2013-06-26

Reversible Reactive Flow Displacements in Porous Media

Alhumade, Hesham Abdulhamed

UNIVERSITY OF CALGARY

Reversible Reactive Flow Displacements in Porous Media

by

Hesham Abdulhamed Alhumade

A THESIS

SUBMITTED TO THE FACULTY OF GRADUATE STUDIES

IN PARTIAL FULFILLMENT OF THE REQUIREMENTS FOR THE

DEGREE OF MASTER OF SCIENCE

DEPARTMENT OF CHEMICAL AND PETROLEUM ENGINEERING

CALGARY, ALBERTA

June, 2013

Abstract

The objective of this research is to investigate the effects of the reversibility of chemical reactions on the instability of reactive fluids displacements in porous media. Such instability is encountered in various fields such as engineering processes, natural phenomena and environmental systems. Therefore, understanding the mechanisms of this instability is key to enhancing the efficiencies of reversible reactive flows in porous media. The reactive displacement was modeled through a bimolecular reversible chemical reaction (BRCR), $A + B \leftrightharpoons C$. In addition, a mathematical model was adopted for the transport of the chemical species through the porous media.

The first part of the research focuses on the horizontal displacement of a reversible reactive interface in homogeneous porous media, where the importance of the reversibility of the chemical reactions in understanding and optimizing reactive displacement processes such as heavy oil recovery as well as underground water treatment techniques was illustrated. The effects of reversibility were found to vary for different scenarios of frontal instability based on the variation of the viscosities of the chemical species. A linear stability analysis of the problem was performed for short time scales, which allowed determining the importance of the different parameters controlling the process. Furthermore, the non-linear interactions between the chemistry and the hydrodynamics were studied by performing numerical simulations. The simulation results revealed that for a particular set of parameters, reversibility can result in an enhancement of the instability of reactive flows.

The research was also extended to address the influence of reversibility on the efficiency of reactive chromatographic process as well as environmental issues related to geological storage of carbon dioxide. The properties of the instability of a horizontal BRCR interface

between a solution of reactant (A) on top of (B) were analyzed. The role of reversibility on the instability of reactive displacements under gravity field where densities mismatch drives the instability was also investigated. The analysis examined the effects of the reversibility where the instability of the flow is driven by the variation of both densities and viscosities of the chemical species. Here too, reversibility enhanced the instability of the flow for some cases of frontal instability.

Acknowledgements

All thanks and praises are for almighty Allah for those kindnesses I am living in everyday in this life. I thank him for making this journey possible and for helping me enriching my knowledge.

I would like to record my gratitude to my supervisor Dr. Jalel Azaiez for his support, advice, and guidance from the beginning of my program. I am indebted and grateful to Dr. Azaiez for all his encouragement and support, which inspired and enriched my knowledge in various ways.

I am grateful to Dr. A. Jeje, Dr. J. Abedi Dr. J. Chen, Dr. N. Mahinpey and Dr. J. Azaiez for their contribution in enhancing my knowledge in various fields. I am also indebted to my fellow colleagues M. Sajjadi and Q. Yuan for their support and suggestions on my research work.

My sincere thanks to my Master committee members, Dr. S. H. Hejazi, Dr. E. Nowicki and Dr. A. D. Visscher for accepting to be members of the committee and for their fruitful comments on my work. I am also grateful to all faculty members and office and technical staff at the department of chemical and petroleum engineering for their support during last years.

I would also like to thanks my wife, my family in Saudi Arabia, especially my parents, brothers and sister for the encouragement, support and their effort during the days of the hard work in making my life more comfortable.

Finally, the financial support by the Saudi cultural bureau in Canada (SACB) is appreciated and also I would like to express my gratitude to all office and technical stuff at the Saudi cultural bureau in Canada and the Ministry of higher education in Saudi.

Dedication

To all of my teachers and my family

Table of Contents

List of Figures and Illustrations

List of Symbols, Abbreviations and Nomenclature

Symbol	Definition
a	Concentrations of chemical components A
a_0	Initial concentrations of reactants B
A	Reactant A (the displacing or injected reactant)
$A_r = L_x/L_y$	Medium aspect ratio
b	Concentrations of chemical components B
b_0	Initial concentrations of reactants B
B	Reactant B (the displaced or *in-situ* reactant)
c	Concentrations of chemical components C
C	Chemical product C
$cas() = cos() + sin()$	cosine and sine function
$2d$	Hele-Shaw cell gap width
D	Diffusion coefficient
$D_a = k\phi a_0 D/U^2$	Damköhler number
$D_r = k\phi D/U^2$	Reversible Damköhler number
$\mathbf{g}$	Gravity acceleration vector
G_i	Dimensionless solutal expansion coefficient $(i = a, b, c)$
$G(s)$	Arbitrary function in Hartley transform domain
$H()$	Heaviside step function
$\mathcal{H}()$	Hartley transformation
$\hat{i}$	Unit vector in $x-$direction
$\hat{j}$	Unit vector in $y-$direction
L	Length
N_x	Number of spectral modes in $x-$ direction

N_y	Number of spectral modes in $y-$ direction
P	Pressure
P_e	Péclet number
$R_b = ln(\mu_B/\mu_A)$	Log viscosity ratio between reactants A and B
$R_c = ln(\mu_C/\mu_A)$	Log viscosity ratio between reactant A and product C
$R_e = \rho UL/\mu$	Reynolds number
$R_{AC} = R_c/2$	Viscosity ratio in the trailing reaction zone
$R_{CB} = R_b - R_c/2$	Viscosity ratio in the leading reaction zone
$R_L = 2R_b/(1 - e^{-R_b})$	Neutral stability curve based on long wave instability.
$R(x,t)$	Chemical production rate
t	Time
t_0	Frozen time
u	Velocity component in $x-$direction
$\mathbf{u}$	Velocity vector in Darcy law
$\hat{\mathbf{u}}$	Velocity vector in Lagrangian frame
U	Injection velocity magnitude
U_c	Critical velocity magnitude
$U_{ch} = \frac{\lvert\bigtriangledown\rho\rvert g}{\mu_A}$	Characteristic velocity
v	Velocity component in $y-$direction
$\vec{v}$	Velocity vector in Navier-Stokes equation
x	$x-$direction coordinate
x_m	Collocation points in $x-$ direction
y	$y-$direction coordinate
z	$z-$direction coordinate
y_n	Collocation points in $y-$ direction
α	Reversibility coefficient

$\delta()$	Delta function
ϵ	Very small and positive value
$\eta = x/\sqrt{t}$	Self-similar dimensionless variable
κ	Medium permeability
μ	Viscosity
μ_0	Base-state viscosity profile
ρ	Density
ω	vorticity
ψ	streamfunction
ϕ	Velocity perturbation eigenfunction, medium porosity
ψ_i	Concentration perturbation eigenfunction ($i = A, B, C$)
σ	Disturbance growth rate
σ_m	Most unstable disturbance growth rate
$\tau_h = D\phi^2/U_c h^2$	Characteristic hydrodynamic time-scale
$\tau_c = \phi/(ka_0)$	Characteristic chemical rate time-scale
*	Dimensionless variable
$^\prime$	disturbance from the base-state value
$^+$	Values at $x > 0$
$^-$	Values at $x < 0$
$\check{}$	variables in Hartley transform domain
$\tilde{}$	Predicted values
$_0$	Base-state variables
$_i$	Related to solution $i = (A, B, C)$
$_{x,\ y,\ z}$	(x, y, z) Cartesian directions
2D	Two-dimensional
BCR	Bimolecular chemical reaction

BRCR	Bimolecular reversible chemical reaction
C_a	Capillary number
CT	Chlorite-tetrathionate
DNAPL	Dense non-aqueous phase liquid
IAA	Iodate-arsenous acid
LBM	Lattice Boltzmann method
LSA	Linear stability analysis
R_a	Rayleigh number
RCA	Relative contact area
RD	Reactive diffusive
TCE	Trichloroethylene
VAPEX	Vapor extraction
VF	Viscous fingering

Chapter 1

Introduction

This thesis focuses on the instability of reversible reactive interfaces in homogeneous porous media. The reactivity of the system may dramatically influence the instability of the displacement process as soon as the chemical reaction produces a new chemical species at the initial interface between the displacing and the displaced fluids, and possibly changes the physical properties of the fluids such as the viscosity, density, diffusion coefficient or surface tension. The interface between the displacing and the displaced fluids can be destabilized as a result of the variations in the viscosities or the densities of the solutions, if not both. This instability may grow to form finger-shaped intrusions of one of the fluids into the other. This instability is referred to as viscous fingering or Saffman-Taylor instability when the variation in the viscosities of the fluids triggers the instability. Whereas, when the density mismatch drives this instability, it is referred to as density fingering or Rayleigh-Taylor instability [3], [4].

There is a growing number of studies that deal with fingering instability of non-reactive flows in porous media where the fingers hydrodynamically interact without affecting the properties of the solutions or the surrounding porous medium [5], [6]. However, the influence of the chemical reaction on the physical properties of the displacing or the displaced fluid finds important applications in fields as the removal of chemical pollutants from underground water, liquid chromatographic separation, heavy oil recovery, fixed bed regeneration and carbon dioxide sequestration [7], [8], [9]. In theses processes, the chemical reaction will change the physical properties of the fluids or the surrounding area if not both, and as a result instability may develop at the reactive interfaces between the chemical species.

Reactive flows are usually encountered in energy and environmental sectors. In particular, the injection of a reactive fluid into a reservoir in order to change the physical properties of the resident fluid such as the viscosity, is an environmentally friendly alternative to current heavy-oil recovery techniques such as Steam Assisted Gravity Drainage ($SAGD$) as well as Vapour extraction ($VAPEX$). Furthermore, the injection of a reactive fluid to remove pollutants from the underground water is also an important application that has shown promising results [10], [11], [12].

The instability of the reactive flows plays an important role in the success and the efficiency of the displacement process. Furthermore, since most homogeneous chemical reactions are reversible [13], it is important to consider the effects of the reversibility on the instability of the reactive displacements. In this study a mathematical model is developed to illustrate the effects of reversibility on the instability of the reactive flows in homogeneous porous media.

The influence of the reversibility is investigated using two techniques, namely linear stability analysis and nonlinear simulations. In the second chapter, a detailed review of the state of the art of literature on experimental and theoretical studies of non-reactive and reactive displacements is presented.

The third chapter presents derivations and results of linear stability analysis (LSA) to illustrate the effects of the various parameters on the instability at early stages where the disturbances are small, by reducing the nonlinear equations to linearized ones. The linear stability analysis is a powerful tool in examining the influence of each of the parameters that control the flow on the instability of the system. In particular, the limits at which reactive flows may switch from stable to unstable regimes were identified. Furthermore, LSA helped

in determining the parameters at which the nonlinear simulations were to be carried.

In the fourth and the fifth chapters, the different scenarios of frontal instability of reversible reactive flows in horizontal and vertical porous media are presented, respectively. In the fourth chapter, the influences of the reversibility on the instability of the reactive flows are illustrated for various possible scenarios of frontal instability. In addition, the efficiency of the displacement process was examined in term of the rate of production as well as the relative total contact area between the chemical species. Similarly in chapter five, the effects of reversibility were also investigated when the variations in the densities or/and the viscosities of the chemical species drive the instability, and the relative total contact area between the species was also analyzed.

Chapters three and four are under review journal articles. In addition, parts of the introduction and the mathematical model presented in chapter three are repeated in chapter four since these two chapters deal with reversible reactive flows in a horizontal geometry. Furthermore, the same mathematical and numerical techniques in chapter four are used in chapter five, while considering the gravity field. Therefore, the reader may omit reading the introduction of chapter four and the mathematical modeling sections in chapters four and five.

1.1 Origin of fingering mechanism

The flow of fluids in porous media was first investigated in (1856) by Darcy [14]. Darcy found that the pressure gradient ($\bigtriangledown P$) along a sand packed column is linearly proportional to the fluid velocity vector ($\mathbf{u}$) according to the following relation, famously known as Darcy's law.

$$\nabla P = -\frac{\mu}{\kappa}\mathbf{u} + \rho\mathbf{g} \tag{1.1}$$

In the above equation, μ/κ represents the proportionality factor, ρg the hydrostatic pressure per unit length, μ the fluid viscosity, ρ the fluid density and κ is the medium permeability.

Such displacements in porous media were found to be unstable, under certain flow conditions. The development of such instability was mathematically modeled in (1952) by Hill [15]. Hill considered a one dimensional displacement process in porous media where a fluid with properties (μ_1, ρ_1) was injected with a uniform velocity to displace a resident fluid with properties (μ_2, ρ_2), while the gravity field was parallel to the direction of the flow. Furthermore, a small disturbance at the initial interface between the fluids will grow in time if the driving force $(\bigtriangledown P)$ across the interface is positive.

$$P_1 - P_2 = -\frac{\mu_1 - \mu_2}{\kappa} U \triangle x + (\rho_1 - \rho_2) g \triangle x \tag{1.2}$$

The conditions at which the initial interface is stable or unstable can be anticipated from the above relation. For example, In the absence of densities mismatch, the interface is unstable if a less viscous fluid is injected to displace another one with higher viscosity $(\mu_1 < \mu_2)$. Whereas, an unstable interface is encountered if a heavier fluid is placed on top of a lighter one $(\rho_1 > \rho_2)$ when the viscosities are equal $(\mu_1 = \mu_2)$. Furthermore, when both densities and viscosities vary, the disturbance will grow if the velocity exceeds a certain value, referred to as the critical velocity.

$$U_c = \frac{(\rho_1 - \rho_2) g \kappa}{\mu_1 - \mu_2} \tag{1.3}$$

Considering the obscure nature of porous media and the difficulty in tracking the interactions between the disturbances in time, the Hele-Shaw cell has been widely used as a prototype to investigate fluid flows in homogeneous porous media.

1.2 Hele-Shaw cell

The complexity of flows in porous media indicates the need to study the flow instability in simpler and more idealized model systems such as the Hele-Shaw cell. This system can be

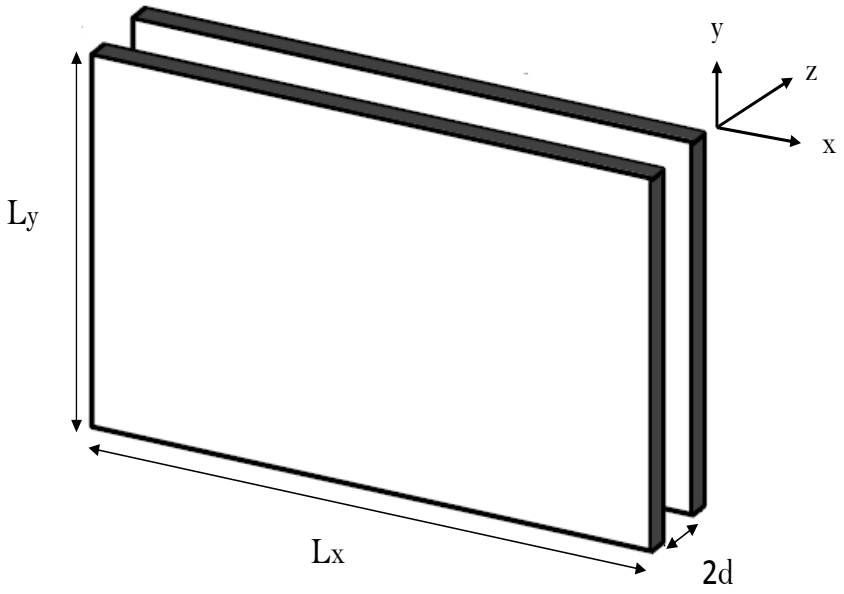

Figure 1.1: Schematic of Hele-Shaw cell.

used to investigate the development of flows in both horizontal and vertical directions for radial and rectilinear geometry. The Hele-Shaw cell consists of two parallel plates separated by a gap that is considered very small compared to the length (L_x) and the width (L_y) of the plates as shown in figure 1.1. In general, the flow through the narrow gap between the plates obeys the Navier-Stokes equation. However, for a small gap and low Reynolds numbers ($R_e << 1$), the flow can be considered to develop only in the x- and y- directions and to be governed by the two dimensional ($2D$) Darcy's law. Under these assumptions, the flow in a Hele-Shaw cell is analogous to a two dimensional incompressible flow in homogeneous porous media and is described by the continuity equation for the conservation of mass and Darcy's law for the conservation of momentum.

1.3 Objectives

A number of studies have focused on the frontal instability of a simple bimolecular $A + B \rightarrow C$ reaction. However, a number of aspects still need to be investigated. It should be noted that most of the bimolecular homogeneous reactions are reversible and this reversibility may

dramatically influence the fate of the reactive displacements and their efficiency in terms of the rate of production and the mixing areas between the chemical species. Therefore, it is interesting to examine the effects of reversibility on the hydrodynamics of fingering instability for the different scenarios of frontal instability.

First, the influence of reversing the chemical reaction $A + B \leftrightharpoons C$ on the instability of a horizontal reactive displacement process where the instability is driven by viscosities mismatch between the fluids is examined analytically and numerically. This is achieved by conducting a linear stability analysis and nonlinear simulations of the fingering instability.

Furthermore, the role of reversibility on the properties of a horizontal reactive interface where both viscosities and densities mismatch trigger the instability is also investigated in the case of a vertical flow geometry.

Chapter 2

Literature Review

This chapter presents and discusses existing studies related to the flow instability in porous media for both non-reactive and reactive flows. Studies on non-reactive flows are presented first. These are followed by a review of experimental work of reactive flow displacements. After that, theoretical studies on reactive flows are presented in two sub-sections, which are auto-catalytic and bimolecular chemical reactions.

2.1 Viscous fingering in non-reactive systems

In this first part, major experimental and theoretical results for non-reactive systems are discussed. The first study on fingering instability was carried out in (1950) by Taylor [16] who proposed a theory about the growth of instability under gravity force at the interface between fluids with different densities. A set of experiments were conducted by Lewis [17] where a high shadow photography was used to confirm Taylor's theory. Hill [15] studied experimentally the development of instability at the interface between sugar liquid and water where the instability was driven by both viscosities and densities mismatch between the fluids. The fingering patterns in Newtonian displacements in porous media were examined in (1952) by Slobod and Caudle [3] using X-ray technique. Saffman and Taylor [4] examined the immiscible displacement of oil by water and air, and derived a mathematical model for the development of the instability.

A number of studies focused on the mathematical and numerical modelling of the development of the instability. These studies date back to the work of Chuoke et al.,[18] as well as that of Peaceman and Rachford [19].

Some experimental studies focused on the effects of different factors on the instability of the non-reactive systems such as surface tension [20], non-Newtonian profiles [21], anisotropy [22] as well as transverse gravity fields [23]. McCloud and Maher [6] presented an extensive review of experimental studies in Saffman-Taylor flows, which detailed the influence of the previous factors on the dynamics of fingering.

A review of relevant literatures and challenges in the simulation of miscible displacements was presented by Homsy [5].

Tan and Homsy [24], [25] investigated analytically and numerically the stability of miscible displacements in porous media, where good agreements with the previous experimental work were observed. The authors presented for the first time the splitting phenomena in miscible displacements and they also reported that the mixing length growths linearly in time.

Yortsos and Zeybek [26] investigated the effect of dispersion on the instability of miscible displacements where it was reported that dispersion has a destabilizing contribution at short wavelengths.

The work of Tan and Homsy [25] was extended by Zimmerman and Homsy [27] where the effects of viscosity contrast, anisotropy and velocity dependence of longitudinal dispersion were studied. It was reported that the combination of high mobility contrast, weak transverse dispersion and and strong dependence of longitudinal dispersion on velocity enhances the long time growth of instability.

Subsequent studies focused on the variation of instability in homogeneous and heterogeneous porous media [28], [29], [30] where it was reported that the intensity of the instability and consequently the mixing zone increase monotonically with the variance of the heterogeneity.

In a vertical geometry, Manickam and Homsy [31] investigated analytically and numerically the instability of miscible displacements driven by both density and viscosity. The authors presented the different scenarios of frontal instability and calculated the growth rate of the mixing zones for different injection velocities and viscosity ratios.

Other studies investigated the role of gravity on the instability of miscible displacement under gravity field [32], [33], [34], [35] where fingering phenomenon such as diagonal fingering, trailing-lobe detachment and secondary side-finger instability were presented.

Singh and Azaiez [36] examined numerically the instability of miscible shear-thinning fluids in a rectilinear Hele-Shaw cell where the authors showed that shear thinning has the effect of accelerating growth rates of fingering patterns in comparison to Newtonian fluids. Furthermore, new fingering mechanism such as mulitiple side-branching, diagonal fingering and trailing-lobe detachment were observed.

De Wit et al. [37] studied numerically the instability of a displacement of a miscible high viscosity slice where the authors showed that fingering contributes transiently to the broadening of the peak in time.

The influences of high mobility ratio and Pèclet number were examined by Islam and Azaiez [38] where new fingers structures such as uneven tip-splitting, partial coalescence, stretched

coalescence, gradual coalescence, single-sided tip-splitting, alternating side-branching, dense branching, skewering, double coalescence, trailing lobe detachment and side-branching were observed. The authors also analyzed qualitatively the relative fingers widths and contact areas.

Rousseaux et al. [39] studied the non-linear instability in packed chromatographic columns. Here the authors focused on the non-linear properties of the instability plus the quantitative measurements in the chromatographic columns. These results can be applied to both numerical and experimental data of such a system in order to understate the effects of the mobility ratio as well as the model's dimensions on the properties of viscous fingering.

The spreading of containments in underground water was investigated by Kim [40]. Here, the author carried a linear stability analysis to investigate the onset of miscible viscous fingering of a high viscous slice of the contaminants in the underground water. It was reported that there is a critical time for the instability to grow and there is a critical width at which the system is always stable. From these results the author concludes that the system is unconditionally stable under critical time and width.

Kim and Choi [41] investigated the effect of shear-thinning on the onset of the instability in porous media using the Carreau model. The stability equations were solved both analytically and numerically with and without the quasi steady state approximation (QSSA). The authors reported that displacing a Newtonian fluid with a shear-thinning one makes the flow more unstable than displacing with a Newtonian fluid. However, when the displacing fluid is Newtonian, then shear-thinning makes the flow, in general, more stable.

Jha et al. [42] examined the mixing efficiency of fluids in porous media at low Reynolds

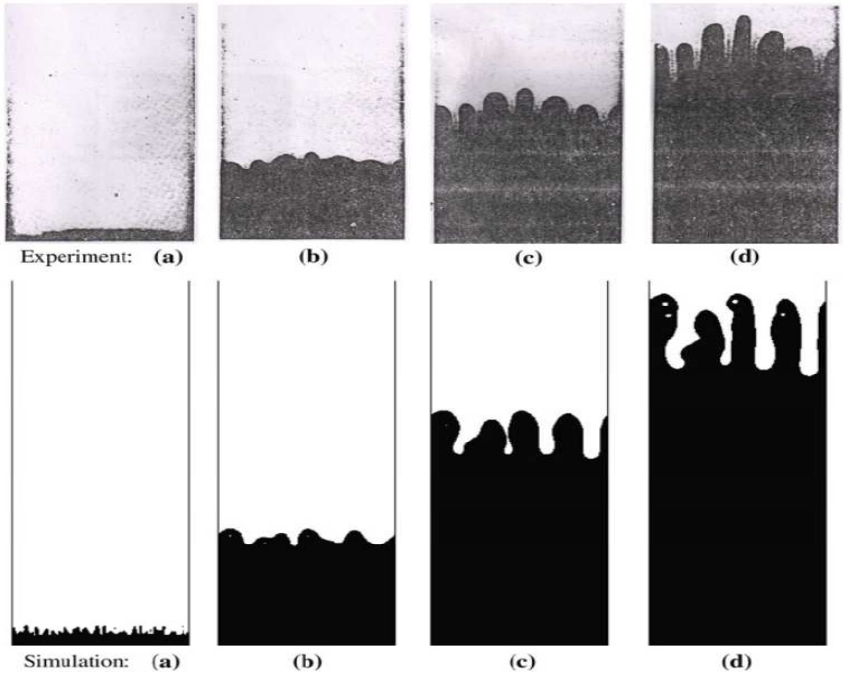

Figure 2.1: Qualitative comparison of viscous fingering in a tilted Hele-Shaw cell: (a) Experiment, (b) Simulation. From Dong et al. [1].

numbers. From the results, it was possible to predict the optimum viscosity ratio for a given Péclet number, which maximizes the interfacial area between the fluids and consequently reduces the mixing time.

The instability of immiscible displacements in porous media was simulated using the lattice Boltzmann Method (LBM) by Dong et al. [1]. The study focused on the effects of capillary force, viscous force, gravity and surface wettability on the fluid behavior. In addition, the areal sweep efficiency was used to evaluate the displacement efficiency. The present study demonstrated that the lattice Boltzmann Method is useful in simulating multiphase flow in porous media as shown in figure 2.1.

The gravity-driven fingering of immiscible flow of water and a dense non-aqueous-phase liquid (DNAPL) such as trichloroethylene (TCE) was experimentally examined in a homogeneous

sand-filled column by Nsir et al. [43]. The spatial distribution of the advancing displacement front in a given control section of the experimental device was examined for different values of the system parameters such as flow rate, flow mode and grain size. It was observed that both higher injection rate of the (DNAPL) and lower medium permeability attenuates the gravity instability.

Dias et al. [44] investigated analytically the possibility of minimizing convectional viscous fingering in an initial unstable immiscible interface in a radial Hele-Shaw cell. It was reported that the optimum injection rate at which the front disturbances can be minimized is a linearly increasing function of time. Furthermore, the authors performed series of experiments and non-linear simulation in order to support the analytical results.

Mishra et al. [45] studied the pressure driven miscible displacement in a channel geometry when a viscous fluid is injected to displace a less viscous one. The problem was governed by the continuity and Navier-Stokes equations along with a concentration-dependent viscosity profile and two convection-diffusion equations for the distribution of the concentrations. The authors focused on the capability of the double diffusive effects on destabilizing the initially stable system. The double diffusive effect is observed when the fluid consists of a solvent that contain two different solutes both influencing the viscosity of the fluid and diffusing at different rates. It was reported that increasing the diffusivity contrast between the faster diffusing and the slower diffusing solutes enhances the intensity of the instability.

2.2 Viscous fingering in reactive systems: Experimental studies

A growing number of experimental studies have focused on reactive viscous fingering. In particular, there is a growing number of studies on viscous fingering coupled with chemical reactions in porous media or Hele-Shaw cells. In most of these studies the initial interface

between the displacing and the displaced fluids was considered unstable without chemical reaction.

One of the first studies on reactive flows was conducted in (1990) by Naser-El-Din et al. [46] where the authors examined the effect of chemical reaction on a secondary oil recovery process. A Hele-Shaw cell filled with glass beads was used as a water wet porous medium saturated with paraffin oil doped with 1 wt linoleic acid. A solution of alkaline ($NaOH$) was used to examine the patterns and the efficiency of the immiscible displacement. A substantial reduction in interfacial tension was observed at the interface between the linoleic acid in the oil phase and the alkaline solution in the water phase as the chemical reaction takes place. The authors also reported that both the interfacial tension and the break-through recovery are functions of the concentration of $NaOH$. Another experimental study on immiscible reactive system was carried out by Hornof and Baig [47] in a Hele-Shaw cell where a mixture of linoleic acid with oil representing the high-viscous phase and a mixture of sodium hydroxide with water as the low-viscous phase, were used in the reactive displacement. Differences between fingering patterns in reactive and non-reactive systems were reported, in addition to a higher oil recovery in reactive than non-reactive displacements.

Carey et al. [48] studied experimentally the instability of a miscible displacement process involving an auto-catalytic iodate-arsenous acid chemical reactive front. These authors reported the onset of buoyancy driven fingering as the density changes with the chemical reaction. Bockmann and Muller [49] focused on a similar buoyancy unstable system where they experimentally defined the growth rate of the unstable modes.

A set of experiments were carried out by Nagatsu and Ueda [50] to examine the effect of the reactants concentrations on the fingering patterns in a miscible displacement. In these

experiments, a Hele-Shaw cell with a centered injection well was considered. The injection was slow enough in order to allow molecular diffusion to control the transport of both the solute and the solution. In addition, it was reported that the initial concentrations of the reactants play a major role in the distribution of the product. Moreover, the reaction zone was located in regions of less concentrated high- or low- viscous fluid. Moreover, it was observed that the chemical product will either accumulate at the fingertips or broadens in the area inside the fingers when the reaction zone was located in the high and low viscous fluids, respectively. The same authors [51] investigated the effects of finger growth velocity on the fingering pattern as well as the distribution of the product. The authors found that the reactants' concentrations ratio has insignificant effects on the reaction pattern and the product will be concentrated around the fingertips when the bulk finger-growth velocity increases.

Another study by Fernandez and Homsy [52] examined the immiscible reactive displacement in a radial Hele-Shaw cell for a liquid-liquid system where the products (surfactants) were able to change the surface tension. The experiments were performed over a wide range of both Capillary C_a, which represents the relative effects of viscous forces against surface tension across immiscible liquid interfaces and Damköhler D_a numbers, which represents the rate of the reaction in order to illustrate the effects of the capillary force and the reaction rate on the fingering patterns. The authors stated that the reduction in the mobility ratio at the interface as a result of the chemical reaction decreases the driving force for instability, which resulted in wider fingers and higher sweep efficiency. A critical Damköhler number was defined ($D_{a_{cr}}$), where the finger width was controlled by D_a above that number, while a similar behavior to that of non-reactive systems was observed below $D_{a_{cr}}$. In addition, the capillary number was found to have stronger influence on the finger width in non-reactive compared to reactive systems.

Zhang [7] conducted laboratory and field experiments where a reactive fluid was injected to remove pollutants from the underground water and promising results were reported.

A study by Nagatsu et al. [53] examined the effect of changing the viscosity of the product on the fingering patterns in an initially unstable miscible reactive displacement. They showed that the existing fingering patterns can be modified as the chemical reaction increases or decreases the viscosity of the product. In addition, they reported that fingers are wider and the product occupied more area as the viscosity of the product increases, while narrower fingers were observed as the product viscosity decreases. This was attributed to the increase in the shielding effect. Effects of the reactants' concentrations were also examined in this study where it was reported that increasing the concentration of the less viscous fluids has a monotonically increasing effect of fingering patterns in cases where the reaction decreases the viscosity of the product. Whereas, when the reaction increases the viscosity of the product, increasing the concentration of the less viscous fluid enhanced the instability up to a threshold value before it starts to attenuate the fingering patterns. The same authors also studied the effect of strong and moderate chemistry on the flow by analyzing the fingering patterns at high and moderated Damköhler numbers [53], [54].

In the same year (2007), Podgorski et al. [55] performed similar experiments where the instability was triggered by a simple chemical reaction of the $A + B \rightarrow C$ type. The system consisted of two reactants with the same viscosity, which made the system neutrally stable before the chemical reaction takes place. Once the reactants come in contact, the product (C) with a higher viscosity than the reactants' appears at the interface and triggers the instability. The results showed that the fingering patterns will be different if the reactant (A) is injected into (B) or vice-versa, which was attributed to differences in the diffusion coefficients of the chemical species.

An experimental study on a reactive miscible displacement process by Nagatsu et al. [56] investigated the effect of precipitation. The results showed that the fingering patterns may change as the precipitation concentration varies. These authors reported that in a reactive displacement process with low Péclet number and stoichiometric ratio of the reactants, fingers will bend and grow in a direction almost perpendicular to the flow when the precipitation concentration exceeds a certain value. Moreover, a higher initial concentration of the less viscous fluid was needed for the bending pattern to be observed at a moderate Péclet number.

Shuwang Li et al. [57] studied numerically and experimentally the viscous fingering patterns in a radial Hele-Shaw cell and it was reported that fingering instability can be suppressed by controlling the injection rate of the less viscous fluid.

A series of core flooding experiments were conducted by Berg et al. [58] in order to investigate the performance of carbon disulfide (CS_2) as a novel agent for enhanced oil recovery. X-ray computed tomography was used to obtain the three dimensional (3D) spatial distribution of the displacing fluid and the displaced oil. Recoveries over 90% were observed at small viscosities ratio and large flow rates. Whereas, high viscosities contrast and slow flows reduced the oil recovery.

The effects of chemical reaction on the fluids' viscosities in miscible displacements in a radial Hele-Shaw cell were investigated experimentally by Nagatsu et al. [59]. It was observed that when the reaction increases the viscosities, the shielding effect is suppressed and the fingers are widened, which result in denser fingering patterns. On the other hand, the shielding effect is enhanced and the fingers are narrowed as the reaction decreases the viscosities, which result in less dense fingering patterns

Buchgraber et al. [60] conducted experimentally and monitored optically water/oil and polymer-solutions/oil displacements in a 2D micro-model. The observed results illustrated the ability of the polymer to stabilize multi-phase flows. At low concentration of polymer, relatively long wide fingers of the displacing fluid were observed, which led to an early water breakthrough and low recovery. On the other hand, as the polymer concentration increased, relatively shorter fingers were observed, which made the displacement front appear to be stabilized at large scales.

In a more recent study, Riolfo et al. [2] analyzed reaction-driven viscous fingering in an initially stable displacement in a horizontal Hele-Shaw cell. Aqueous solutions of polymers were used in order to benefit from the dependence of their viscosities on the pH. Two cases where instability developed in the upstream or the downstream directions of a bimolecular reaction system were presented as shown in figure 2.2. Non-linear simulations were also performed to support the experimental results.

2.3 Viscous fingering in reactive systems: Theoretical studies

A growing number of theoretical studies dealt with the reactive flows. Some of these studies focused on reactions between the fluid and the surrounding porous media while others dealt with the auto-catalytic fluid-fluid reactions. Some recent theoretical works investigated the instability of simple type of bi-molecular chemical reactions $A + B \longrightarrow C$. In addition there is a limited number of studies that have examined the instability of reversible reactive interfaces $A + B \rightleftharpoons C$. In this section, studies dealing with reactions between the fluid and the porous media are presented first followed by those related to auto-catalytic fluid-fluid reactions and then recent studies on both complete and reversible chemical bi-molecular reactions.

2.3.1 Auto-catalytic and infiltration reactive systems

The modelling study by Chadam [61] is considered one of the first studies that modelled mathematically the ability of the chemical reaction in changing the macroscopic patterns of the media. In this study, the authors investigated infiltration flow in addition to the variation in the porosity of the media as a result of the reaction. The possibility of fingering instability in such a process was confirmed by both linear stability analysis as well as non-linear simulations.

In parallel, Lichtner et al. [62] used the numerical finite difference technique to study diffusion mass transport accompanied with reversible auto-catalytic chemical reaction in porous media. A porous medium consisting of an inert solid matrix and a reactive solid phase in equilibrium with an aqueous solution was considered. When the solute concentration was fixed at one end of the porous medium at fluid composition that is under-saturated with respect to the reactive solid phase, the solid starts to dissolve at a reversible reactive interface that propagates along the porous medium. Here, the authors were able to determine the position of the dissolving front as well as the concentration distribution of the different solute species. Furthermore, the numerical results were validated against exact analytical solutions.

Another mathematical model that simulates the carbon-cemented sandstone system was proposed by Wei and Ortoleva [63] where the reactive flow can decrease or increase the porosity and consequently the permeability of the medium by dissolving the matrix. The study revealed that fingering instability may exist at such a system as a result of the dissolution of the matrix and the changes in the properties of the medium. Furthermore, different dynamics of fingering such as tip splitting were observed for different types of rocks and fluids properties.

A linear stability analysis for acid flows through porous rocks was conducted by Hinch and Bhatt [64] where the injected acid dissolved the matrix and increased the permeability. In this study, reaction convection equations coupled with Darcy's law were used to control the transport of the acid and the dissolved materials. Moreover, it was assumed that the medium's porosity was not affected significantly with the dissolution of the materials, while permeability varied significantly with the concentration of the dissolved materials. This study showed that changes in the permeability can destabilize the reactive front. In addition, it was observed that the growth rates were small at long wavelengths, while they increased at short wavelengths.

Another linear stability analysis where the reactive fluid can dissolve the matrix, but for a vertical slab was carried out by Aharonov et al., [65]. These authors studied the formation of conducts as melt flowed from the Earth's mantle. The mass conservation equations along with Darcy's law were used to model the propagation of the reactive flow as well as the deformation of the matrix. The authors showed that increasing the diffusion coefficient decreases the instability and that the reactive-infiltration instability is a significant factor in the up-welling melt in the mantle.

De Wit and Homsy [66] simulated the instability of auto-catalytic miscible horizontal displacements in the Hele-Shaw cell geometry. Here too, the reaction convection diffusion equations along with Darcy's law were used to model the propagation of the concentration of the fluids. In addition, a third order auto-catalytic chemical reaction as a function of the concentration of the displacing fluid was used. The authors showed that this type of reactions can result in a sharper displacement front as well as in stronger tip-splitting mechanisms along with droplet formation.

Another study by Jahoda and Hoenof [67] modelled the reactive displacement of two immiscible fluids in porous media. A two-dimensional reactive-convective-diffusion model was adopted to investigate the instability of the oil-water interface in addition to the interactions with the medium. The objective of this study was to illustrate the effect of the concentration of the product, which is alkaline, on the fate of the displacement process. Furthermore, the authors observed a decrease in the concentration of the product in the water phase especially at the fingertip.

The previous work by Chadam [61] was subsequently improved by the same authors where a velocity-dependent hydrodynamic dispersion was adopted [68]. Here, a dispersion-convection-reaction equations coupled with Darcy's law were used for mass and flow field modeling. The authors found that the rate of increase in the porosity of the medium was proportional to the reaction rate. Moreover, the study showed that transverse dispersion had a stabilizing effect of the system, but without eliminating the reaction-infiltration instability.

De Wit [69] performed a linear stability analysis on the system introduced in the previous study with Homsy [66] in order to illustrate the effects of the reaction parameters on the instability of the system. In this study, the author reported that the stability of the system depends on both the width and the speed of the reactive front. Furthermore, De Wit reported that the major difference between pure and chemically driven fingering is that the dispersion curves do not vary in time in absence of chemical reactions. In a subsequent study, Yang et al., [70] studied the buoyancy driven instability for a chlorite-tetrathionate reaction in a Hele-Shaw cell where good agreements between the linear stability analysis, non-linear simulations and experimental measurements were observed.

A numerical model based on the lattice Boltzmann model (LBM) for the transport and

reactions of fluids in porous media was developed by Kang et al., [71]. This study focused on the acid stimulation properties in an enhanced oil recovery process. It was found that highly conductive channels wormholes can be formed in the carbonate rocks as the acid's injection dissolves the matrix. In addition, the dependence of the dissolution process and the wormholes patterns on the acid type as well as the injection rate was successfully simulated using the LBM and the results confirmed the existence of an optimal injection rate at which the wormholes are formed. Furthermore, good qualitative agreements between the results and other experimental and theoretical studies were reported.

Considering a vertical Hele-Shaw cell geometry, Demuth and Meiburg [72] conducted a linear stability analysis for an auto-catalytic miscible reactive front. In their study, the viscosity was assumed to be constant, while the instability was driven by the variation in the density of the product. The reaction-convection-diffusion equations were coupled with the three-dimensional Stokes equations to model the process and the results were compared to the linear stability analysis presented by De Wit [69]. From this comparison, the authors observed that the maximum growth rate and the cut off wave-numbers were under-predicted by a factor of three. This variations in the results were attributed to the applicability of the Darcy's law for small Rayleigh numbers (R_a). The authors also reported that three-dimensional effects become more significant as the Rayleigh number increases and therefore, the linear stability analysis should be based on the three-dimensional Stokes equations.

The applicability of the lattice Boltzmann method for the non-linear simulation of a miscible reactive and an immiscible displacement in a vertical Hele-Shaw cell were illustrated by Grosfils and Boon [73] and Grosfils et al. [74], respectively. In these studied, the auto-catalytic chemical reactions had the similar effects on the surface tension by sharpening the interface, which may affect the fingering patterns.

Similarly, Vasquez and De Wit [75] conducted a linear stability analysis for a chlorite-tetrathionate (CT) auto-catalytic reaction in a vertical Hele-Shaw cell. In this study, four different models resulting from coupling Darcy's law or Brinkman's equation for flow field to an eikonal equation or a one variable reaction diffusion model, were adopted. The authors reported that the combination of Darcy's law with the eikonal equation failed in predicting the dispersion curves, while other three models resulted in good agreements with experimental results for narrow gaps. However, the Darcy-reaction-diffusion model showed poor results as the cell gap increased as reported previously by Demuth and Meiburg [72]. The Brinkman's model resulted in a good agreement between the experimental and the theoretical results when the diffusion coefficients were assumed to be equal.

The infiltration instability problem for in-situ leaching Uranium mining was investigated by Kai-Xuan et al. [76]. It was shown numerically that the feedback between the reactive fluid and the dissolved minerals can result in a frontal instability which affects the rate of recovery of the mineral resource.

The work of Yang et al., [70] was extended by Kalliadasis et al., [77] where the heat of an exothermic reaction was considered in a vertical Hele-Shaw system with insulated plates. Moreover, it was assumed that the auto-catalytic reactions take place at both ends of the vertical cell. In absence of thermal effects, the heavier products invaded the reactants and resulted in stable ascending and unstable descending fronts. It was observed that, thermal effects have opposite contribution to that of the solutal ones on the density. The linear stability analysis as well as the nonlinear simulations showed that the heat of the reaction may actually result in an unstable ascending front.

In a similar geometry, De Wit [78] conducted a non-linear simulation to investigate the development of fingers in an auto-catalytic iodate-arsenous-acid front. Here, the reaction diffusion equations coupled with Darcy's law and a concentration dependent density profile were used in the analysis. Here, the author illustrated the effects of the different parameters modeling the flow on the fingering dynamics.

D'Hernoncourt et al., [79] investigated the role of heat loss when auto-catalytic reactions were triggered at both the top and bottom of a vertical Hele-Shaw cell. Here, a density mismatch at both reactive fronts was considered as a function of both the thermal and the solutal profiles. The reaction produced a hot-light product, which resulted in unstable upward propagating and stable descending, fronts. The linear stability analysis showed that the dispersion curves for the ascending front can be similar to those of the isothermal system when the Hele-Shaw cell is insulated. In addition, the authors found that the heat losses may stabilize a system with perfectly insulated walls. However, heat losses through the walls may result in a non-monotonic density profile at the descending front, which may destabilize the front at a certain range of thermal parameters.

Miscible displacements of radionuclide leaks from underground containers in a water saturated heterogeneous porous media were analyzed by Bruneau et al., [80]. The authors modelled mathematically and numerically the changes in the concentration of the radioactive element in the medium. It was found that the radionuclide coming from a leak of a buried container may reach the surface even in a slow flow.

Zadrazil et al., [81] conducted a linear stability analysis as well as non-linear simulations to examine the effects of an external electric field on the buoyancy driven instability in a vertical geometry. A light product was produced at the bottom of the Hele-Shaw cell as a

result of a third order auto-catalytic reaction, which destabilized the upward propagating front. The transport of the negative ions in the opposite direction of the propagation was increased when a negative electric field was applied. This resulted in an increase in the density mismatch across the front and consequently a more unstable system. On the other hand, applying a positive electric field, increased the transport of the ion in the direction of the propagation and as a result decreased the frontal instability. However, it was reported that a high enough strength of the electric field may stabilize the buoyancy unstable system.

The non-linear interactions of buoyancy driven instability of the auto-catalytic reaction diffusion acidity front of the chlorate-tetrathionate were examined by Lima et al., [82]. A two-variables reaction diffusion equation coupled with Darcy's law were used to model the instability between the heavy product and the fresh reactants in a vertical Hele-Shaw cell. It was found that the development of the fingers is a function of the Damköler number D_a, the diffusivity ratio δ of the chemical species and the Rayleigh number R_a. Simulations showed that for a moderate R_a number, the developed fingers merged to a single symmetric finger. However, tip splitting was observed above a certain value of R_a. Also, a faster travelling front was observed when the chemical product diffused faster than the reactants. Finally, a less elongated but faster developing single finger was observed as the D_a increased.

The buoyancy driven instability of a chemical reaction was classified by D'Hernoncourt et al., [83]. In this study, the authors considered exothermic auto-catalytic miscible fronts in a vertical Hele-Shaw cell where a temperature and density dependant density profile was used. Here, the system can be destabilized by the buoyancy-driven convection. This convection was driven by the solutal and thermal effects on the variation in the density profile of the product. Furthermore, a linear stability analysis was conducted and showed that a counter-intuitive unstable region exists between the hot light and the heavy cold solutions. This

observation was identified as a localized reaction area coupled with variation in the diffusion of heat and concentration.

Adiabatic reactive miscible displacements were also investigated by Swernath and Pushpavanam [84] where, using solutal and thermal expansion constants, the viscosity was considered to be a function of both concentration and temperature. It was observed that the growth rates of the unstable wave-numbers were increased and decreased by increasing the solutal and the thermal expansion constants, respectively. Furthermore, a higher thermal expansion constant had stabilizing and destabilizing effects for exothermic and endothermic reactions, respectively. Finally, a non-linear simulation was carried out in order to support the reported results.

The fingering patterns in a miscible reactive displacement where both the viscosity and the density were modified by the concentration across the auto-catalytic bi-stable front were investigated by Swernath and Pushpavanam [85]. In this study, the authors examined the conditions under which the viscosity profile can stabilize a density unstable profile in a vertical geometry where the auto-catalytic reaction can be triggered either at the top or at the bottom of the surface. When the chemical reaction is triggered at the bottom, the interface between the product and the reactant is buoyancy unstable when the density of the product is lower than that of the reactant. Both linear stability analysis and non-linear simulation confirmed that the interface of such a system can be stabilized when the viscosity of the product is much larger than that of the reactant. Results showed that even when the reaction is triggered at the top to result in an unstable gravitational front, the unstable front may be stabilized if the viscosity of the product is very high compared to that of the reactant.

In a miscible reactive displacement, the effects of the velocity dependent transverse dis-

persion and the longitudinal dispersion on the fingering patterns were examined by Ghesmat and Azaiez [86]. Darcy's law and the reaction diffusion convection equation were used for the velocity field and the continuity of the solute and the solution, respectively. The authors considered second and third-order auto-catalytic reactions and it was reported that the fingering dynamics in dispersive flows with high reaction rates are similar to those observed in a high mobility ratio displacement. Moreover, the authors reported that dispersion had more pronounced effects on the fingering patterns of the reactive flows than on the non-reactive ones.

2.3.2 Bimolecular reactive flows

The previous reviewed studies are related either to the interactions between the fluids and the porous medium or to auto-catalytic reactions. However, there is a growing number of studies on the frontal instability of non-auto-catalytic reactions where the instability is driven by the variation in the physical properties of the reactants and the products. Here, studies on irreversible bimolecular chemical reactions (BCR) will be presented first, followed by studies on bimolecular reversible chemical reactions (BRCR).

Irreversible chemical reactions:

The stability of the $A + B \rightarrow C$ front was examined by Rongy et al. [87] where the chemical reaction takes place at the interface between horizontal layers of the initially separated reactants. The model was governed by the two dimensional incompressible Stokes equations for the flow field along with the reaction diffusion convection equation for the conservation of mass. Here, the density profile was assumed to be linearly dependant on the local concentration of the chemical species (A), (B) and (C). The authors reported that the stability of the reactive interface may be influenced by the buoyancy-driven convection as a result of densities mismatch between the reactants and the product even if the diffusion coefficients of the chemical species are equal and the initial concentrations of both reactants are equal.

Furthermore, the authors supported the reported results by numerical simulations and the various dynamics of frontal propagation were classified based on the solutal expansion coefficients.

For the same type of chemical reactions $A + B \rightarrow C$, Gerard and De Wit [88] numerically investigated the viscous fingering in a miscible displacement in a horizontal Hele-Shaw cell geometry. Here, it was assumed that the viscosities of both reactants are equal, which resulted in a neutrally stable initial interface. Furthermore, the viscosity of the product was assumed to be different than the viscosities of both reactants, while an exponential variation of the viscosity of the fluid with the concentration of the product was adopted. The authors reported that the viscous fingering patterns were similar whether (A) is displacing (B) or vice verse when the initial concentrations of the reactants are equal as well as the diffusion coefficients. This study confirms the asymmetry in fingering patterns observed in the experiments by Podgorski et al. [55].

Hejazi et al. investigated analytically [89] and numerically [90] the different scenarios of frontal instability in a horizontal miscible displacement process that involves a simple chemical reaction $A + B \rightarrow C$. The authors adopted a slab configuration where each half of the slab was filled with only one of the reactants. In this study, the authors focused on the instability of the interfaces between the reactants and the product based on the mobility ratio at each interface.

Hejazi and Azaiez also examined the displacement of a reactive slice of pollutant solution in a carrier solution [91]. Here, the dynamics of the flow as well as the rate of consumption of the pollutant were investigated when a chemical reaction takes place between the two solutions $A + B \rightarrow C$. It was reported that the widest distribution of the pollutant is

observed when the pollutant's viscosity is smaller or larger than those of the carrier solution and the product, while the highest consumption rate is reported when the chemical product is the least or the most viscous solution. Furthermore, the authors observed that the carrier solution may break through the pollutant when the viscosity of the product is larger than that of the carrier solution.

Almarcha et al. [92] studied the buoyancy chemically driven instability experimentally and numerically in a vertical reactive displacement. Here, the authors confirmed the unstable nature of the system when the chemical product is heavier than the reactants or when the diffusion rates of the chemical species vary.

Nagatsu and De Wit [93] conducted non-linear simulations in the same model considered by Hejazi and Azaiez [90], but for an infinite Damköler number ($D_a \to \infty$). Here, the authors characterized quantitatively the fingering patterns in terms of the mixing lengths, the fingering density (FD) as well as the total amount of the product (C). Furthermore, they validated the results with previous linear stability analysis and experimental studies.

The stability of the horizontal reactive interface under gravity field in the presence of transverse velocity was recently examined by Hejazi and Azaiez [94]. In this system, a bimolecular chemical reaction (BCR) $A + B \to C$ takes place between the displacing and the displaced reactants. A linear stability analysis was performed to determine the stability of the purely buoyancy driven flow as well as where the density contrast is combined with the viscosity one at the presence of transverse flow. It was reported that a chemical reaction may destabilize a buoyancy stable initial interface.

In a horizontal geometry Davison et al. [95] studied numerically the instability of paral-

lel reactants streams flow through porous media and react transversely at the centerline to produce a product that may increase or decrease the fluid viscosity. The authors observed that a reduction in fluid velocity and consequently a higher production rate as the product increases the fluid viscosity. Here, the increased production rate was attributed to the increases in the diffusion time as the velocity decreases. In contrast, higher fluid velocity and slower production rate were observed as the fluid viscosity decreases.

Reversible chemical reactions:

Chopard et al. [96] analyzed the properties of the interface of a reversible reactive process with initially separated reactants. In this study, the authors focused on determining the width of the reaction zone numerically. The authors reported that the dynamics of the reactive front can be described as a crossover between irreversible and reversible regimes at short and long times, respectively. Moreover, the existence of this crossover between short time "irreversible" and long time "reversible" regimes was confirmed by Sinder et al. [97]. In addition to the previous confirmation, the authors investigated analytically and numerically the reaction rate profile in an immobilized reaction zone and it was found that at long times, the reaction rate will encounter two maxima and may attain negative values in between.

Benes et al. [98] developed a numerical simulation of multi-component gas transport accompanied with reversible reactions in porous media. Here, the authors built the simulation based on the *dusty gas model* and the simulation results were validated against the analytical solution for a simple system. Furthermore, the simulation showed accurate results of the distribution of the chemical species in the porous media.

Gopich and Szabo [99] studied the long time behavior of the concentrations of the chemical species involved in a reversible reaction $A + B \rightleftharpoons C$ as they approach their equilibrium values. The authors used the Poisson representation, where the asymptotic of the relaxation

function was transformed into a FokkerPlanck or equivalent Langevin equation. The amplitude of the power law ($t^{-\frac{d}{2}}$ in d dimensions) decay of the concentrations to equilibrium for constant diffusion coefficients and concentrations of the reactants, was determined.

Mayer [100] illustrated the important role of reversibility on the efficiency of the underground water treatment process examined by Zhang [7].

Koza [101] developed a method for studying analytically and numerically the long-time properties of a reaction-diffusion system with a reversible reaction $A + B \rightleftharpoons C$. The study focused on the expansion of the concentrations of the chemical species as series in $\tau \equiv \frac{1}{t}$, which was useful in deriving some interesting conclusions analytically. From the observed results, the author concluded that systems with irreversible reactions can be studied by taking the limit where the reversibility coefficient approaches zero for reversible reactions.

Sinder et al., [102] investigated the reaction rate of a reversible reactive-diffusive process where the reactants are initially mixed with different diffusion coefficients. It was reported that the reactive-diffusive process for this case can be considered as a quasi-equilibrium process. Furthermore, the authors analyzed the dependence of the reaction rate on the initial distribution of the concentration of the reactants and it was observed that the number of the reaction zones varies with time and can be determined by the initial conditions.

In all previous studies on reversible reactive process, the spatial distributions of the chemical species were controlled by diffusion and none of the these studies has considered the effects of convection. Furthermore, the non-linear interactions between the different chemical species involved in the process have never been investigated. Since the injection of one of the reactants into the other is encountered in various applications and the frontal instability is a key

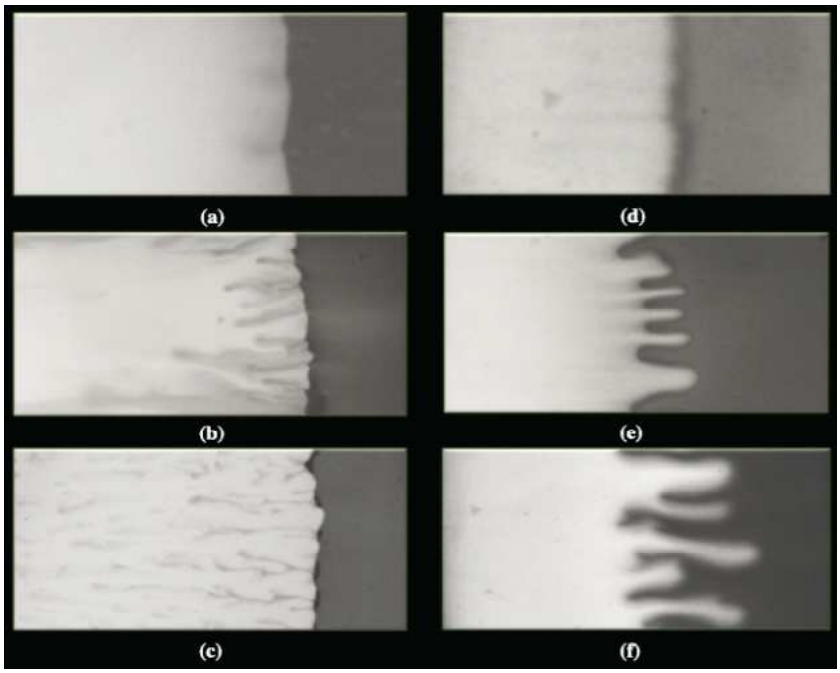

Figure 2.2: Reaction driven viscous fingering when a polymer solution displaces from left to right a less vsicous aqueous dyed solution. Left: polyacrylic acid (PAA) displacing NAOH solution with concentration (a) 0 M Stable front, (b) 0.01 M, (c) 0.06 M at $t = 225s$. Right: Salt sodium polyacrylate (SPA) displacing aqueous solutions of 60 wt% glycerol + HCl in concentration (a) 0 M, (b) 0.3 M, (c) 0.5 M at $t = 360s$. From Riolfo et al. [2].

factor to improve the efficiency of these processes, it is important to examine analytically and numerically the frontal instability of reversible reactive flows in porous media.

Chapter 3

Stability Analysis of Reversible Reactive flow displacements in Porous Media

[1] The effects of reversibility on the viscous fingering of miscible reactive flow displacement processes are examined. A model, where the viscosity mismatch between the reactants and the product triggers instability is adopted. The stability of the flow displacement is examined in the case of initial sharp front between the two reactants as well as when the reactants are given time to diffuse. In the case of a sharp front, a transformation allows to map the reversible case to that of the non-reversible one and an analysis of the effects of chemical reversibility is presented. In general, faster attenuation in the development and growth of instability is reported as the reversibility of the chemical reaction increases. However, it was found that reversibility can actually enhance the instability when a critical reversibility coefficient that depends on the mobility ratios of the chemical species, is exceeded. Different trends for the effects of reversibility were obtained for initially diffusing chemical reactants and the results are discussed in terms of the mobility ratios of the different species. It was found that the effects of stronger chemical reversibility on the stability of the flow are qualitatively similar to those induced by slower chemical reactions in non-reversible cases, however quantitative differences are reported and discussed.

3.1 Introduction

When a viscous fluid is used to displace another one of a larger viscosity, a frontal instability appears at the interface between the two fluids, which may affect dramatically the

[1]This chapter is the exact reproduction of the following submitted journal article:
H. Alhumade and J. Azaiez (2013). Stability Analysis of Reversible Reactive flow displacements in Porous Media. *Chemical Engineering Science*

overall efficiency of the displacement process. This instability may grow to form fingers that propagate in both upstream and downstream directions and is referred to as fingering or Saffman-Taylor instability [15, 3, 4]. The instability can be triggered by either viscosity mismatch and is referred to as viscous fingering or density mismatch, where it is known as the Rayleigh-Taylor instability.

Many experimental and theoretical studies have focused on the frontal instability of non-reactive displacement process, where hydrodynamic interactions between the fluids result in the viscous fingering instability. In these studies the effects of different parameters were examined and most of these studies were reviewed by [5] and [6]. However, the effects of these parameters on the fate and the efficiency of the displacement process may change when chemical reactions take place between the displacing and the displaced fluids, since chemical reactions can change the physical properties of the fluids as well as those of the porous medium.

Reactive flow displacements are encountered in processes such as underground water treatment, heavy oil recovery, chromatographic separation, polymer processing and fixed bed regeneration. In such applications involving chemical reactions, the efficiency and viability of the process strongly depend on the flow instability.

There is a number of experimental studies that deal with reactive flow displacements. The first such a study was carried out by [46], where the reaction leads to an interfacial tension decrease in a secondary oil recovery process. In 1995, Hornof and Baig studied flows in a secondary oil recovery process where the chemical reaction leads to a modification of the viscosity ratio at the reactive interface. Subsequent studies examined the role of stoichiometry [50], finger growth rate [51], precipitation [56] as well as that of elastic mi-cellar product de-

veloping at the interface between the reactants [55]. Similar experiments were conducted to study the effect of high [53] and moderate [54] Damköhler numbers on the fingering patterns in miscible displacements.

The dynamics of a bi-molecular $A + B \rightarrow C$ reactive front in horizontal reactive displacements were investigated by [88]. In their study, the viscosity of both reactants were assumed to be equal while the product (C) was more viscous than the reactants. In a series of studies, Hejazi and Azaiez investigated analytically [89] and numerically [90] the different scenarios of frontal instability in a horizontal miscible displacement process that involves a non-autocatalytic chemical reaction. The same authors also examined the displacement of a reactive slice of pollutant solution in a carrier solution [91]. Here, the dynamics of the flow as well as the rate of consumption of the pollutant were analyzed.

[59] studied experimentally the effects of changing the viscosity of the displacing less-viscous fluid by chemical reaction for miscible displacements in a radial Hele-Shaw cell. In a subsequent study, [93] conducted non-linear simulations in the same model considered by [90], but for an infinite Damköler number and characterized quantitatively the fingering patterns. In a more recent study, [2] analyzed experimentally reaction-driven viscous fingering in an initially stable horizontal displacement involving aqueous polymer solutions. Non-linear simulations were also performed to support the experimental results.

In all previous studies, the chemical reactions were assumed to be complete, which is not always the case in a reactive fluid displacement process. The reversibility of the reaction actually plays an important role in many phenomena studied in physics, chemistry, biology, and geology [104]. For example, in the in-situ soil remediation, promising results were reported by [7], where a reactive fluid was injected to remove the pollutant from the un-

derground water and the important role of reversibility on the efficiency of such a process was discussed by [100]. Reversibility is also an important factor in the study of the effects of the transport of reactive tracers on the dispersion coefficients at pore-level [105]. The first study on reactive-diffusive systems with reversible reaction was carried out by [96] who analyzed the properties of a reversible reactive front with initially separated reactants. It was reported that the dynamics of the reactive front can be described as a crossover between irreversible and reversible regimes at short and long times, respectively. Another study [97] confirmed the results obtained by [96] regarding the existence of a crossover between short time "irreversible" and long time "reversible" regimes. The authors also investigated analytically and numerically the reaction rate profile in an immobilized reaction zone and it was found that as $t \to \infty$, the reaction rate will encounter two maxima where it might attain negative values in between. In a more recent study, [102] investigated the reaction rate of a reversible reactive-diffusive process when the reactants are initially mixed with different diffusion coefficients. The authors reported that the reactive-diffusive process for this case can be considered as a quasi-equilibrium process. Furthermore, they analyzed the dependence of the reaction rate on the initial distribution of the reactants and it was reported that the number of reaction zones is determined by the initial conditions and varies with time.

In all previous studies of reversible reactive displacement processes, only the diffusive effects were considered. However, when the injection of one of the reactants is required, the convective term must be considered in addition to the diffusive one. In such a case, the displacement process is expected to be dominated by convection rather than diffusion. Therefore, it is important to conduct a full analysis of a reversible reactive-diffusive-convective flow displacement to understand the effects of reversibility on the flow dynamics as well as on the overall efficiency of the displacement process.

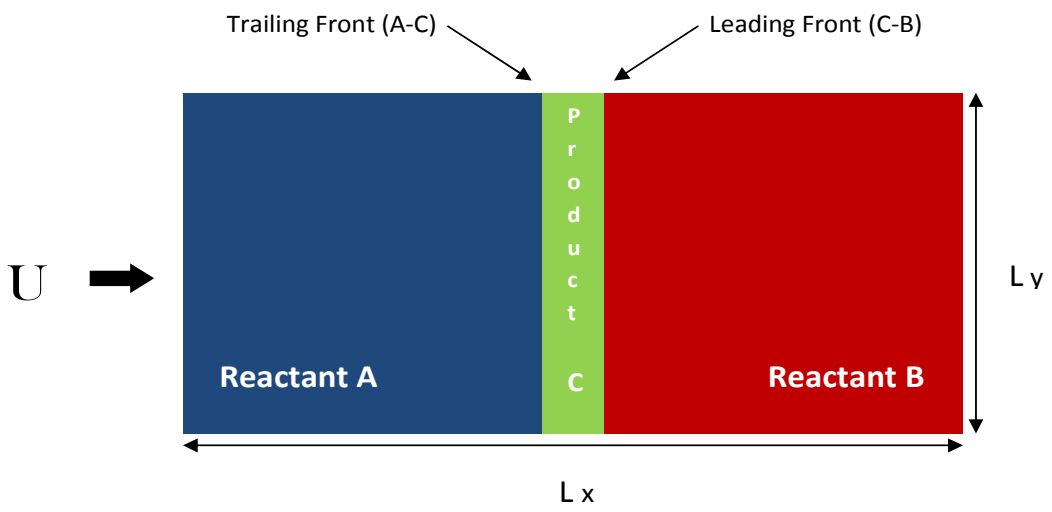

Figure 3.1: Schematic of a reactive front displacement process.

3.2 Mathematical model

3.2.1 Physical problem

In this study, miscible reactive flows in a rectilinear Hele-Shaw cell which is an analogous of a homogeneous porous medium, are examined. The cell is assumed to be initially filled with a miscible solution of reactant (B) with viscosity μ_B. A miscible solution of reactant (A) with viscosity μ_A is injected at a constant velocity U to displace fluid B as shown in Figure 3.1. It is assumed that both reactants (A) and (B) have an equal initial concentration, a_0. Furthermore, all fluids are assumed to be incompressible and Newtonian. In addition, an instantaneous reversible reaction takes place between the reactants as soon as they come in contact to generate a chemical product (C) with viscosity μ_C.

$$(A) + (B) \rightleftharpoons (C) \tag{3.1}$$

As time proceeds, more product accumulates at the interface between the two reactants. Figure 3.1 shows an idealized distribution of the two reactants (A) and (B) and the product (C).

3.2.2 Governing equations

The flow is governed by the equations for conservation of mass, momentum (Darcy's Equation) and the transport of the three chemical species.

$$\nabla.\mathbf{u} = 0 \tag{3.2}$$

$$\nabla p = -\frac{\mu}{\kappa}\mathbf{u} \tag{3.3}$$

$$\phi\frac{\partial A}{\partial t} + \mathbf{u}.\nabla A = \phi D_A \nabla^2 A - kAB + k_r C \tag{3.4}$$

$$\phi\frac{\partial B}{\partial t} + \mathbf{u}.\nabla B = \phi D_B \nabla^2 B - kAB + k_r C \tag{3.5}$$

$$\phi\frac{\partial C}{\partial t} + \mathbf{u}.\nabla C = \phi D_C \nabla^2 C + kAB - k_r C \tag{3.6}$$

In the above equations, the superficial velocity is denoted by $\mathbf{u} = u\hat{i} + v\hat{j}$ where $\hat{i}$ and $\hat{j}$ are the unit vectors along x and y, respectively. Furthermore, p represents the pressure, k the forward reaction constant, k_r the reverse reaction constant, ϕ the medium porosity, and μ is the ratio of the solution viscosity to the constant permeability of the porous medium, which will be simply referred to as viscosity. The concentrations of the two reactants and the product are denoted by A, B and C, respectively while D_A, D_B and D_C represent their corresponding diffusion coefficients. In the present study, it will be assumed that all species have the same diffusion coefficient, i.e. $D_A = D_B = D_C = D$. Furthermore, since the initial concentrations as well as the diffusion coefficients of all reactants are equal, the maximum concentration of the product (C) remains at the location of the initial interface between the reactants [106, 107].

Following [90], a Lagrangian reference frame moving with the injection velocity U is adopted. The equations are made non-dimensional using $\phi D/U$ and $D\phi^2/U^2$ as the reference length and time, respectively. Furthermore, the velocity, viscosity, pressure and concentrations are scaled using U, μ_A, $\mu_A D\phi$ and a_0, respectively. The resulting dimensionless equations are:

$$\nabla \cdot \mathbf{u} = 0, \tag{3.7}$$

$$\nabla p = -\mu(\mathbf{u} + \mathbf{i}), \tag{3.8}$$

$$\frac{\partial A}{\partial t} + \mathbf{u} \cdot \nabla A = \nabla^2 A - D_a AB + D_r C, \tag{3.9}$$

$$\frac{\partial B}{\partial t} + \mathbf{u} \cdot \nabla B = \nabla^2 B - D_a AB + D_r C, \tag{3.10}$$

$$\frac{\partial C}{\partial t} + \mathbf{u} \cdot \nabla C = \nabla^2 C + D_a AB - D_r C, \tag{3.11}$$

The Damköhler number $D_a = ka_0\phi D/U^2$ represents the ratio between the characteristic hydrodynamic time scale and the chemical time scale, while $D_r = k_r\phi D/U^2$ represents a reversible Damköhler number. Furthermore, for non-zero D_a, a parameter $\alpha = \frac{D_r}{D_a} = \frac{k_r}{ka_0}$ which involves the ratio of both reaction constants k and k_r is defined and will be referred to as the reversibility coefficient. It should be noted that α is actually the inverse of the equilibrium constant of the reaction K_c in dimensionless form. The reversibility coefficient varies between zero and one, with the limiting values $\alpha = 0$ and $\alpha = 1$ corresponding to non-reversible and completely reversible reactions, respectively.

Following previous studies [90], a concentration dependent viscosity profile is adopted to complete the model:

$$\mu = \mathrm{e}^{R_b B + R_c C} \tag{3.12}$$

In the above equation R_b and R_c are the log mobility ratios between the viscosity of (B) to (A) and (C) to (A), respectively.

$$R_b = \ln(\frac{\mu_B}{\mu_A}) \qquad and \qquad R_c = \ln(\frac{\mu_C}{\mu_A}) \tag{3.13}$$

3.2.3 Base-State profiles

In the absence of any disturbances, the system admits a base-state solution corresponding to $u_0 = v_0 = 0$, where the base-state concentrations $A_0(x,t)$, $B_0(x,t)$ and $C_0(x,t)$ and viscosity $\mu_0(x,t)$ are solutions of the following equations:

$$\frac{\partial A_0}{\partial t} = \frac{\partial^2 A_0}{\partial x^2} - D_a A_0 B_0 + D_r C_0, \tag{3.14}$$

$$\frac{\partial B_0}{\partial t} = \frac{\partial^2 B_0}{\partial x^2} - D_a A_0 B_0 + D_r C_0, \tag{3.15}$$

$$\frac{\partial C_0}{\partial t} = \frac{\partial^2 C_0}{\partial x^2} + D_a A_0 B_0 - D_r C_0, \tag{3.16}$$

$$\mu_0(x,t) = \mathrm{e}^{R_b B_0(x,t) + R_c C_0(x,t)}. \tag{3.17}$$

A linear combination of the above equations leads to:

$$\frac{\partial (A_0 + B_0 + 2C_0)}{\partial t} - \frac{\partial^2 (A_0 + B_0 + 2C_0)}{\partial x^2} = 0. \tag{3.18}$$

The above set of base-state equations has no exact analytical solution. However, given the initial and boundary conditions, one can show that the base state concentration satisfies $A_0 + B_0 + 2C_0 = 1$. Furthermore, by analyzing the viscosity profiles, it is possible to show that the reactive system will be always stable when $R_b \leq \frac{R_c}{2} \leq 0$, and that the case $R_b = R_c$ reduces to the non-reactive flow [89]. Therefore, the effects of reversibility on these special cases will not be discussed.

Before discussing the results of the stability analysis, it is worth examining the influence of the chemical reversibility on the base-state viscosity profile. Figure 3.2 depicts the logarithm of the viscosity as a function of the self-similar variable $\eta = \frac{x}{2\sqrt{t}}$. These profiles were obtained by solving numerically equations (3.14) - (3.16) in conjunction with equation (3.17) and are presented for asymptotically long times when the product (C) reaches its maximum concentration at the initial interface ($\eta = 0$). The code has been checked for numerical convergence and was validated by reproducing the results for non-reversible reactions for long time asymptotic derived by [106] and presented by [89]. From the figure, it can be seen that the viscosity exhibits different profiles depending on whether $\eta > 0$ or $\eta < 0$ with either a positive or negative gradient that corresponds to an unstable or stable front, respectively. Therefore following [89], one zone between (A) and (C) and referred to as the trailing zone, and another between (C) and (B) and referred to as the leading zone, can be defined (see

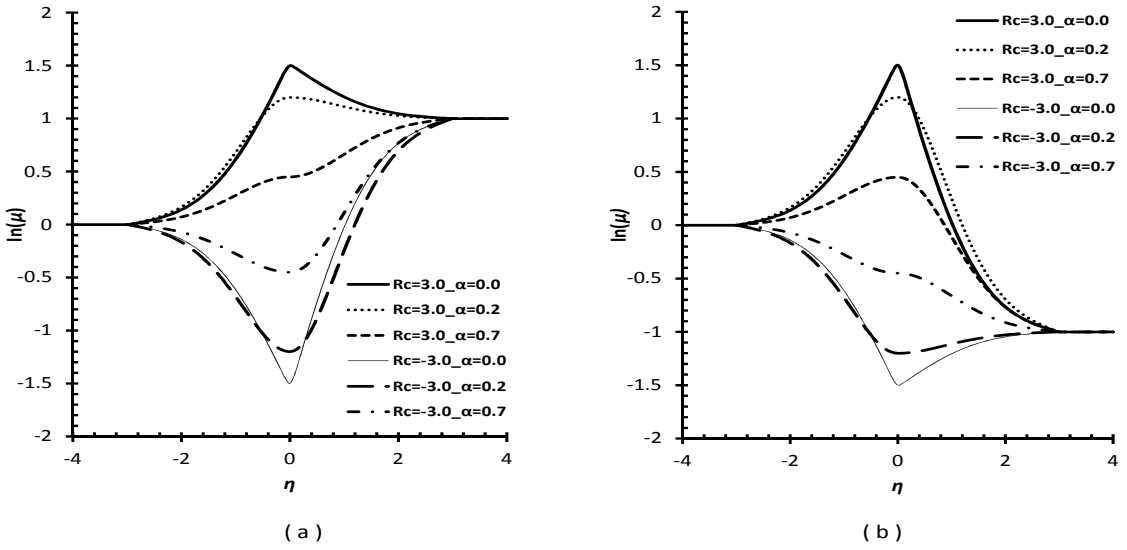

Figure 3.2: Logarithm of the viscosity profiles as a function of the self-similar η for asymptotic large time ($t \to \infty$) at (a) $R_b = 1, R_c = 3, -3$, (b) $R_b = -1, R_c = 3, -3$ for different α.

Figure 3.1). The mobility ratios at these trailing and leading zones will be referred to as:

$$R_{AC} = \ln(\frac{\mu_C(C = 0.5)}{\mu_A}) = \frac{R_c}{2} \qquad and \qquad R_{CB} = \ln(\frac{\mu_B}{\mu_C(C = 0.5)}) = R_b - \frac{R_c}{2} \quad (3.19)$$

It can be seen from Figure 3.2 that for the different combinations of mobility ratios, the reversibility coefficient α affects the viscosity profiles and can actually change them from non-monotonic to monotonic. As we shall see later, this will result in changes of the stability characteristics.

3.3 Linear stability analysis

3.3.1 Linearized equations

In this section, in order to conduct the stability analysis, all dependent variables are expressed as the sum of the base-state solution and a perturbation :

$$\begin{aligned}
A(x,y,t) &= A_0(x,t) + A'(x,y,t),\\
B(x,y,t) &= B_0(x,t) + B'(x,y,t),\\
C(x,y,t) &= C_0(x,t) + C'(x,y,t),\\
p(x,y,t) &= p_0(x,t) + p'(x,y,t),\\
\mu(x,y,t) &= \mu_0(x,t) + \mu'(x,y,t),\\
u(x,y,t) &= u'(x,y,t),\\
v(x,y,t) &= v'(x,y,t),
\end{aligned} \tag{3.20}$$

The resulting linearized equations for the perturbation terms, which are indicated with prime, are:

$$\frac{\partial u'}{\partial x} + \frac{\partial v'}{\partial y} = 0, \tag{3.21}$$

$$\frac{\partial P'}{\partial x} = -\mu_0 u' - \mu'; \frac{\partial P'}{\partial y} = -\mu_0 v', \tag{3.22}$$

$$\frac{\partial A'}{\partial t} + u'\frac{\partial A_0}{\partial x} = \left(\frac{\partial^2}{\partial x^2} + \frac{\partial^2}{\partial y^2}\right) A' - D_a(A'B_0 + A_0B') + D_rC', \tag{3.23}$$

$$\frac{\partial B'}{\partial t} + u'\frac{\partial B_0}{\partial x} = \left(\frac{\partial^2}{\partial x^2} + \frac{\partial^2}{\partial y^2}\right) B' - D_a(A'B_0 + A_0B') + D_rC', \tag{3.24}$$

$$\frac{\partial C'}{\partial t} + u'\frac{\partial C_0}{\partial x} = \left(\frac{\partial^2}{\partial x^2} + \frac{\partial^2}{\partial y^2}\right) C' + D_a(A'B_0 + A_0B') - D_rC', \tag{3.25}$$

$$\mu' = \mu_0(R_bB' + R_cC'). \tag{3.26}$$

The following relation between the perturbation of the reactants and the product is used to eliminate the product's concentration C':

$$A' + B' + 2C' = 0. \tag{3.27}$$

Furthermore, the transverse velocity and pressure disturbances are eliminated by applying the curl to Darcy's equation and using the continuity equation:

$$\left(\frac{\partial^2}{\partial x^2}+\frac{\partial^2}{\partial y^2}\right)u'+\frac{1}{\mu_0}\frac{\partial \mu_0}{\partial x}\frac{\partial u'}{\partial x}=(\frac{R_c}{2}-R_b)\frac{\partial^2 B'}{\partial y^2}+\frac{R_c}{2}\frac{\partial^2 A'}{\partial y^2}. \tag{3.28}$$

As a result, the stability can be analyzed in terms of the disturbances A', B' and u'.

3.3.2 Quasi-Steady-State approximation

The coefficients of the above equations (3.23) - (3.25) and (3.28) are functions of one of the dimensions (x) and time, therefore the quasi-steady-state approximation ($QSSA$) where the base-state solution is frozen at a certain time t_0 was adopted to solve the problem [24]. The disturbances are expanded in terms of Fourier components in order to determine the stability of the frozen system.

$$(u', A', B') = (\phi, \psi_A, \psi_B)\mathrm{e}^{\mathrm{i}ky+\sigma(t_0)t}, \tag{3.29}$$

In the above equations, ϕ, ψ_A and ψ_B are functions only of (x), while $\sigma(t_0)$ is the disturbance's growth rate at wave-number k.

Applying the QSSA to equations (3.23), (3.24) and (3.28) leads to:

$$[\sigma(t_0)-\frac{d^2}{dx^2}+k^2+D_aB_0+\frac{D_r}{2}]\psi_A=-\frac{\partial A_0}{\partial x}\phi-(D_aA_0+\frac{D_r}{2})\psi_B, \tag{3.30}$$

$$[\sigma(t_0)-\frac{d^2}{dx^2}+k^2+D_aA_0+\frac{D_r}{2}]\psi_B=-\frac{\partial B_0}{\partial x}\phi-(D_aB_0+\frac{D_r}{2})\psi_A, \tag{3.31}$$

$$[\frac{d^2}{dx^2}+([R_b-\frac{R_c}{2}]\frac{\partial B_0}{\partial x}-\frac{R_c}{2}\frac{\partial A_0}{\partial x})\frac{d}{dx}-k^2]\phi=k^2[(R_b-\frac{R_c}{2})\psi_B-\frac{R_c}{2}\psi_A]. \tag{3.32}$$

In what follows the above system of eigenvalue differential equations is solved analytically and numerically to determine the growth rate σ at $t_0=0$ and $t_0>0$, respectively.

3.4 Results

In this section the instability characteristics are obtained and the effects of the chemical reaction reversibility on the flow instability are presented. Results are first obtained in the

case of an initial concentration step profile ($t_0 = 0$) and then for a diffuse initial profile ($t_0 > 0$).

3.4.1 Dispersion curves at $t_0 = 0$

Characteristics equation

In this section, an analytical solution for the growth rate will be derived at $t_0 = 0$. The Heavy-side step function is used to represent the concentrations of reactants A and B.

For $x < 0$: (A_0=1, B_0=0), Equations (3.30)-(3.32) become:

$$[\sigma - \frac{d^2}{dx^2} + k^2 + \frac{D_r}{2}]\psi_A = -(D_a + \frac{D_r}{2})\psi_B, \tag{3.33}$$

$$[\sigma - \frac{d^2}{dx^2} + k^2 + D_a + \frac{D_r}{2}]\psi_B = -\frac{D_r}{2}\psi_A, \tag{3.34}$$

$$[\frac{d^2}{dx} - k^2]\phi = k^2([R_b - \frac{R_c}{2}]\psi_B - \frac{R_c}{2}\psi_A), \tag{3.35}$$

The solutions of the above equations are:

$$\psi_A^- = A^- exp(\gamma_1 x) + B^- exp(\gamma_0 x), \tag{3.36}$$

$$\psi_B^- = -\frac{D_r}{2D_a + Dr} A^- exp(\gamma_1 x) + B^- exp(\gamma_0 x), \tag{3.37}$$

$$\phi^- = G^- exp(kx) - \frac{k^2(R_b D_r + R_c D_a)}{(2D_a + D_r)({\gamma_1}^2 - k^2)} A^- exp(\gamma_1 x) + \frac{k^2(R_b - R_c)}{{\gamma_0}^2 - k^2} B^- exp(\gamma_0 x), \tag{3.38}$$

Where

$$\gamma_0 = \sqrt{\sigma + k^2 + D_a + D_r}, \qquad \gamma_1 = \sqrt{\sigma + k^2} \tag{3.39}$$

For $x > 0$: (A_0=0, B_0=1), equations (3.30)-(3.32) simplify to:

$$[\sigma(t_0) - \frac{d^2}{dx^2} + k^2 + \frac{D_r}{2} + D_a]\psi_A = -(\frac{D_r}{2})\psi_B, \tag{3.40}$$

$$[\sigma(t_0) - \frac{d^2}{dx^2} + k^2 + \frac{D_r}{2}]\psi_B = -[D_a + \frac{D_r}{2}]\psi_A, \tag{3.41}$$

$$[\frac{d^2}{dx^2} - k^2]\phi = k^2([R_b - \frac{R_c}{2}]\psi_B - \frac{R_c}{2}\psi_A), \tag{3.42}$$

The solutions of the above equations are:

$$\psi_A^+ = A^+ exp(-\gamma_0 x) - \frac{D_r}{2D_a + Dr} B^+ exp(-\gamma_1 x), \tag{3.43}$$

$$\psi_B^+ = A^+ exp(-\gamma_0 x) + B^+ exp(-\gamma_1 x), \tag{3.44}$$

$$\phi^+ = G^+ exp(-kx) + \frac{k^2(R_b - R_c)}{{\gamma_0}^2 - k^2} A^+ exp(-\gamma_0 x) + \frac{k^2(R_b(2D_a + D_r) - R_c D_a)}{({\gamma_1}^2 - k^2)(2D_a + D_r)} B^+ exp(-\gamma_1 x), \tag{3.45}$$

Where A^+, B^+, G^+, A^-, B^- and G^- are constant coefficients and the following continuity conditions are used at x=0, to evaluate these constants.

$$\begin{aligned} &[\mu_0 \frac{d\phi}{dx}]_{0^-}^{0^+} = 0, \qquad [\phi]_{0^-}^{0^+} = 0, \\ &[\frac{d\psi_B}{dx}]_{0^-}^{0^+} = \phi(0), \qquad [\psi_A]_{0^-}^{0^+} = 0, \\ &[\frac{d\psi_A}{dx}]_{0^-}^{0^+} = -\phi(0), \qquad [\psi_B]_{0^-}^{0^+} = 0, \end{aligned} \tag{3.46}$$

The following relation between the growth rate σ and disturbance wave-number k is obtained by requiring the determinant of the coefficient matrix to be zero for a non-trivial solution:

$$\begin{aligned} &[-2k\gamma_1(1 + \frac{D_r}{2D_a + D_r}) - \frac{k^2(R_b - R_c)}{{\gamma_0}^2 - k^2}(\gamma_0 - k)(1 - \frac{D_r}{2D_a + D_r}) \\ &+ 2\frac{k^2(R_b(2D_a + D_r) - R_c D_a)}{({\gamma_1}^2 - k^2)(2D_a + D_r)}(\gamma_1 - k)](1 + e^{R_b}) \\ &+ 2\frac{k^2(R_b - R_c)}{{\gamma_0}^2 - k^2}(\gamma_0 - k)(1 - \frac{D_r}{2D_a + D_r}) + \frac{4D_a(R_c - R_b)}{(2D_a + D_r)({\gamma_1}^2 - k^2)} k^2(\gamma_1 - k) = 0, \end{aligned} \tag{3.47}$$

The above characteristic equation can be further simplified to:

$$(e^{R_b} + 1)(\gamma_0 + k)(D_a + D_r)[R_b k - 2\gamma_1(k + \gamma_1)] + kD_a(e^{R_b} - 1)(R_c - R_b)(\gamma_1 - \gamma_0) = 0. \tag{3.48}$$

The values of the growth rate, which can be complex, determine the stability of the system. If Re(σ) is always negative for all values of k, then the system will be stable. On the other hand, the system will be unstable if Re(σ) is positive for some values of k. The effects of the flow parameters on the stability of the system can be examined by plotting the Re(σ)

against the wave-number k for various values of those parameters. The dispersion curves obtained by plotting $\mathrm{Re}(\sigma)$ against the wave-number k have been classified into three types by Cross and Hohenberg [108]. The first type of dispersion curves (Type I) cross the line $\mathrm{Re}(\sigma) = 0$ at two different values of k along with $k = 0$. In this type of dispersion curves, the long wave instabilities are absent and the fingers maintain a finite wave-number in time [109]. The second type of dispersion curves (Type II), cross the line $\mathrm{Re}(\sigma)$=0 at one value of k along with $k = 0$, where the growth rate is positive between the two values of k. This kind of dispersion curves may include long-wave instabilities. In the third type of dispersion curves (Type III) $\sigma \neq 0$ for $k = 0$, which does not satisfy (3.48).

First, it should be noted that in the special case of a non-reversible reaction ($D_r = 0$), equation (3.48) reduces to the one reported by Hejazi et al., [89]. Furthermore, in the absence of chemical reaction ($D_a = 0$), equation (3.48) results in the classical dispersion equation obtained by Tan and Homsy [24] for miscible viscous fingering in non-reactive systems.

$$\sigma = \frac{k}{2}[R_b - k - \sqrt{k(k + 2R_b)}] \tag{3.49}$$

Equation (3.49) corresponds to a type II dispersion curves since $\sigma > 0$ for $0 < k < \frac{R_b}{4}$.

It is important at this stage to determine if it is possible to find a relationship that allows to predict the stability nature of the reversible-reaction flow from that of the non-reversible one when $t_0 = 0$. A close examination of equation (3.48) reveals that the characteristics of the reversible case with parameters $[R_b, R_c, D_a, \alpha]$ are the same as those of a non-reversible reactive flow displacement with the corresponding parameters $[R'_b = R_b, R'_c = \frac{R_c+\alpha R_b}{1+\alpha} = R_b + \frac{R_c-R_b}{1+\alpha}, D'_a = D_a(1 + \alpha)]$. This indicates that the corresponding non-reversible flow will have a different Damköhler number and mobility ratio R_c and implies that stronger reversibility is equivalent to an increase of D_a in conjunction with a change in R_c which would increase with α for flows where $R_b > R_c$ and decrease for $R_b < R_c$. However, it is

not easy to infer the effects of reversibility from this transformation, since the stability of the non-reversible system depends on both the Damköhler number and the mobility ratios R_b and R_c. In what follows the effects of the reversibility coefficient α are examined using equation (3.48).

Long-wave instability

Before proceeding with the numerical solution of the algebraic equation (3.48), some general information can be obtained by examining few special limits. In particular, it is interesting to examine the long-wave instability of the flow when $k \longrightarrow 0$. A series expansion resulted in a first order approximation of the growth rate as $\sigma = \Lambda k + o(k)$, where

$$\Lambda = \frac{e^{R_b}[R_b(2+\alpha) - R_c] + R_c + \alpha R_b}{2(1+\alpha)(e^{R_b}+1)}. \tag{3.50}$$

It is worth noting that the above expansion can be obtained from the expression reported by [89] for a non-reversible case using the transformation mentioned previously, and that it reduces to that expression when $\alpha = 0$. Furthermore, unlike the non-reversible case where the above term does not depend on the reaction constants, the first order term for the reversible case does depend on the reaction constants through the reversibility coefficient $\alpha = \frac{D_r}{D_a}$.

Neutral stability in the long-wave regime is defined by imposing $\Lambda = 0$, which from equation (3.50) leads to $R_c = R_L$, where:

$$R_L = \frac{[e^{R_b}(2+\alpha) + \alpha]R_b}{(e^{R_b}-1)}. \tag{3.51}$$

Note that R_L is always positive for any value of R_b. Long wave instability will take place if $\Lambda > 0$, which requires that

$$e^{R_b}[R_b(2+\alpha) - R_c] + R_c + \alpha R_b > 0. \tag{3.52}$$

The above condition will require $R_c < R_L$ if the initial reactive front is unstable, *i.e.* $R_b > 0$, and $R_c > R_L$ otherwise. The critical value of α for long wave instability is:

$$\alpha_c = \frac{(R_c - 2R_b)e^{R_b} - R_c}{R_b(e^{R_b} + 1)} \tag{3.53}$$

Note that α_c will be positive if $R_c \geq \frac{2R_b e^{R_b}}{(e^{R_b}-1)} = 2R_b + \frac{2R_b}{(e^{R_b}-1)}$ and is less than one only if $R_c \leq \frac{R_b(3e^{R_b}+1)}{(e^{R_b}-1)} = 3R_b + \frac{4R_b}{(e^{R_b}-1)}$.

Few general conclusions can be drawn from the above results. First, since for any given R_b, R_L is a monotonically increasing function of α, the range of the parameter R_c for which long wave instability is expected, will expand (contract) with α for positive (negative) values of R_b. As a result, for any given values of R_b and R_c, the stability to long wave disturbances can be changed as the reversibility factor α increases. Furthermore, one can easily show that $R_L > 2R_b$ for any value of R_b and α. Therefore, for an initially unstable reactive front ($R_b > 0$), if the mobility ratios are such that at least the leading $(C - B)$ front is unstable, *i.e.* $R_b > R_c/2$; then the condition for long wave instability $R_c < R_L$ is automatically satisfied, regardless of the value of α. Hence the flow will be unstable for any value of the reversibility coefficient α and the instability characteristics will be of type II. On the other hand if the leading front is stable, *i.e.* $R_b < R_c/2$ then the flow may be stable or unstable to long wave disturbances since, depending on the value of α, the condition $R_c < R_L$ may or may not be satisfied. In particular, the flow will be unstable to long-waves disturbances if $\alpha > \alpha_c$ and stable otherwise. Note that since $\alpha \leq 1$, the condition $\alpha > \alpha_c$ is possible only if $\alpha_c < 1$ or equivalently if $R_c < \frac{R_b(3e^{R_b}+1)}{(e^{R_b}-1)}$.

Different conclusions are obtained when the initial reactive front is stable, $(R_b < 0)$. In this case, the flow will be always stable to long wave disturbances if $R_c < R_L$ while for $R_c > R_L > 0$, the flow is unstable and the characteristics will be of type II.

Cut-off wave-numbers

It is possible to determine the wave-numbers at which the growth rate is zero. These wave-numbers will include the cut-off wave-numbers beyond which the flow is stable. These wave-numbers can be determined by requiring σ in (3.48) to be identically zero. In addition to the trivial solution $k = 0$, these wave-numbers are solution of the following equation:

$$\Gamma(k) = (\sqrt{k^2 + D_a + D_r} + k)^2(R_b - 4k) - \frac{D_a(R_c - R_b)(e^{R_b} - 1)}{(e^{R_b} + 1)} = 0 \tag{3.54}$$

Few general conclusions can be actually drawn without solving equation (3.54). First, it can be shown that for $R_c \leq R_b < 0$, the above equation has no positive solution and hence the flow is stable for all wave-numbers. Furthermore, by inspecting the sign of the two terms in equation (3.54), it is possible to determine the upper and lower bounds of the cut-off wave-numbers. First, it should be noted that the cut-off wave-number of the non-reactive flow is $k_{cut-nr} = \frac{R_b}{4}$. For a reactive flow with an initially unstable front ($R_b > 0$) and where the chemical product is less viscous than the displaced reactant (B); *i.e.* $R_c < R_b$, the cut-off wave-number will be always larger than that of the non-reactive flow; $\frac{R_b}{4}$. On the other hand, if the product is more viscous than the reactant (B), then the cut-off wave-number will be smaller than that of the non-reactive system. In all these cases, the cut-off wave-numbers and hence the range of unstable wave-numbers depend on the reversibility coefficient α. Furthermore noting that:

$$\Gamma(+\infty) = -\infty, \Gamma(0) = D_a[(1+\alpha)R_b - \frac{(R_c - R_b)(e^{R_b} - 1)}{(e^{R_b} + 1)}] = D_a(R_L - R_c)\frac{(e^{R_b} - 1)}{(e^{R_b} + 1)} \tag{3.55}$$

It is possible to show that if $\Gamma(0)$ is positive ($R_b > 0$ and $R_c < R_L$ or $R_b < 0$ and $R_c > R_L$), then equation (3.54) has one root in $[0, +\infty]$ and the characteristics are of type II. On the other hand, if $\Gamma(0)$ is negative, then equation (3.54) will either have no positive roots (stable flow) or two roots (type I characteristics). In particular, one can show that for $R_b \leq 0$, $\Gamma(k)$ is a monotonically decreasing function (see equation (3.56)) and therefore, if $\Gamma(0)$ is

negative, the flow will be stable.

$$\Gamma'(k) = 2(\sqrt{k^2 + D_a + D_r} + k)^2[\frac{R_b - 4k}{\sqrt{k^2 + D_a + D_r}} - 2] \tag{3.56}$$

Furthermore, for $R_b > 0$ and $R_c > R_L$, it is possible to show that the flow can actually be unstable (type I characteristics) for $R_c < R_s$ with a critical wavenumber for the onset of such instability obtained by requiring $\Gamma(k_c) = \Gamma'(k_c) = 0$, leading to:

$$k_c = \frac{R_b}{3} - \frac{\sqrt{R_b^2 + 12(D_a + D_r)}}{6} \tag{3.57}$$

$$R_s = R_b + \frac{[R_b^3 + 18R_b(D_a + D_r) + (R_b^2 + 12(D_a + D_r))^{3/2}]}{54} \frac{(e^{R_b} + 1)}{D_a(e^{R_b} - 1)} \tag{3.58}$$

The above expressions which depend on both D_a and D_r, reduce to the ones reported in [89] for a non-reversible reaction. The previous results confirm and extend the conclusions obtained from the long-wave analysis.

Parametric analysis

In this section, the effects of the reversibility coefficient on the instability of the system are examined. The results which are based on numerical solutions of the algebraic equation (3.48) will give a general picture of the instability that goes beyond the previous analysis restricted to special limit cases. In particular, the effect of reversibility on the stability will be examined. The discussion will be presented for cases where one of the leading or trailing fronts is unstable followed by flows where the viscosity distribution is such that both leading and trailing fronts are expected to be unstable.

Unstable trailing or leading front:

Figure 3.3 depicts instability characteristics for a system where the initial reactive front is unstable ($R_b > 0$) with $R_b = 1$ and $R_c = -3$, which corresponds to a stable trailing ($R_c/2 = -1.5$) and an unstable leading ($R_b - R_c/2 = 2.5$) fronts. The non-reversible case

($\alpha = 0$) and the non-reactive one ($D_a = 0$) are shown with solid lines. For this choice of mobility ratios $\alpha_c = -2.85$ and the instability characteristics as expected are of type II. The flow is found to be unstable for all values of the reversibility coefficient and the instability decreases as reversibility increases. Note that the attenuating effects of chemical reversibility are more pronounced for large Damköhler numbers, and that a completely reversible reaction ($\alpha = 1$) is more unstable than the non-reactive flow.

A scenario with an initial unstable front but where the trailing front is unstable while the leading one is stable has also been examined ($R_b = 1, R_c = 2$). Here, the flow is also unstable at large wavelengths for all values of α (Type II curves). It is however interesting to note that in this case, reversibility actually makes the flow more unstable, leading to larger maximum growth rates as well as a wider spectrum of unstable wave-numbers (Figure 3.4-a). A similar scenario with an unstable trailing front and a stable leading one was also considered but with a different set of mobility ratios ($R_b = 5, R_c = 12$). This example that results in a value of $\alpha_c = 0.38$, illustrates well the case where an increase of α changes the characteristics from type I to type II (Figure 3.4-b). Here too, stronger reversibility leads to a more unstable flow. Note that in both cases, flows with a fully reversible reaction are always less unstable than the non-reactive case.

Similar trends were obtained in the case of an initially stable front ($R_b < 0$). Figure 3.5 depicts instability characteristics for $R_b = -1$ and $R_c = 3$, which corresponds to unstable trailing ($R_c/2 = 1.5$) and stable leading ($R_b - R_c/2 = -2.5$) fronts. The instability decreases as reversibility increases and in fact, the system is expected to shift from an unstable to a stable regime for long wave-numbers when α reaches or exceeds the critical value for instability as obtained from equation (3.53), in this case $\alpha_c = 0.85$.

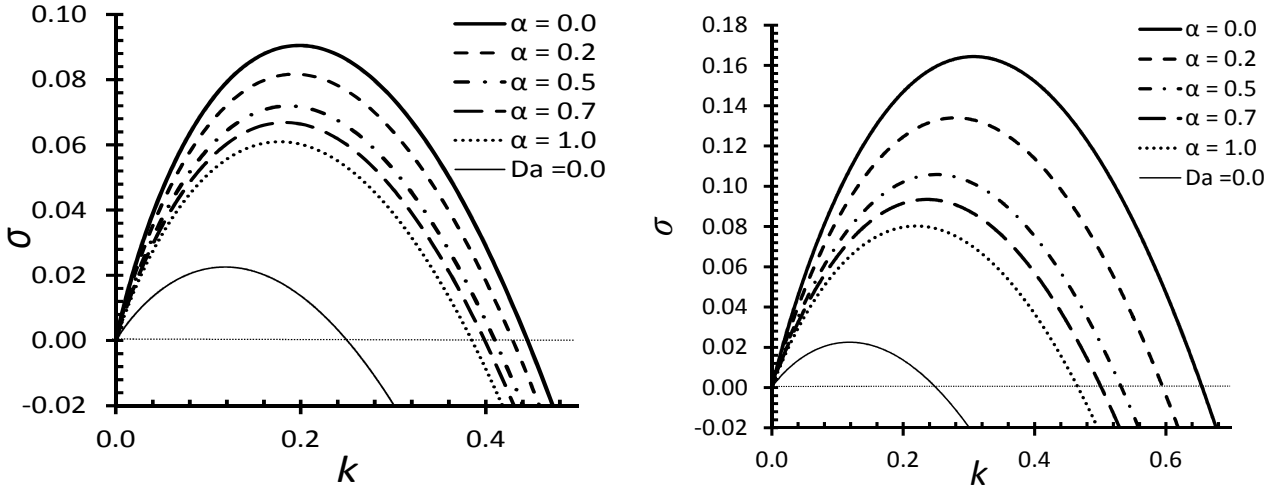

(a) (b)

Figure 3.3: Dispersion Curves at $t_0 = 0$ showing the influence of D_r at (a) $D_a = 1.0$, (b) $D_a = 100.0$ for $R_b = 1$ and $R_c = -3$.

The above results show that if the initial front is stable ($R_b < 0$), then reversibility tends to attenuate any instability that may develop in the flow. On the other hand, if the initial front is unstable ($R_b > 0$) and the distribution of the viscosities is such that the leading front is stable while the trailing one is unstable, then reversibility makes the flow more unstable.

Unstable trailing and leading fronts:

The case where both trailing and leading fronts are unstable, which can be achieved only when the initial front is unstable ($R_b > R_c/2 > 0$), is now considered.

Figure 3.6-a shows instability characteristics in the case $R_b = 2$ and $R_c = 3$ which lead to positive values of $R_{AC} = 1.5$ and $R_{CB} = 0.5$. It is interesting that in this case reversibility actually enhances the flow instability. Indeed both the maximum growth rate and the spectrum of unstable wave-numbers are increased with increasing α. However, it was found that reversibility is not always in favour of the growth of instability when both the trailing and the leading fronts are unstable. To illustrate this, another example was considered with a

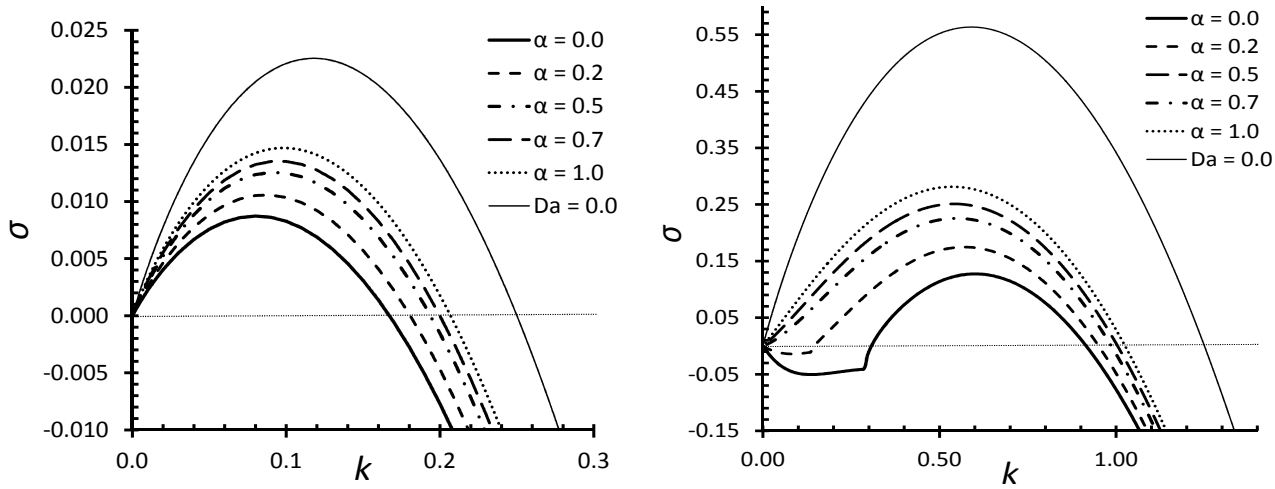

(a) (b)

Figure 3.4: Dispersion Curves at $t_0 = 0$ showing the influence of D_r at $D_a = 1.0$ for (a) $R_b = 1$ and $R_c = 2$, (b) $R_b = 5$ and $R_c = 12$.

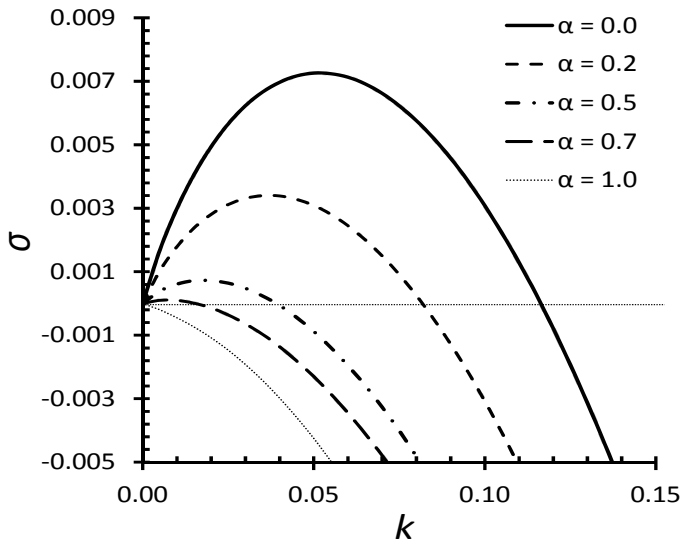

Figure 3.5: Dispersion Curves at $t_0 = 0$ showing the influence of D_r at $D_a = 1.0$ for $R_b = -1$ and $R_c = 3$.

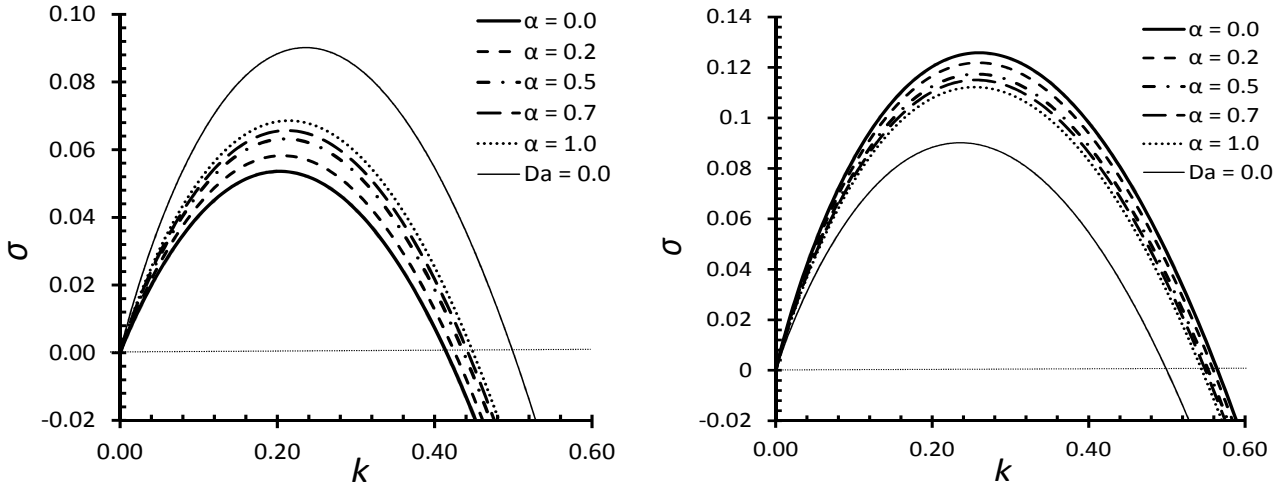

(a) (b)

Figure 3.6: Dispersion Curves at $t_0 = 0$ showing the influence of D_r at $D_a = 1.0$ for (a) $R_b = 2$ and $R_c = 3$, (b) $R_b = 2$ and $R_c = 1$.

different set of mobility ratios $R_b = 2$ and $R_c = 1$, which leads to $R_{AC} = 0.5$ and $R_{CB} = 1.5$. For this particular choice of mobility ratios, reversibility actually attenuates the instability as shown in figure 3.6-b.

These different effects of reversibility could have actually been anticipated from the previous analytical discussion. Indeed, in the case $R_b > R_c/2 > 0$, the flow is expected to be unstable to long wave disturbances and the characteristics to be of Type II. Furthermore the parameter Λ in equation (3.50) is positive and its derivative with respect to the reversibility coefficient α is:

$$\frac{\partial \Lambda}{\partial \alpha} = \frac{R_c - R_b}{2(1+\alpha)^2} \frac{(e^{R_b} - 1)}{(e^{R_b} + 1)}. \tag{3.59}$$

Clearly, the slope is positive if $R_c > R_b$ and negative otherwise. This implies that the flow will be more unstable with increasing α if $R_c > R_b$ and less unstable if $R_c < R_b$. Noting that $R_c - R_b = R_{AC} - R_{CB}$, the previous results show that reversibility attenuates the flow instability if $R_b < 0$ while for $R_b > 0$ it will enhance the instability if the trailing front is more unstable than the leading one *i.e.* $R_c > R_b$ and will reduce it otherwise.

3.4.2 Instability at later times ($t_0 > 0$)

In the previous section, the stability of the system was examined at $t_0 = 0$. However, the initial front is typically diffuse and the chemical reaction will change the base state as time proceeds. In this section, the development of the instability is examined by solving numerically the eigenvalue problem described by equations (3.30)-(3.32) using base-state profiles obtained from the numerical solution of equations (3.14)-(3.16). A finite difference method allowed to transform the eigenvalue differential problem into a generalized eigenvalue problem. The general real matrix of the eigenvalue problem was converted to an upper Hessenberg form to obtain the eigenvalues and eigenfunctions. The computational domain was chosen wide enough to capture all eigenfunctions and the code was validated by comparing the results at $D_r = 0$ to those presented by [89] for non-reversible reactions. The effects of reversibility on the instability will be illustrated for all possible scenarios in cases where the chemical reaction is complete ($\alpha = 0$) or reversible ($\alpha \neq 0$).

It was found that for cases where the initial front is stable ($R_b < 0$) and those where the initial front is unstable with $R_b > R_c$, the effects of reversibility on the instability at $t_0 > 0$ are similar to what was observed for $t_0 = 0$ where reversibility attenuates the instability. In addition, the strength of the attenuating effects were found to depend on t_0 and α. For brevity and following [89], the effects are analyzed in terms of the maximum growth rate. In all figures, the non-reversible case ($\alpha = 0$) and the non-reactive one ($D_a = 0$) are shown with thick and thin solid lines, respectively. The fully reversible reaction flow is shown with thin dotted lines and a result for a non-reversible reaction with a small Damköhler number ($D_a = 0.01$) is included for the purpose of the discussion.

Figure 3.7-a shows the variations of the maximum growth rate with t_0 in the case $R_b = -1, R_c = 3$. Results for $D_a = 0$ are not shown since the non-reactive flow is stable. The

variation with time is non-monotonic and in this case, the maximum growth rates decreases monotonically with increasing α. Note that for large times t_0, all curves of the non-reversible reaction merge together regardless of the value of D_a while those corresponding to different reversible coefficients α are still distinct.

Results for a flow displacement with $R_b = 1, R_c = 2$ which corresponds to an unstable trailing and a neutrally stable leading fronts, are depicted in figure 3.7-b. For short times, the non-reversible reaction flow ($\alpha = 0$) has the smallest growth rate and the larger the reversibility coefficient α the larger the maximum growth rate. these effects are similar to what was observed at $t_0 = 0$ where reversibility enhanced the instability. Furthermore, the non-reactive flow has in this case the largest maximum growth rate and the one with small Damköhler number ($D_a = 0.01$) was still more unstable the the fully reversible case ($\alpha = 1$). However, reversibility had an opposite effect on the instability at later time where the maximum growth rate decreases with increasing α, though the effects are less marked. Furthermore, similar results were observed for cases where both the trailing and the leading fronts are unstable, but the instability of the trailing front is more than that of the leading one ($R_c > R_b > 0$). However, for this case, a less noticeable variation between the maximum growth rates was observed as the reaction reverses.

3.5 Conclusions and discussion

The main objective of this study is to determine the effects of reversibility on the instability of a horizontal reactive displacement where the frontal instability is triggered by the viscosity mismatch between the chemical species. The study revealed that the fate of the displacement process can be dramatically influenced when a reversible chemical reaction takes place between the displacing and the displaced fluids. The effects of chemical reversibility which were observed in terms of the longwave instability as well as the whole range of unstable

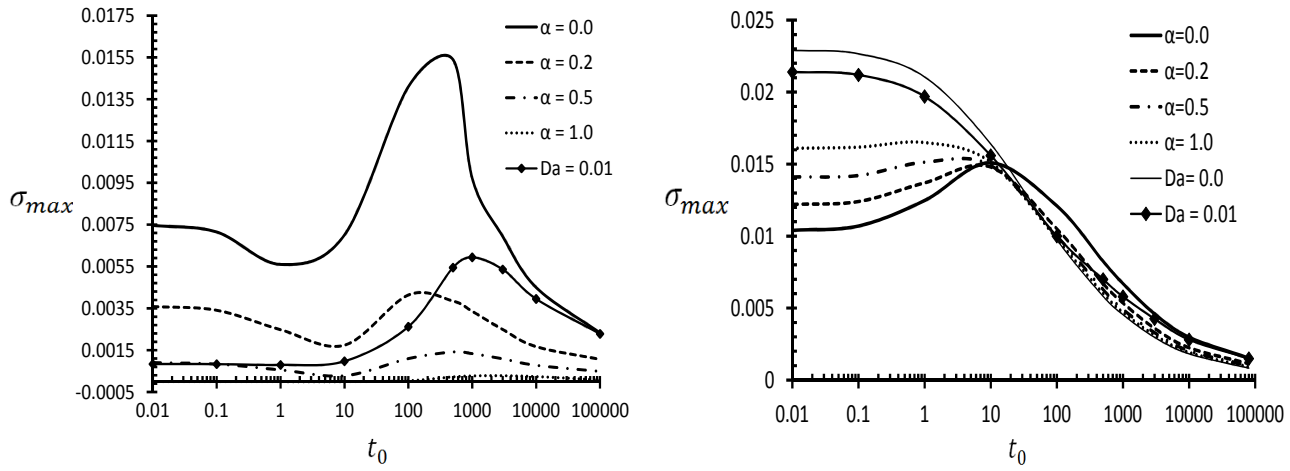

Figure 3.7: Dispersion Curves at $t_0 > 0$ showing the influence of D_r at $D_a = 1.0$ for (a) $R_b = -1$ and $R_c = 3$, (b) $R_b = 1$ and $R_c = 2$.

wavenumbers and the maximum growth rates, were found to depend on the initial profile of the front between the two reactants.

For an initial sharp concentration front, ($t_0 = 0$), it was found that beyond a certain critical coefficient α_c, a flow which is unstable to longwave disturbances may actually become stable and vice versa, as a result of chemical reversibility. This critical reversibility coefficient is a function of the mobility ratio of the three chemical species. In particular, for an initially unstable reactive front where the displacing reactant (A) has a smaller viscosity than the displaced reactant (B), *i.e.* $R_b > 0$, the flow is unstable to longwave disturbances only for reversibility coefficients larger than α_c. On the other hand for an initially stable front ($R_b < 0$), longwave instability is observed only for reversibility coefficients smaller than α_c while for larger values of the reversibility coefficient, the flow is intrinsically stable. Furthermore, chemical reversibility tends to attenuate the flow instability in all cases except for initially unstable flows ($R_b > 0$) where the chemical product is more viscous than the displaced reactant; *i.e.* $R_c > R_b$.

For diffusing initial fronts ($t_0 > 0$), the trends reported in the case of a sharp front are also observed, at least for short times. However, the effects of reversibility tend to weaken at very long times, and actually the trends are reversed from enhancing to attenuating the instability in the cases where at $t_0 = 0$ reversibility was found to make the flow more unstable.

The effects of reversibility are qualitatively similar to those of the Damköhler number D_a as reported in [89], where it was found that for $t_0 = 0$, a decrease of D_a will attenuate the flow instability for $R_b < 0$ as well as for $R_b > 0; R_b > R_c$ and enhances it for $R_c > R_b > 0$. This result is expected since chemical reversibility can be considered to have a similar effect as a slowing down of the rate of the chemical reaction. However the similarities between a decrease of the Damköhler number and an increase of the strength of the chemical reversibility do not extend beyond this qualitative similarity in how both affect the flow instability. First based on the long wave expansion in [89], changes in the rate of the reaction do not affect the instability for short wave numbers and depend only on R_b and R_c (see equation (4.15) in [89]). This implies that decreasing the Damköhler number does not affect the instabilities at small wavenumbers, and a flow will be always stable or unstable to longwave disturbances regardless of the reaction rate, at least for non-complex growth rates [89]. The present results however show that chemical reversibility can switch the flow from being stable to unstable to longwave disturbances or vice versa. Furthermore, increasing the reversibility to the highest limit ($\alpha = 1$) does not lead to the results obtained when the Damköhler number is reduced to its minimum zero value. In fact, except for an initially stable reactive front ($R_b < 0$) where the curves for $D_a = 0$ and $\alpha = 1$ superpose, in all other scenarios the characteristics of these two limiting cases are different resulting in the complete reversible reaction always leading to a system that is either more unstable or less unstable than the non-reactive flow.

The trends reported in this study can be explained through the mobility ratios of the vari-

ous species. The interpretation makes use of the concepts of the leading and trailing fronts, which though are an idealization of the flow, can help in elucidating the effects of chemical reversibility. First, It should be noted that as the chemical reaction reverses, part of the chemical product (C) is converted into the reactants (A) and (B). This implies that in the two zones of the flow where instability may develop, *i.e.* the leading and trailing fronts, more regions of the flow which initially involved the product, will now involve more of the reactants and hence the mobility ratios are shifted towards $R_b = \ln(\frac{\mu_B}{\mu_A})$. For cases where the initial interface is stable ($R_b \leq 0$), only the leading or the trailing fronts of the reactive flow can be unstable. Furthermore, the mobility ratio between the reactants is in this case always smaller than that at the unstable trailing or leading front. As a result of chemical reversibility, the mobility ratio at the unstable front, whether the leading ($C-B$) or the trailing ($A-C$) one, will decrease since part of the chemical product (C) is converted into the reactants. As a consequence, the instability will be systematically attenuated. However, reversibility may have different effects on the instability when the initial front is unstable ($R_b > 0$). In such a case, there are three possible scenarios for the instability to develop. In the first one the instability develops only at the trailing front ($R_c > 2R_b$), in the second only the leading front will be unstable ($R_c < 0$) while in the third both trailing and leading fronts are unstable ($2R_b > R_c > 0$). In the first two scenarios the mobility ratio of the two reactants R_b is always less than that of the unstable front, be it the leading or the trailing one, while in the third one it is larger than those of the unstable leading and trailing fronts. As a consequence as the reaction reverses, the mobility ratio at the stable front in the first two scenarios, or both unstable fronts in the third one, will be enhanced. When this enhancement of the instability is combined with the influence of the direction of injection, which is in favour of the growth of the instability at the leading but not the trailing front [110], chemical reversibility will result in a more unstable displacement. This explains the enhancement of instability by chemical reversibility in flow displacements where

$R_c > R_b$. Finally, the growth of the instability in a reactive displacement process depends on the mobility ratios as well as the amount of the chemical species at the reactive fronts. As time proceeds, the chemical species diffuse and the influence of the mobility mismatches in enhancing the instability decreases for both complete and reversible reactions, which explains the systematic attenuation of the instability at very large times, whether the reaction reverses or not.

The present analysis can serve as a guide in determining the conditions of instability of displacements involving reversible reactions and in choosing the parameters when examining the full non-linear development of the flow.

Chapter 4

Numerical Simulations of Reversible Reactive Flows in Homogeneous Porous Media

[1] The effects of reversibility on the viscous fingering of miscible reactive flow displacements in homogeneous porous media are examined through numerical simulations. A model, where the viscosities mismatch between the reactants and the chemical product triggers the instability, is adopted. The problem is governed by the continuity equation, Darcy's law and the convection-diffusion-reaction equations which are solved using a pseudo-spectral method. It was found that in general, chemical reversibility tends to attenuate the instability at the fronts resulting in less complex fingers than in the non-reversible case. However, stronger chemical reversibility also leads to less diffuse and thinner finger structures. Furthermore, the chemical product was found to be homogeneously distributed in the porous medium in the case of the reversible reaction, while strong concentration gradients are observed in the non-reversible case. The study has also revealed that chemical reversibility is capable of enhancing the instability of a stable reactive front. It is also found that the rate of production can be the same for different cases of frontal instability for a period of time that increases with the increase in the magnitude of chemical reversibility.

4.1 Introduction

In a fluid displacement process, the interface between the displacing and the displaced fluids is unstable when the viscosity of the displaced fluid is higher than that of the displacing one. When the instability between the fluids is triggered by viscosity mismatch, the instability is

[1]This chapter is the exact reproduction of the following submitted journal article:
H. Alhumade and J. Azaiez (2013). Numerical Simulations of Reversible Reactive Flows in Homogenous Porous Media. *Journal of Porous Media*

referred to as viscous fingering or Saffman-Taylor. This instability may grow to form fingers that propagate in both upstream and downstream directions. The instability between the fluids may also take place as a result of density mismatch, in which case it is referred to as the Rayleigh-Taylor instability [15, 3, 4].

Many experimental and theoretical studies have examined the instability in the absence of chemical reactions in the flow. In these studies the effect of different parameters on the instability were examined and most of these studies were reviewed by [5] and [6]. However, the fate of the displacement process can be dramatically influenced when a chemical reaction takes place between the displacing and the displaced fluids. Reactive flow displacements are encountered in various important fields such as underground water treatment, heavy oil recovery, chromatographic separation, polymer processing and fixed bed regeneration. Furthermore, an environmental friendly approach was explored for heavy oil upgrading and in-situ recovery as an alternative to current techniques that have strong impact on the environment [111]. In all different sectors involving a reactive displacement process, the flow instability is an important factor in measuring the efficiency and the viability of that process.

There is a growing number of studies on reactive flow displacement processes. The first study on reactive flows was carried out on a secondary oil recovery process by [46] where the chemical reaction led to an interfacial tension decrease in the process. The capacity of chemical reactions to also modify the viscosity ratio at the interface of a secondary oil recovery process was investigated by [47]. A number of subsequent studies investigated the influence of other aspects on the efficiency of the reactive displacement such as the dimensions of the Hele-Shaw cell [49], stoichiometry [50], geometry orientation [112], finger growth rate [51], chemical composition [113], external electrical field [114], variation in the physical properties of the phases [115], and precipitation [56]. Other experiments studied the effect

of the chemical reactions in changing the viscosities of the chemical species and consequently the fingering patterns of miscible displacements at high [53] and moderate [54] Damköhler numbers.

A limited number of studies have also focused on modeling the reactive displacement process. One of the first studies is the mathematical model by [61], where the macroscopic patterns of the medium can be changed as a result of the reactive displacement process. This mathematical model focused on the infiltration flow as well as the variation in the porosity of the medium as a result of the reaction. A number of subsequent studies investigated different aspects such as medium dissolution [63], acid flow through porous rocks [64], auto-catalytic reactions in immiscible [116] and miscible [117] displacements, buoyancy driven displacement [118] and displacement of immiscible fluids with a reactive interface [67]. Furthermore, the influence of various factors on the reactive displacements have been investigated such as, the role of velocity dependant hydrodynamic dispersion [68, 119], reaction parameters [69], buoyancy [70], cell gap-width [72], heat of reaction [109, 77, 79] and external electrical field [81]. [84] analyzed adiabatic reactive miscible displacements for both endothermic and exothermic reactions where the viscosity was considered to be a function of both concentration and temperature.

Most of the previous studies are related to cases involving either interactions between the fluids and the porous medium or auto-catalytic reactions. However, a growing number of studies have investigated the cases where non-auto-catalytic reactions drive the instability of the process. The dynamics of a bimolecular reaction $A + B \rightarrow C$ were investigated by [88] where the viscosity of both reactants were assumed to be equal, which resulted in a neutrally stable initial interface, while the viscosity of the product was assumed to be larger than that of both reactants. The authors adopted the configuration where reactant (B) was

sandwiched inside reactant (A). Different scenarios of frontal instability in a horizontal miscible displacement process that involves a chemical reaction $A + B \rightarrow C$ were investigated by [90]. A slab configuration where each half of the slab was filled with only one of the reactants was adopted and the authors focused on the instability of the interfaces between the reactants and the product based on the mobility ratio at each interface as well as the effect of Péclet number on the rate of production. [93] conducted non-linear simulations in the same model considered by [90], but for a infinite Damköler number ($D_a \rightarrow \infty$). Here, the authors characterized quantitatively the fingering patterns in terms of the mixing lengths, the fingering density (FD) as well as the total amount of the product (C). Furthermore, the authors validated the results with previous linear stability analysis and experimental studies. In a more recent study, [2] analyzed reaction-driven viscous fingering in an initially stable displacement in a horizontal Hele-Shaw cell. In this experiment, aqueous solutions of polymers were used in order to benefit from the dependence of their viscosities on pH. Two cases where instability developed at the upstream or the downstream directions of a bi-molecular reaction, were presented. Non-linear simulations were also carried out for comparisons with the experimental results.

In all previous studies, the chemical reactions were always assumed to be complete. However in certain applications, chemical reactions can be reversible and this can influence the effects of different factors on the instability of the process. Reversibility of the chemical reaction has major influence on many phenomena studied in physics, chemistry, biology, and geology [104]. For example, In the in-situ soil remediation, promising results were reported by [7], where a reactive fluid was injected to remove the pollutant from the underground water and the important role of reversibility on the efficiency of such a process was examined by [100]. Moreover, reversibility is an important factor in the study of the effect of the transport of reactive tracers on the dispersion coefficients at pore-level [105]. The first study on reactive-

diffusive systems with reversible reaction was carried out by [96] who have analyzed the properties of the interface of a reversible reactive process with initially separated reactants. In this study, the authors focused on calculating the width of the reaction zone numerically and it was reported that the dynamics of the reactive front can be described as a crossover between irreversible and reversible regimes at short and long times, respectively. Furthermore, the existence of a crossover between short time "irreversible" and long time "reversible" regimes was confirmed by [97]. In addition, the authors also investigated analytically and numerically the reaction rate profile in an immobilized reaction zone and it was found that at long times, the reaction rate will encounter two maxima and may attain negative values in between. Recently, [102] investigated the reaction rate of a reversible reactive-diffusive process where the reactants are initially mixed with different diffusion coefficients, by using the boundary layer function method. It was reported that the reactive-diffusive process for this case can be considered as a quasi-equilibrium process. Furthermore, the authors analyzed the dependence of the reaction rate on the initial distribution of the reactants and it was reported that the number of the reaction zones varies with time and can be determined by the initial conditions.

In all previous studies of reversible reactive displacement processes, only the diffusive term was considered. However, when one of the reactants is injected to displace the other as in most applications, the convective term must be considered in addition to the diffusive one. In such cases, the displacement process is expected to be dominated by convection rather than diffusion. A recent study [103] used linear stability analysis to determine how chemical reversibility may influence the stability of the reactive flow displacement. Various possible scenarios of instability were determined based on the mobility ratios between the chemical species as well as the strength of the reversibility. However, even though linear stability analysis did lead to interesting conclusions about the effects of different parameters on the

instability, it cannot extend beyond the linear regime and therefore does not provide any information about the non-linear regime and hence about the actual growth and development of the fingers. In the present study, full non-linear simulations of reversible reactive-diffusive-convective flow displacements are conducted in order to understand the effects of reversibility on the flow dynamics as well as on the overall efficiency of the displacement process.

4.2 Mathematical model

4.2.1 Physical problem

The non-linear simulations of a two dimensional displacement process will be carried out in a homogeneous porous medium with constant permeability and porosity. The flow is in the horizontal direction referred to by the x-axis, whereas the y-axis is perpendicular to the direction of the flow. Furthermore, both the displacing and displaced fluids are assumed to be incompressible, Newtonian and miscible with equal initial concentrations. A schematic of the process is shown in Figure 4.1, where L_x and L_y are the length and width of the medium, respectively.

A fluid (A) of viscosity μ_A is injected with a constant velocity U from the the left-hand side to displace fluid (B) of viscosity μ_B. A reversible reaction results in a chemical product (C) of viscosity μ_C:

$$A + B \rightleftharpoons C \tag{4.1}$$

As time proceeds, more products will accumulate at the interface between the two reactants. Figure 4.1 shows an idealized distribution of the two reactants (A) and (B) and the product (C), with two fronts. The first one is between the reactant (A) and the product (C); $(A-C)$ while the other is between the reactant (B) and the product(C); $(C-B)$, and they will be referred to as the trailing and leading front, respectively.

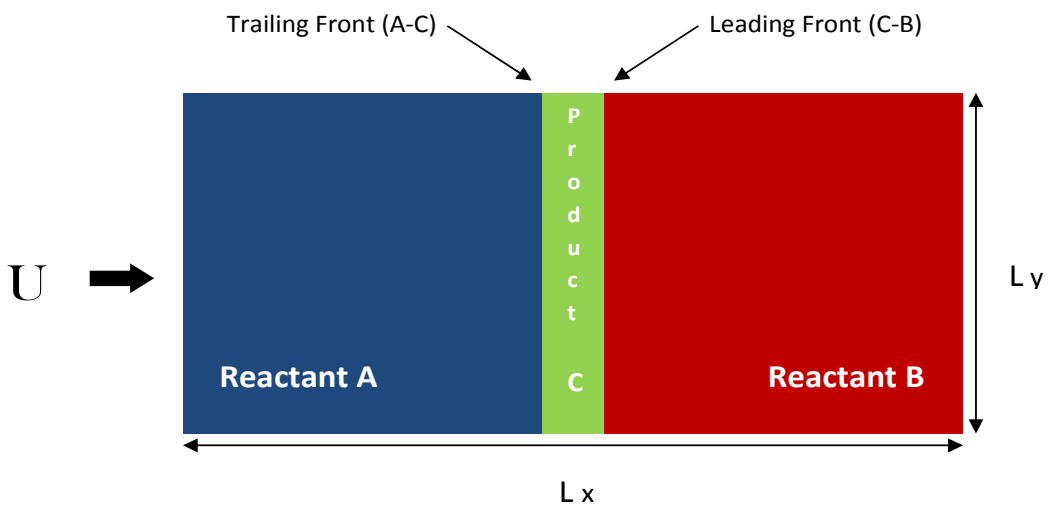

Figure 4.1: Schematic of a reactive front displacement process.

4.2.2 Governing equations

The flow is governed by the equations for conservation of mass, momentum (Darcy's Equation) and the transport of the three chemical species.

$$\nabla.\mathbf{u} = 0 \tag{4.2}$$

$$\nabla p = -\frac{\mu}{\kappa}\mathbf{u} \tag{4.3}$$

$$\phi\frac{\partial A}{\partial t} + \mathbf{u}.\nabla A = \phi D_A \nabla^2 A - kAB + k_r C \tag{4.4}$$

$$\phi\frac{\partial B}{\partial t} + \mathbf{u}.\nabla B = \phi D_B \nabla^2 B - kAB + k_r C \tag{4.5}$$

$$\phi\frac{\partial C}{\partial t} + \mathbf{u}.\nabla C = \phi D_C \nabla^2 C + kAB - k_r C \tag{4.6}$$

In the above equations, the superficial velocity is denoted by $\mathbf{u} = u\hat{i} + v\hat{j}$ where $\hat{i}$ and $\hat{j}$ are the unit vectors along x and y, respectively. Furthermore, p represents the pressure, k the forward reaction rate constant, k_r the reverse reaction rate constant, ϕ the medium porosity, κ the medium permeability and μ is the viscosity. The concentrations of the two reactants and chemical product are denoted by A, B and C, respectively while D_A, D_B and D_C represent their corresponding diffusion coefficients. In the present study, it will be assumed

that all species have the same diffusion coefficient, i.e. $D_A = D_B = D_C = D$. Furthermore, the maximum concentrations of both reactants are equal, *i.e.* $a_0 = b_0$ and under these conditions, the center of the reaction region remains at the initial frontal locations between the two reactants [106]. The above equations are expressed in a Lagrangian reference frame moving with the constant injection velocity and the equations are made non-dimensional using U, $D\phi/U$ and $D\phi^2/U^2$ as the reference velocity, length and time, respectively. In addition, the constant permeability is integrated in the expression of the viscosity as μ/κ and this expression is simply treated as μ, which is referred to as the mobility or viscosity ratio. Furthermore, the viscosity, pressure and concentrations are scaled using μ_A, $\mu_A D\phi$ and a_0. The resulting dimensionless equations are:

$$\nabla \cdot \mathbf{u} = 0, \tag{4.7}$$

$$\nabla p = -\mu(\mathbf{u} + \mathbf{i}), \tag{4.8}$$

$$\frac{\partial A}{\partial t} + \mathbf{u} \cdot \nabla A = \nabla^2 A - D_a AB + D_r C, \tag{4.9}$$

$$\frac{\partial B}{\partial t} + \mathbf{u} \cdot \nabla B = \nabla^2 B - D_a AB + D_r C, \tag{4.10}$$

$$\frac{\partial C}{\partial t} + \mathbf{u} \cdot \nabla C = \nabla^2 C + D_a AB - D_r C, \tag{4.11}$$

The Damköhler number $D_a = k\phi a_0 D/U^2$ represents the ratio between the characteristic hydrodynamic time scale and the chemical time scale, while $D_r = k_r \phi D/U^2$ represents the reversible Damköhler number. In all what follows, the ratio $\alpha = \frac{D_r}{D_a}$ for $D_a \neq 0$ is referred to as the reversibility coefficient.

Following a previous study [90], a concentration dependent viscosity profile is adopted to complete the model:

$$\mu = \mathrm{e}^{R_b B + R_c C} \tag{4.12}$$

In the above equation R_b and R_c are the log mobility ratios of the viscosity of (B) to (A) and (C) to (A), respectively.

$$R_b = \ln(\frac{\mu_B}{\mu_A}) \qquad and \qquad R_c = \ln(\frac{\mu_C}{\mu_A}) \tag{4.13}$$

Furthermore, the mobility ratios at the trailing and leading fronts are referred to as:

$$R_{AC} = \ln(\frac{\mu_C}{\mu_A}) = \frac{R_c}{2} \qquad and \qquad R_{CB} = \ln(\frac{\mu_B}{\mu_C}) = R_b - \frac{R_c}{2} \tag{4.14}$$

Following previous studies [88, 90], the problem is formulated in terms of stream-function ψ and vorticity ω, which are related to velocity in the stream-wise and transverse directions by the following equations:

$$u = \frac{\partial \psi}{\partial y}, \qquad v = -\frac{\partial \psi}{\partial x}. \tag{4.15}$$

$$\omega = \frac{\partial v}{\partial x} - \frac{\partial u}{\partial y}. \tag{4.16}$$

Furthermore, the stream-function and vorticity are related by the following equation:

$$\bigtriangledown^2 \psi = -\omega. \tag{4.17}$$

Where $\bigtriangledown^2$ is the Laplacian operator.

The curl of the Darcy's law, equation (4.8), is taken in order to eliminate the pressure, resulting in the following equation:

$$\omega = R_b(\frac{\partial \psi}{\partial x}\frac{\partial B}{\partial x} + \frac{\partial \psi}{\partial y}\frac{\partial B}{\partial y} + \frac{\partial B}{\partial y}) + R_c(\frac{\partial \psi}{\partial x}\frac{\partial C}{\partial x} + \frac{\partial \psi}{\partial y}\frac{\partial C}{\partial y} + \frac{\partial C}{\partial y}) \tag{4.18}$$

The partial differential equations are solved using the following initial conditions:

$$A = 1, B = 0, C = 0 \quad for \quad x < 0 \tag{4.19}$$

$$A = 0, B = 1, C = 0 \quad for \quad x > 0 \tag{4.20}$$

While the boundary conditions at the streamwise direction in dimensionless form are:

$$u = 0, v = 0, A = 1, B = 0, C = 0 \quad at \quad x = -\frac{P_e}{2} - t \tag{4.21}$$

$$u = 0, v = 0, A = 0, B = 1, C = 0 \quad at \quad x = \frac{P_e}{2} - t \tag{4.22}$$

and at the transverse direction:

$$(u, v, A, B, C)(x, -\frac{P_e}{2A_r}, t) = (u, v, A, B, C)(x, \frac{P_e}{2A_r}, t) \tag{4.23}$$

In the above equations $P_e = \frac{UL_x}{D\phi}$ is the Péclet number and $A_r = \frac{L_x}{L_y}$ is the cell aspect-ratio.

4.2.3 Numerical technique

The variables in the problem can be decomposed as the sum of the base-state and a perturbation. The base-state is a numerical solution of the reactive-diffusive-convective equations (4.4)-(4.6) while the adopted initial perturbation consists of a random noise with values between -1 and 1. The random noise is introduced at the initial interface between the reactants, with a magnitude that decays rapidly away from the initial interface. The magnitude of the initial perturbation may increase, decrease or stay constant based on the mobility ratio at the initial interface and the final solution will be a combination of the perturbation that has evolved in time and space and the base-state solutions.

Following previous studies [120, 90], the Hartley-Pseudo-spectral method is used to determine the perturbation part of the problem. This method allows recasting the partial differential equations in time and space into an ordinary differential equations in time. The resulting ordinary differential equations are stepped in time using a semi-implicit predictor-corrector method along with an operator-splitting algorithm.

4.3 Results

4.3.1 Validation and convergence of the numerical code

The numerical convergence was tested by using different spatial resolutions (up to 512 x 512) and corresponding time steps. Based on the results of these tests, it was found that a

spatial resolution of 256 x 256 and a time step $\triangle t = 0.005$ allow to ensure the numerical convergence for the cases discussed in this study. Furthermore, the code was validated by comparing the time evolution and the related viscous fingers interactions to those presented by [90] for the non-reversible case ($\alpha = 0$). It was found that the dynamics of fingering were identical when the same parameters were used along with the same spatial resolution and time step size.

4.3.2 Concentration iso-surfaces contours

The flow evolution will depend on the mobility ratios of the different species; R_b and R_c as well as Pe, A_r, D_a and α. In order to limit the analysis to the effects of the reversibility of the chemical reaction, the following parameters are fixed as $A_r = 2$, $P_e = 1000$ and $D_a = 1$. Furthermore, the analysis will examine separately the cases where the initial front between the two reactants is unstable ($R_b > 0$) and that where it is stable ($R_b \leq 0$). In each of these cases, the roles of the reversibility coefficient and the mobility ratios are investigated. For each case, concentration iso-surfaces of the product (C) are presented for a complete chemical reaction ($\alpha = 0$) and for two different non-zero values of the reversibility coefficient (α).

Unstable initial interface ($R_b > 0$)

When a less viscous fluid (A) is used to displace another one (B) with a higher viscosity, the initial interface between the two fluids is unstable ($R_b >0$). The viscosity of the chemical product (C) can be either smaller than, larger than or in between the viscosities of (A) and (B). As a result, regardless of the viscosity of the product (C), instability will take place at least at the trailing or the leading front, if not at both. In what follows, various cases of instability are discussed.

Concentration contours of the chemical product (C) are depicted in Figure 4.2 for the case

where the product's viscosity is smaller than those of both reactants; i.e. $R_{AC}(=\frac{R_c}{2}) < 0$ and $R_{CB}(= R_b - \frac{R_c}{2}) > 0$. The results are presented for the cases where the chemical reaction is complete ($\alpha = 0$), weakly reversible ($\alpha = 0.3$) and strongly reversible ($\alpha = 0.8$). It is worth noting that in all three cases the instability develops mainly on the leading front and the fingers extend in the downstream direction. Furthermore, it is clear that in this case reversibility tends to attenuate the instability of the flow. In particular, fingers are less developed and are more diffuse than in the non-reversible case. However, reversibility also increased the number of developed fingers. Moreover, it should be noted that the distribution of the chemical product is more homogeneous and shows less gradients than in the non-reversible reaction flow. This indicates that in such reversible-reaction flows, the chemical product will be more uniformly distributed in the medium.

When the viscosity of the product (C) is larger than those of both reactants, the viscosity ratio will be in favour of the growth of instability at the trailing ($R_c > 0$), but not the leading one ($R_b - \frac{R_c}{2} < 0$). As a result, fingers will appear on the trailing front and extend in the opposite direction of the flow, while the leading front will be stable. Figure 4.3 depicts the case $R_b = 1$ and $R_c = 2$, which corresponds to unstable trailing and neutrally stable leading fronts. It is interesting to note that in this case, reversibility does actually enhance the instability particularly at the leading front, where the fingers become more developed and narrower with increasing α. This is also the case on the trailing front, though the fingers extend less in the upstream direction. Furthermore here too, reversibility leads to a more homogeneous distribution of the product. These results are to be compared with the predictions of the linear stability analysis that have indicated that for ($R_b = 1$, $R_c = 2$), the maximum growth rate increases with chemical reversibility at short times, but are smaller than those of the irreversible ones at later times [103].

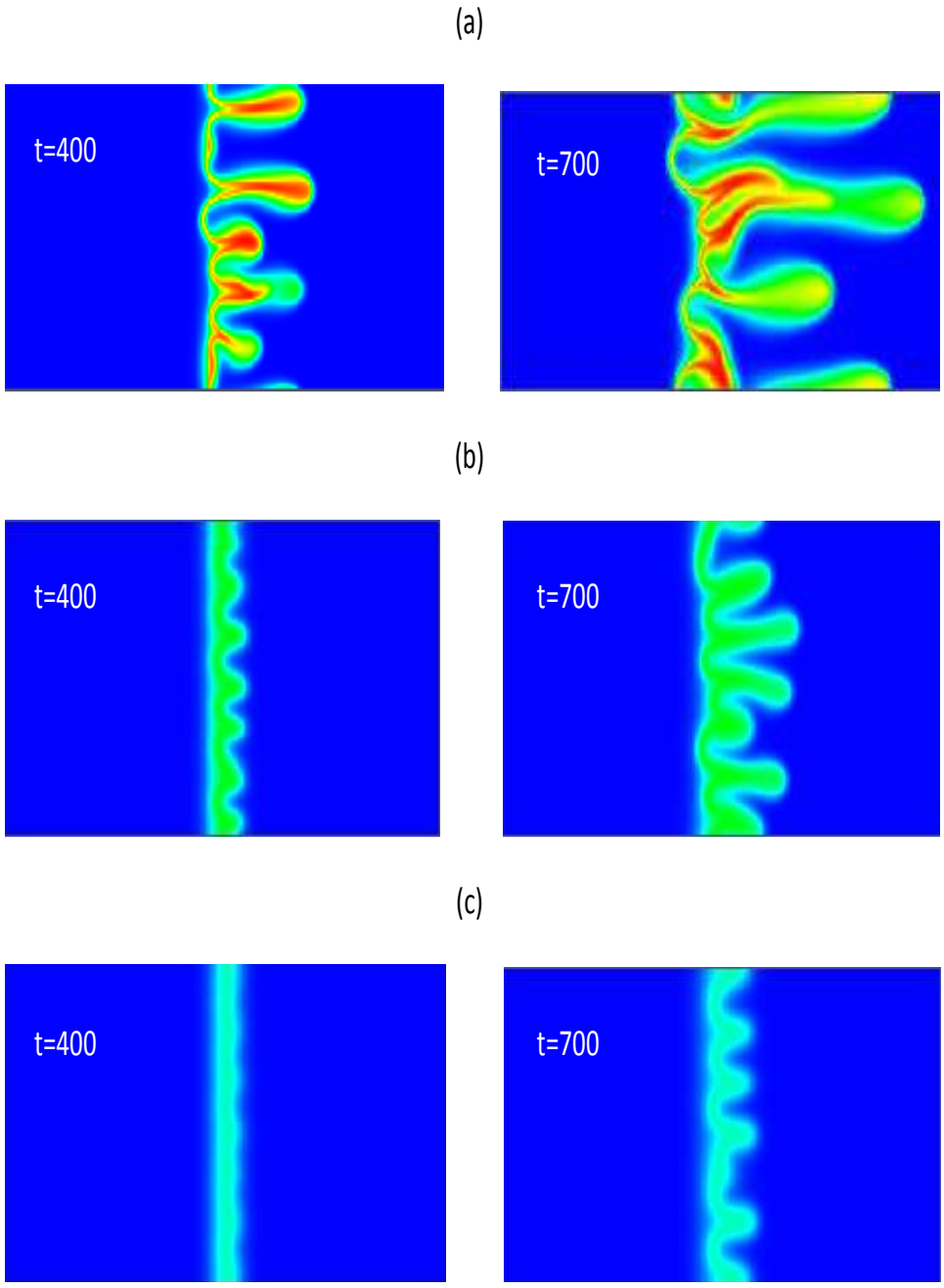

Figure 4.2: Concentration iso-surfaces for $R_b = 1$, $R_c = -3$ (stable trailing front, unstable leading front): (a) $\alpha = 0.0$, (b) $\alpha = 0.3$, (c) $\alpha = 0.8$

Figure 4.4 depict results for reactive flow displacements where the viscosity of (C) lies between those of the two reactants. In this case both the trailing and the leading fronts are unstable ($R_c > 0$, $R_b - \frac{R_c}{2} > 0$). The non-linear simulations indicate that reversibility does not actually have a major effect on the finger structure, and aside from the fact that the chemical product is more uniformly distributed in the porous medium when the reaction reverses, the number and overall structures of fingers are virtually unchanged. It should be finally noted that in all previous cases where the initial reactive front is unstable, stronger reversibility systematically leads to thinner and less diffuse fingers with a uniform distribution of the chemical product.

The previous results can be explained by examining the effects of the chemical reversibility on the distribution of the viscosity on the different fronts. First, it should be noted that in a reactive displacement process, instability will not grow until a certain amount of the product (C) is generated. Furthermore, for the unstable initial reactive front case ($R_b > 0$), when the instability develops at one of the trailing or the leading fronts, the mobility ratio at that unstable front is always larger than that of the initial reactive front. As the reaction reverses and (C) is converted back into (A) and (B), the favourable mobility ratio between the reactants will increase and decrease the mobility ratios at the stable and the unstable front, respectively. Furthermore, it is known that the direction of injection is in favour of the growth of the instability at the leading $(C - B)$, but not the trailing $(A - C)$ front [121]. These two factors explain the influence of reversibility in attenuating or enhancing the instability of the cases where instability developed at the leading ($R_b = 1$, $R_c = -3$ and $R_{CB} > R_b$) or the trailing ($R_b = 1$, $R_c = 2$ and $R_{CB} < R_b$) front, respectively.

The less noticeable effects of reversibility in Figure 4.4 corresponding to $(Rb = 2, Rc = 3, R_{AC} = 1.5, R_{CB} = 0.5)$ can be attributed to the fact that in this case the trailing *and* lead-

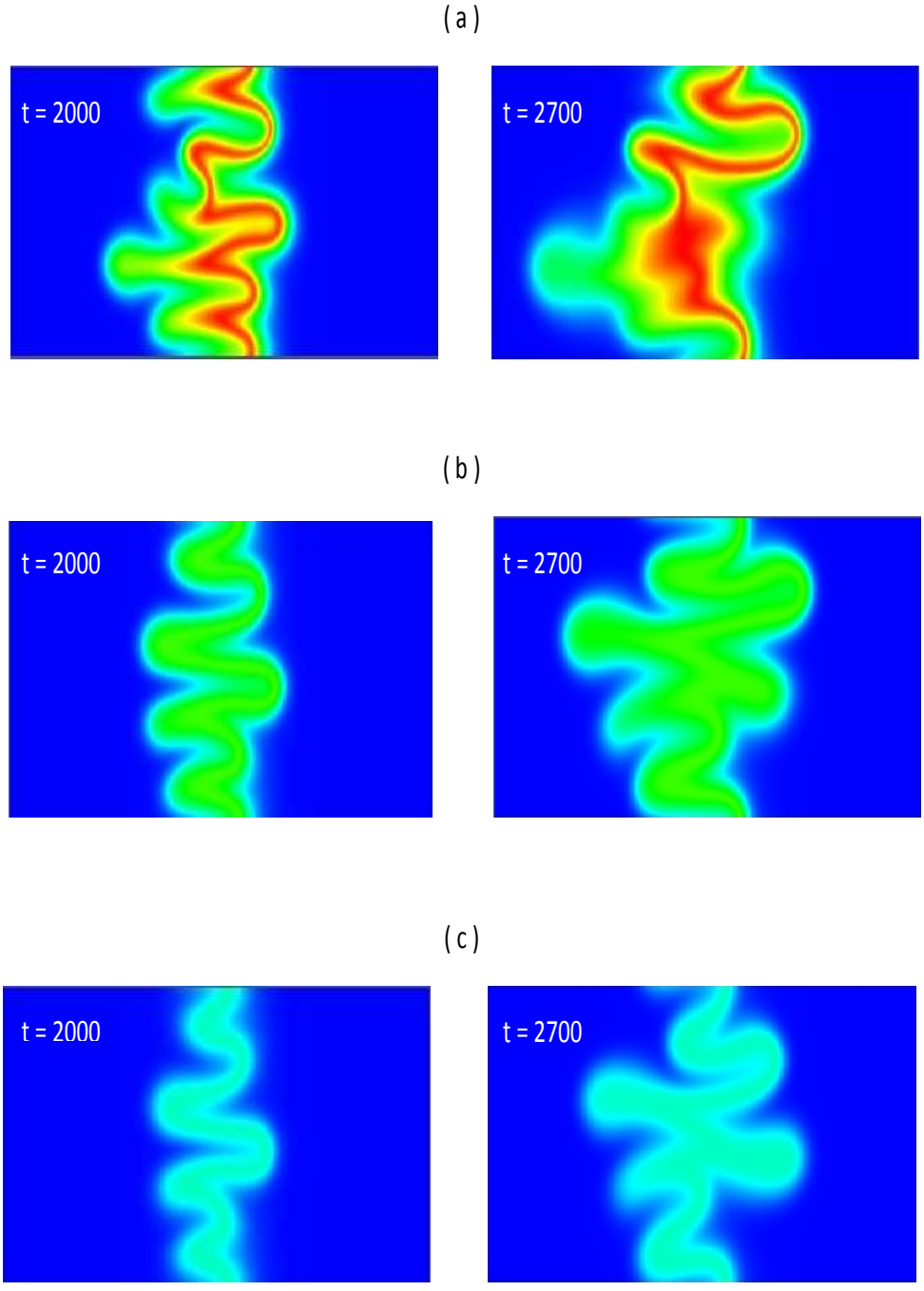

Figure 4.3: Concentration iso-surfaces for $R_b = 1$, $R_c = 2$ (unstable trailing front, neutrally stable leading front): (a) $\alpha = 0.0$, (b) $\alpha = 0.3$, (c) $\alpha = 0.8$

ing fronts are unstable, resulting in a stronger mixing of the chemical species. Furthermore, the favorable mobility ratio between the reactants (R_b) increases the mobility ratios at both the trailing and the leading fronts as the reaction reverses. This helps the instability to keep growing regardless of how fast the product (C) is converted back to (A) and (B).

Stable or neutrally stable initial interface ($R_b \leq 0$)

The initial interface between the two reactants is stable or neutrally stable if the viscosity of the displacing fluid is larger than or equal to that of the displaced one ($R_b \leq 0$). However, as the reaction takes place and chemical product is generated, instability may develop at either the trailing or the leading front but not at both. The case where the viscosity of (C) lies between those of (B) and (A) or equal to both or any of them ($\mu_A \geq \mu_C \geq \mu_B$) results in a stable displacement process and therefore, will not be discussed. In what follows, the two cases where instability appears at only the trailing or the leading front are examined.

A stable trailing front and an unstable leading front is observed in the case where the viscosity of (C) is smaller than that of both reactants. On the other hand, a stable leading front and an unstable trailing will occur when the viscosity of the product (C) is larger than the viscosities of both reactants. It is worth mentioning that unlike the previously discussed cases of an unstable initial front, the mixing between the two reactants for a stable initial front is mainly controlled by diffusion. As a result, the growth of fingers is rather slow compared to cases with an unstable initial front.

In such cases involving stable initial reactive fronts, reversibility tends to attenuate the instability at the unstable trailing or leading front and may actually result in a completely stable system for a period of time. Figure 4.5 depicts the case where the instability takes place at the leading front when the chemical reaction is complete ($\alpha = 0$), while the system was found to be stable when the reaction reverses ($\alpha \neq 0$). This can be attributed to the fact

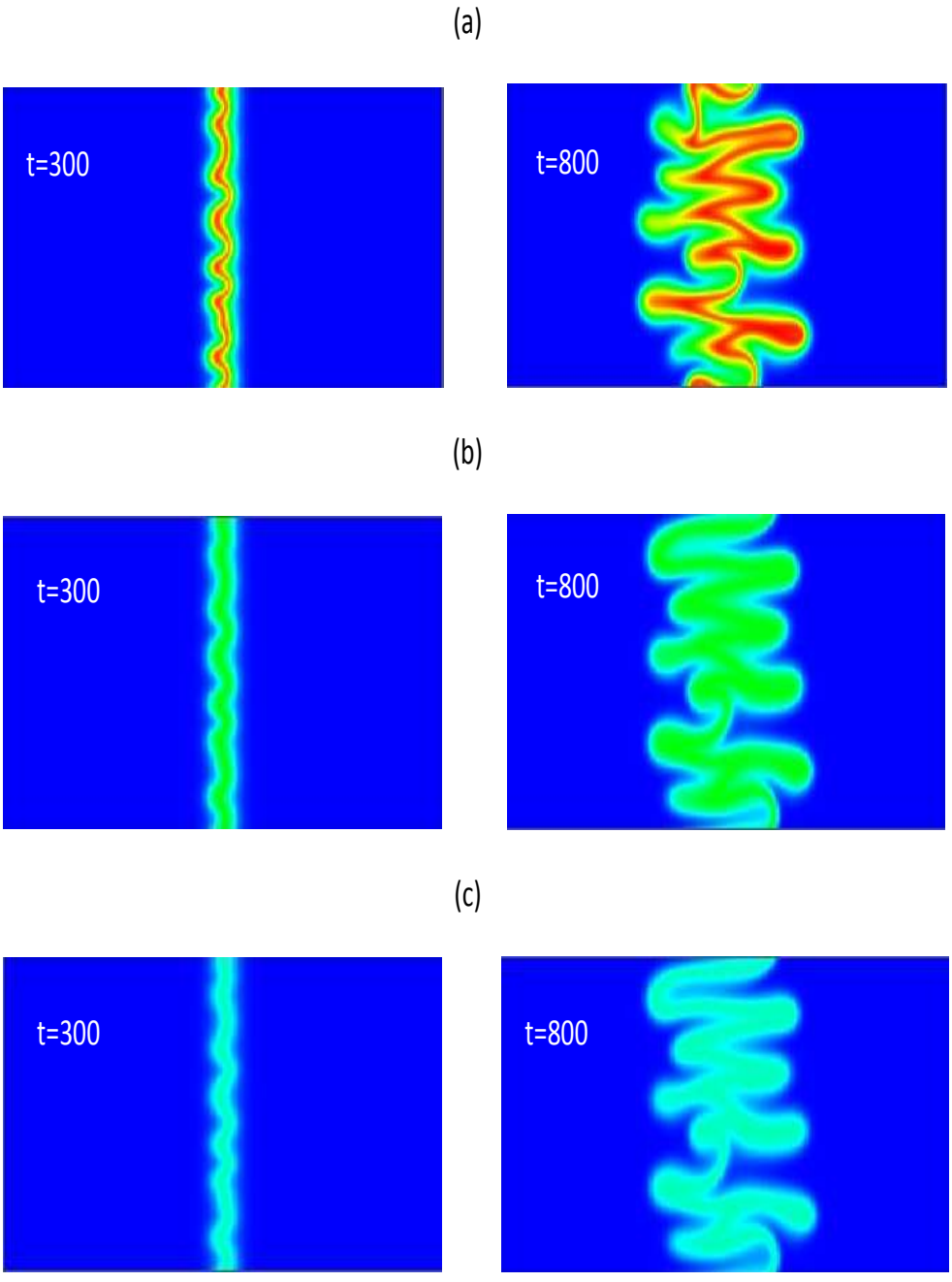

Figure 4.4: Concentration iso-surfaces for $R_b = 2$, $R_c = 3$ (unstable trailing front, unstable leading front): (a) $\alpha = 0.0$, (b) $\alpha = 0.3$, (c) $\alpha = 0.8$

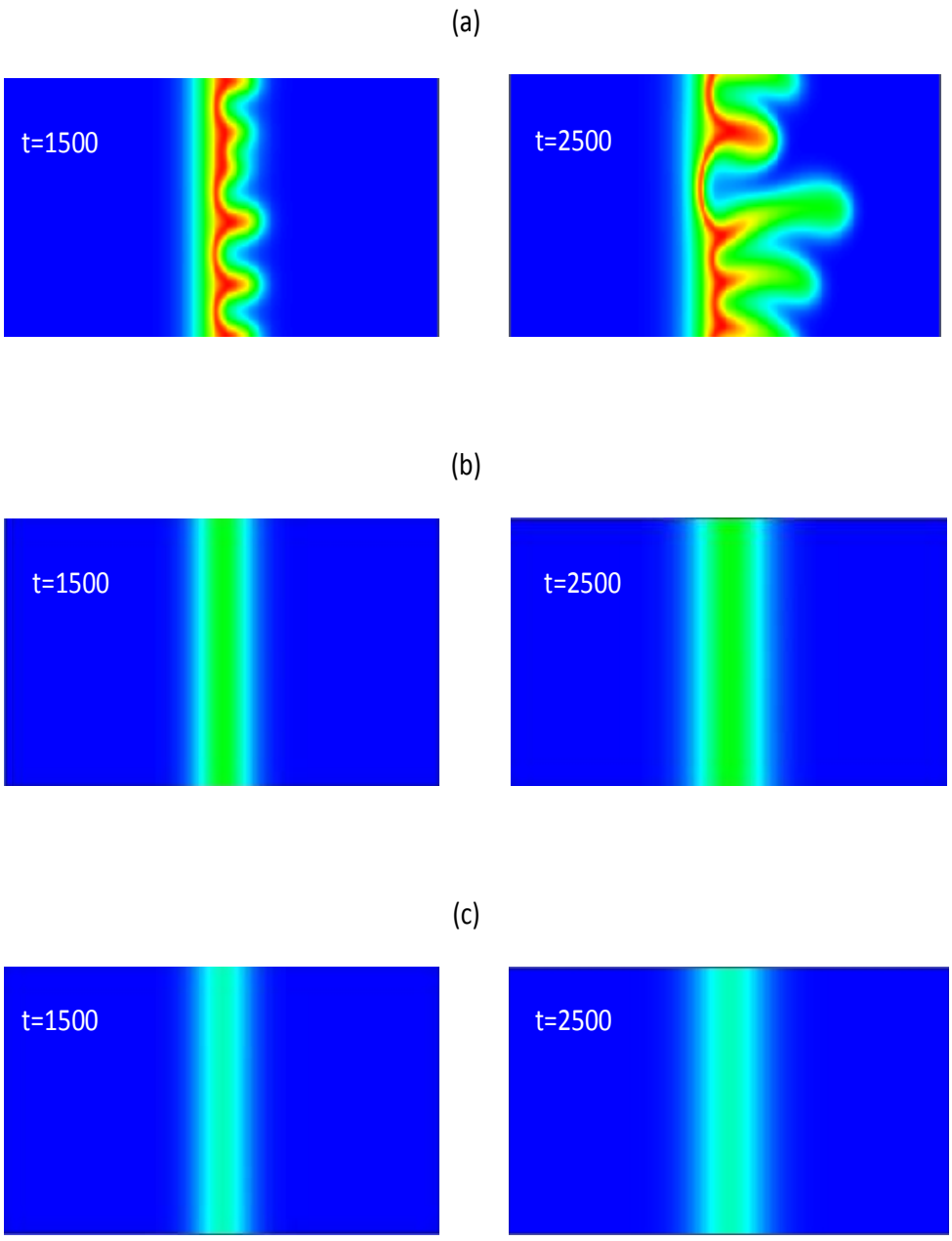

Figure 4.5: Concentration iso-surfaces for $R_b = -0.5$, $R_c = -3$ (stable trailing front, unstable leading front): (a) $\alpha = 0.0$, (b) $\alpha = 0.3$, (c) $\alpha = 0.8$

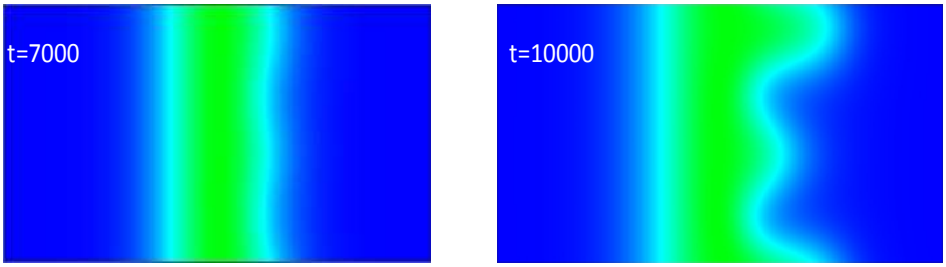

Figure 4.6: Concentration iso-surfaces for $\alpha = 0.3$, $R_b = -0.5$, $R_c = -3$ (stable trailing front, unstable leading front)

that in the initial stages of the flow, the mixing of the different species is governed by diffusion and reversibility perpetuates this state by preventing more of the product to accumulate and to trigger instability at the leading front. However, the amount of chemical product will still keep growing with time, though slowly, and instability will eventually appear at the unstable leading front at later times (see Figure 4.6). The time for the instability to appear depends on the rate of chemical reversibility, with smaller reversibility coefficients leading to an earlier growth of fingers. This time also depends on the mobility ratios of the different chemical species, with distributions that lead to a more unstable leading front resulting in the instability developing earlier in time. To illustrate this, the results for ($R_b = -0.01$, $R_c = -3$, $R_{CB} = 1.49$) depicted in Figure 4.7 show that the instability develops earlier in time in comparison with the case in Figure 4.6 where $R_{CB} = 1$. Similar conclusions were reached for the case where the instability takes place at the trailing front, and for brevity the corresponding contours are not shown.

4.3.3 Quantitative analysis

In this part, the efficiency of the displacement process is quantified through the total amount of (C) produced for different scenarios of frontal instability. In addition the complexity of the fingering structure is examined by determining the relative contact area between the chemical species.

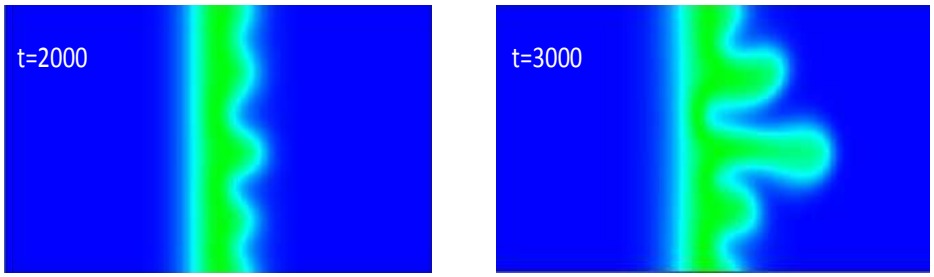

Figure 4.7: Concentration iso-surfaces for $\alpha = 0.3$, $R_b = -0.01$, $R_c = -3$ (stable trailing front, unstable leading front)

Total amount of Product C

The total amount of product (C) is determined using the following equation:

$$C(t) = \int_{\frac{Pe}{2}}^{\frac{-Pe}{2}} \int_{\frac{Pe}{2A_r}}^{\frac{-Pe}{2A_r}} C(x, y, t) dx dy \tag{4.24}$$

It is obvious that reversibility will decrease the total amount of the chemical product. However, this part will focus on the variation on the total amount of the product for all possible scenarios of instability. The total amounts of the product (C) for different cases of frontal instability at $\alpha = 0.5$ are presented in Figure 4.8-a. Similar to the non-reversible cases presented in [90], the total amount of (C) is larger in cases with an unstable ($R_b > 0$) compared to those with a stable ($R_b < 0$) initial front. However, it can be noticed that unlike the results obtained for non-reversible reactions, the normalized number of moles of product (C) for both cases with a stable initial front ($R_b < 0$) are overlapping for a longer period of time.

From Figure 4.8-b, it is found that increasing the magnitude of α results in the total amount of the product (C) for both cases ($R_b = -0.5$, $R_c = -3$) and ($R_b = -1$, $R_c = 3$) being equal for a longer period of time. From the figure, it can also be seen that the production rate was higher in the case where instability takes place at the trailing front. This is due to the higher mobility ratio at the unstable trailing front ($R_c/2 = 1.5$) than that at the unstable leading front ($R_b - R_c/2 = 1.0$).

For cases with unstable initial fronts, the effect of increasing the magnitude of reversibility on the total amount of the product (C) has also been investigated when instability takes place at the trailing ($R_b = 1$, $R_c = 3$), the leading ($R_b = 1$, $R_c = -3$) as well as both fronts ($R_b = 2$, $R_c = 3$). Here, it was observed that the trends for the accumulation of the product (C) are similar to those obtained for non-reversible cases and furthermore as expected, the total amount of the product decreases as reversibility increases. Similar to the results obtained for the cases with stable initial fronts, increasing α equalizes the total amount of (C) for the above three scenarios for a longer period of time. However, the variation in the total amount of (C) was observed at earlier times compared to those where the initial front is stable. Furthermore, the total amount of (C) for the case with an unstable leading front ($R_b = 1$, $R_c = -3$) was at later time larger than that where the trailing front is unstable ($R_b = 1$, $R_c = 3$) and this is again attributed to the higher mobility ratio at the leading ($R_b - R_c/2 = 2.5$) than the trailing front ($R_c/2 = 1.5$).

In summary, for a fixed R_b, stronger chemical reversibility leads to total amounts of the product (C) that superpose for different scenarios of instability for a longer period of time. Increasing the mobility ratios at the unstable fronts results in an earlier variation in the total amount of (C) for fixed α and R_b.

Relative Contact Area

The effect of reversibility on the instability of the reactive system will be quantified by examining the relative contact areas (R.C.A.). The relative contact area which is defined as the area of contact between the species involved in the displacement process scaled by the cross-sectional area of the cell, is a good criterion to quantify the complexity of the insta-

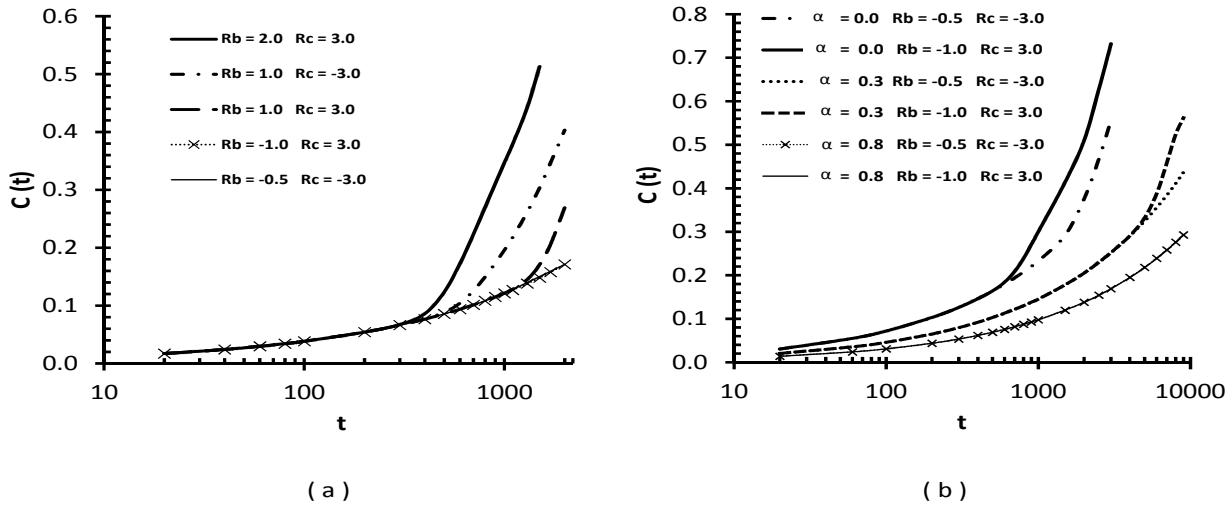

Figure 4.8: Normalized number of moles of product C for $P_e = 1000, D_a = 1.0$: (a) $\alpha = 0.5$, (b) $\alpha = 0.0$, $\alpha = 0.3$ and $\alpha = 0.8$

bility. For a stable front, the R.C.A. at one front will be equal to one, while it is larger than one once instabilities develop. This contact area is determined by measuring the length of a contour that corresponds to a specific concentration value of one of the species. In this study, three chemical species are involved in the process and therefore, there are two contact interfaces to be measured, one corresponding to the leading and the other to the trailing front. For both cases where the chemical reaction is either complete or reversible, the contour that corresponds to concentration of 0.01 of the chemical product ($C = 0.01$), is used to determine the length of the contact areas at both fronts.

The numerical data on the curves that represent the contact areas have been extracted using an algorithm and the results are presented in terms of the variation of the (R.C.A.) with time. This analysis focuses on the case where an increase in the instability of the system has been observed. Figure 4.9 illustrates the variation in R.C.A with time for the case where reversibility triggers instability at the neutrally stable leading front ($R_b = 1, R_c = 2$). It is clear that at early times, R.C.A. is virtually constant and equal to one, indicating a stable flow. However at later times, the relative contact area increases and the increase is found to

be stronger for stronger chemical reversibility. Furthermore, this increase is most noticeable at the trailing front, where the values of R.C.A. of the reversible reaction flow actually becomes larger than that of the non-reversible reactive displacement. It is also worth noting that for a large value of the reversibility coefficient ($\alpha = 0.8$), R.C.A. at the trailing front also can exceed that of the non-reversible reaction flow.

These trends for the variation of the R.C.A can be explained by the fact that the growth of instability is influenced by both the total amount of the chemical species and the mobility ratios at both reactive fronts. The reduction in the total amount of the chemical product (C) as the reaction reverses, explains the slower growth of instability at early stages at both the trailing and the leading fronts. However, the favourable mobility ratio between the reactants (R_b) increases the mobility ratio at the neutrally stable leading front as the reaction reverses, which explains the faster growth of the R.C.A at the leading front as α increases (Figure 4.9-a). Furthermore, it is interesting to notice that even though the mobility ratios at the trailing and initial reactive fronts are equal ($\frac{R_c}{2} = R_b = 1$), the R.C.A for the extremely reversible reaction ($\alpha = 0.8$) is at some later times larger than that for the complete one. This is attributed to the strong instability of the leading front which in turn enhances that of the trailing front. This is confirmed by noting that the relative contact area reaches its maximum on both fronts around the same time.

4.4 Conclusion

The main objective of this study is to determine the effects of chemical reversibility on the overall efficiency of bi-molecular reactive displacements in homogeneous porous media. The viscous fingering instability in these flows is triggered by the viscosity mismatch between the reactants and the product. The non-linear interactions between the fluids were captured for different scenarios of frontal instability at a specific set of parameters. It was found that the

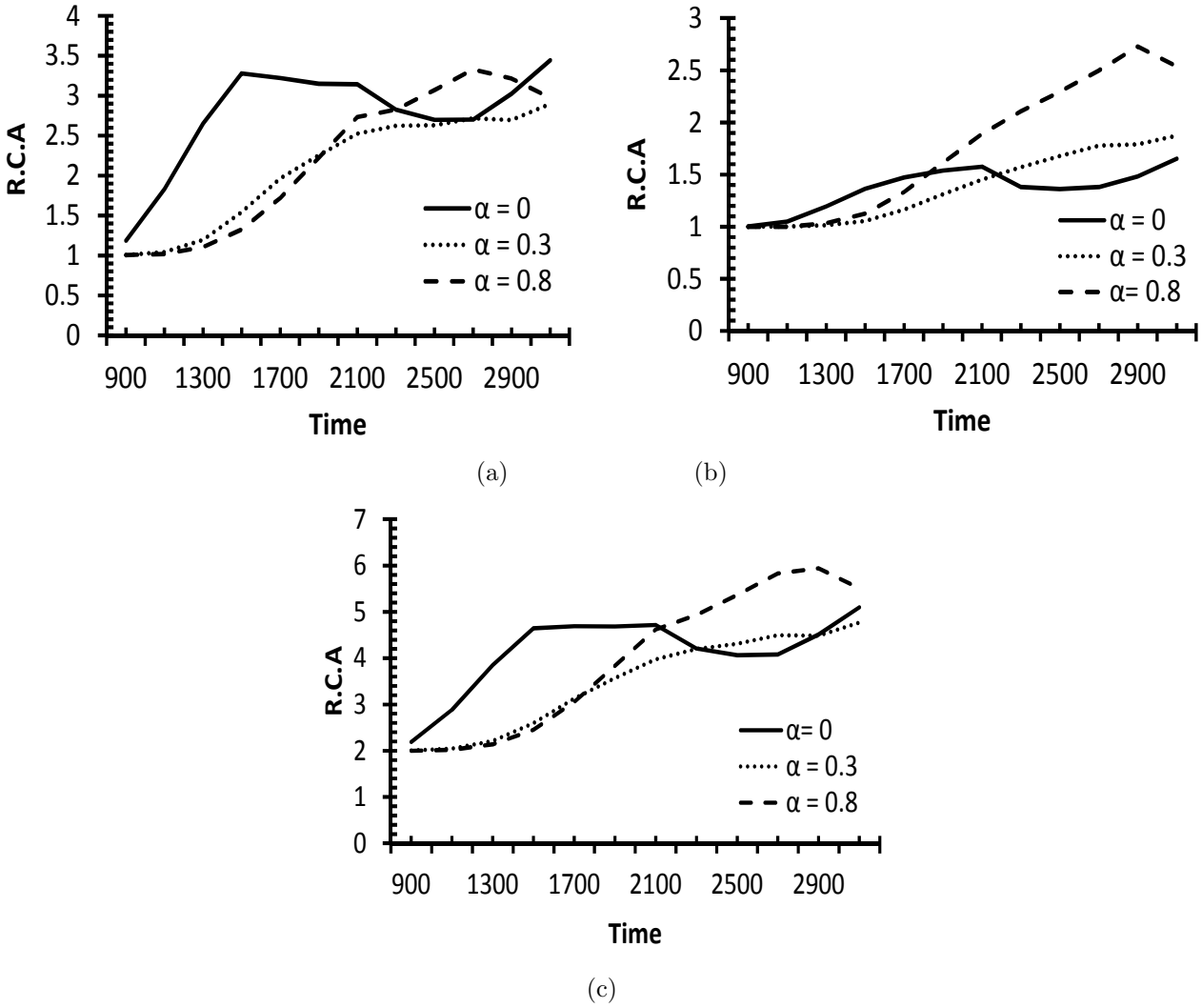

Figure 4.9: Variations of the Relative Contact Area (R.C.A.) for $R_b = 1$, $R_c = 2$: (a) at Trailing Front, (b) at Leading Front, (c) Total R.C.A.

fate of the displacement process can be dramatically influenced as a result of the reversibility of the chemical reaction.

The development of viscous fingering is much faster in cases where the initial front between the reactants was unstable ($R_b > 0$) compared to cases with a stable initial front. This is due to the larger production rate in the former cases, as a result of the rapid mixing between the reactants. It was found that in all cases, reversibility tends to result in a more homogeneous spatial distribution of the chemical product in the porous medium. However, the effects of reversibility on the viscous fingering instability were found to depend on the distribution of the viscosity of the different reactants. In particular, in all flow displacements where the initial front is stable or where the initial front is unstable with unstable leading and stable trailing fronts, stronger chemical reversibility leads to less unstable flows. Furthermore, for viscosity distributions that result in unstable initial reactive front as well as unstable trailing and leading fronts, reversibility has virtually no effects on the development of the flow instability. The intense mixing between the reactants in addition to the favourable mobility ratio of the initial front help the continuous growing of the instability regardless of the speed of the reversibility. On the other hand, for unstable initial and trailing fronts and stable leading one, reversibility was found to enhance the instability of the stable leading front as the favourable mobility ratio between the reactants increases the mobility ratio at that front in addition to the fact that the direction of injection is in favour of the growth of the instability at the leading front.

Chapter 5

Reversible Reactive Flow Displacements in Vertical Homogeneous Porous Media

The effect of reversibility on the instability of a miscible vertical reactive flow displacement is examined. A model, where densities and viscosities mismatches between the reactants and the product trigger instability is adopted. The problem is governed by he continuity equation, Darcy's law and the convection-diffusion-reaction equations and is solved using a pseudo-spectral method. A non-linear simulation was carried out to illustrate the effect of reversibility on the instability at different scenarios of frontal instability. In general, faster attenuation in the development and growth of instability is reported as the reversibility of the chemical reaction increases. However, it was observed that reversibility is capable of triggering instability at a particular choice of densities and viscosities mismatches. In addition, the effect of reversibility in enhancing the instability was illustrated by presenting the total relative contact area between the reactants and the product.

5.1 Introduction

Instability at the interface between flowing solutions in a porous media may take place as a result of viscosities and/or densities mismatch between the fluids. This instability will develop in shape of fingers and will be referred to as viscous fingering or Saffman-Taylor instability in case of viscosity mismatch or as density fingering or Rayleigh-Taylor instability in case of densities mismatch between the fluids [15], [3], [4], [5], [6].

The simultaneous variation in viscosities and densities is encountered in various applica-

tions. An analytical expression for the growth of instability in a non-reactive system with variation in viscosities and densities was driven by Bacri et al.[122]. In 1993, Rogerson and Meiburg carried out a linear stability analysis to investigate the interface of a non-reactive system with densities and viscosities mismatch in a porous media where both normal and tangential velocities can be observed [32]. It was reported that the growth rate of instability was not affected by tangential velocity in immiscible displacements, unlike the miscible displacements where a stabilizing role was observed. In the same year, the same authors investigated the non-linear evolution in instability for the unstable modes of the same system [33], where remarkable features of instability such as diagonal fingering and secondary side-finger instability were observed. The effect of non-monotonic viscosities and densities profiles on the instability of a vertical non-reactive displacement process was investigated by Manickam and Homsy by running a no-linear simulation of the system [31]. Authors found that, a stable viscous interface between the fluids can break the symmetry of buoyancy driven instability by acting as a barrier against the upward growth of instability.

A simple chemical reaction $A + B \longrightarrow C$, can change the physical properties such as viscosity or density of the fluids, which might change the fate of the displacement process. Reactive flows are encountered in many applications such as in-situ oil recovery, carbon dioxide sequestration, in-situ groundwater re-mediation and chromatographic columns. It has been shown that frontal instability can be purely driven by a chemical reaction, where a viscous product is generated at the interface of two reactants with smaller viscosities [55]. In a series of experiments, the effect of chemical reaction on the viscosity profile of an initially unstable system was investigated by Nagatsu et al. [53], [54], [123]. The properties of the unstable miscible reactive displacements were analysed by a number of theoretical and numerical studies. For example, Rongy et al. [87] showed that the instability of the interface in a vertical displacement process can be influenced by buoyancy-driven convection

once the densities of the species are changed by a chemical reaction even for equal diffusion coefficients and equal initial concentrations of the reactants. Another study examined the buoyancy chemically driven instability where the reaction introduces a heavier product at the initial interface and where a variation in the diffusion rates of the solutions exist [92]. In a horizontal geometry, Alhumade and Azaiez carried out a linear stability analysis [103] followed by non-linear simulations [124] of the reversible reactive flow displacements. Authors investigated quantitatively and qualitatively and influence of the reversibility on the instability of the flows. Hejazi and Azaiez conducted a detailed linear stability analysis [94] followed by a non-linear simulation [125] of a miscible vertical reactive displacement processes with transverse velocity.

The instability of miscible reactive solutions under gravity force is involved in many underground flows applications. For example, geological storage of CO_2 in addition to mixing of brine [126]. The former process involve dissolution of carbon dioxide in the reservoir's fluid and this can be modelled by a chemical reaction [8], [127]. A heavier solution will be introduced on top of the reservoir's lighter fluid as a result of the CO_2 dissolution, which will establish instability at the fluids interface.

The reversibility of the chemical reaction plays an important role in various fields such as in-situ soil remediation [100] and liquid chromatographic columns [128]. This triggers the need to investigate the effect of reversibility on the frontal instability of miscible vertical reactive displacements. In this study, a system where the variation in viscosities and densities between the reactants and the product initiate frontal instability in absence of injection or transverse velocities is examined.

5.2 Mathematical model

5.2.1 Physical Problem

Non-linear simulations of a two dimensional displacement process are carried out in a homogeneous reservoir, where the porosity and permeability are assumed to be constant. The displacement takes place in the vertical direction, which is referred to as the x-axis, while the y-axis is perpendicular to the direction of the flow. Furthermore, both the displacing and displaced fluids are assumed to be incompressible, Newtonian and miscible. A schematic of the process is shown in figure 5.1, where L_x, L_y and w are the length, width and thickness of the medium, respectively. When the thickness of the medium is small compared to the other dimensions, the system corresponds to a Hele-Shaw cell, which is a common prototype for homogeneous porous media [5].

Fluid (A) of viscosity μ_A is on top of fluid (B) of viscosity μ_B. The two fluids react to generate a chemical product (C) of viscosity μ_C that can be different than the viscosities of both reactants. The chemical reaction is first order and can be reversible:

$$A + B \rightleftharpoons C \tag{5.1}$$

As time proceeds, more product accumulates at the interface between the two reactants. Figure 5.1 shows an idealized distribution of the two reactants (A) and (B) and the product (C), with two fronts. One front is between reactant (A) and product (C); $(A$ - $C)$ while the other is between reactant (B) and product (C); $(C$ - $B)$, and these fronts are referred to as the trailing and leading front, respectively.

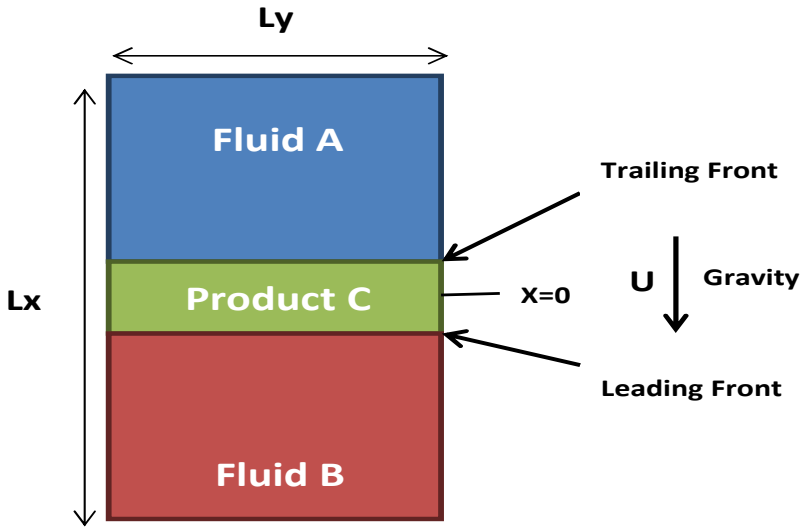

Figure 5.1: Schematic of a reactive front displacement process.

5.2.2 Governing equations

The flow is governed by the equations for conservation of mass, momentum (Darcy's Equation) and the transport of the three chemical species.

$$\nabla.\mathbf{u} = 0 \tag{5.2}$$

$$\nabla p = -\frac{\mu}{\kappa}\mathbf{u} + \rho\mathbf{g} \tag{5.3}$$

$$\phi\frac{\partial A}{\partial t} + \mathbf{u}.\nabla A = \phi D_A\nabla^2 A - kAB + k_r C \tag{5.4}$$

$$\phi\frac{\partial B}{\partial t} + \mathbf{u}.\nabla B = \phi D_B\nabla^2 B - kAB + k_r C \tag{5.5}$$

$$\phi\frac{\partial C}{\partial t} + \mathbf{u}.\nabla C = \phi D_C\nabla^2 C + kAB - k_r C \tag{5.6}$$

In the above equations, the superficial velocity is denoted by $\mathbf{u} = u\hat{i} + v\hat{j}$ where $\hat{i}$ and $\hat{j}$ are the unit vectors along x and y, respectively. Furthermore, p represents the pressure, k the forward reaction constant, k_r the reverse reaction constant, ϕ the medium porosity, and μ is the viscosity and κ is the constant medium permeability. Here, the constant permeability is integrated in the expression of the viscosity as μ/κ and this expression is simply treated as μ, which is referred to as the mobility or viscosity ratio. The concentrations of the two

reactants and chemical product are denoted by (A), (B) and (C) respectively while D_A, D_B and D_C represent their corresponding diffusion coefficients. In the present study, it will be assumed that all species have the same diffusion coefficient, i.e. $D_A = D_B = D_C = D$. Furthermore, the maximum concentrations of both reactants are equal, *i.e.* $a_0 = b_0$. Under these conditions, the center of the reaction region remains at the initial frontal locations between the two reactants.

The above equations are expressed in a Lagrangian reference frame moving with constant velocity $U_{ch} = \frac{|\bigtriangledown \rho| g}{\mu_A}$ where $|\bigtriangledown \rho|$ is the absolute value of the difference between the densities of the displacing and displaced fluids. The equations are made non-dimensional using U_{ch}, $D\phi/U_{ch}$ and $D\phi^2/{U_{ch}}^2$ as the reference velocity, length and time, respectively. Furthermore, the viscosity, pressure and concentrations are scaled using μ_A, $\mu_A D\phi$ and a_0. The resulting dimensionless equations are:

$$\nabla \cdot \mathbf{u} = 0, \tag{5.7}$$

$$\nabla p = -\mu(\mathbf{u} + U\widehat{i}) + \rho\widehat{i}, \tag{5.8}$$

$$\frac{\partial A}{\partial t} + \mathbf{u} \cdot \nabla A = \nabla^2 A - D_a AB + D_r C, \tag{5.9}$$

$$\frac{\partial B}{\partial t} + \mathbf{u} \cdot \nabla B = \nabla^2 B - D_a AB + D_r C, \tag{5.10}$$

$$\frac{\partial C}{\partial t} + \mathbf{u} \cdot \nabla C = \nabla^2 C + D_a AB - D_r C, \tag{5.11}$$

The Damköhler number $D_a = ka_0 D\phi/{U_{ch}}^2$ represents the ratio between the characteristic hydrodynamic time scale and the chemical time scale, while $D_r = kD\phi/{U_{ch}}^2$ represents the reversible Damköhler number. In all what follows, the ratio $\alpha = \frac{D_r}{D_a}$ for $D_a \neq 0$ is referred to as the reversibility coefficient. U is the injection velocities in the direction of the flow, which is included only to provide a complete framework model, and is assumed to be zero in this study.

Following previous studies [125], concentration dependant viscosity and density profiles are adopted to complete the model:

$$\mu = \mathrm{e}^{R_b B + R_c C} \tag{5.12}$$

$$\rho = G_a A + G_b B + G_c C \tag{5.13}$$

In the above equation G_i is the density expansion coefficient of specie i and is defined as $G_i = \frac{\partial \rho}{\partial C_i}$, while R_b and R_c are the log mobility ratios between the viscosity of (B) to (A) and (C) to (A), respectively. In what follows, these log mobility ratios are simply referred to as the mobility or viscosity ratios

$$R_b = \ln(\frac{\mu_B}{\mu_A}) \qquad and \qquad R_c = \ln(\frac{\mu_C}{\mu_A}) \tag{5.14}$$

Furthermore, the mobility ratios at the trailing and leading fronts are referred to as:

$$R_{AC} = \ln(\frac{\mu_C}{\mu_A}) = \frac{R_c}{2} \qquad and \qquad R_{CB} = \ln(\frac{\mu_B}{\mu_C}) = R_b - \frac{R_c}{2} \tag{5.15}$$

Following previous studies; [38], [88], [90], the problem is formulated in term of vorticity ω and streamfunction ψ, which are related to velocity field as follows:

$$u = \frac{\partial \psi}{\partial y}, \qquad v = -\frac{\partial \psi}{\partial x}. \tag{5.16}$$

$$\omega = \frac{\partial v}{\partial x} - \frac{\partial u}{\partial y} = - \bigtriangledown^2 \psi. \tag{5.17}$$

The curl of the Darcy's law equation (5.8) is taken in order to eliminate the pressure, which shows that vorticity is produced by concentration gradients according to the following equation:

$$\begin{aligned} \omega = R_b(\frac{\partial \psi}{\partial x}\frac{\partial B}{\partial x} + \frac{\partial \psi}{\partial y}\frac{\partial B}{\partial y} + U\frac{\partial B}{\partial y}) \\ +R_c(\frac{\partial \psi}{\partial x}\frac{\partial C}{\partial x} + \frac{\partial \psi}{\partial y}\frac{\partial C}{\partial y} + U\frac{\partial C}{\partial y}) \\ -\frac{1}{\mu}(G_a\frac{\partial A}{\partial y} + G_b\frac{\partial B}{\partial y} + G_c\frac{\partial C}{\partial y}) \end{aligned} \tag{5.18}$$

The partial differential equations are solved using the following initial conditions:

$$A = 1, B = 0, C = 0 \quad for \quad x < 0 \tag{5.19}$$

$$A = 0, B = 1, C = 0 \quad for \quad x > 0 \tag{5.20}$$

While the boundary conditions at the streamwise direction in dimensionless form are:

$$u = 0, v = 0, A = 1, B = 0, C = 0 \quad at \quad x = -\frac{P_e}{2} - t \tag{5.21}$$

$$u = 0, v = 0, A = 0, B = 1, C = 0 \quad at \quad x = \frac{P_e}{2} - t \tag{5.22}$$

and at the transverse direction:

$$(u, v, A, B, C)(x, -\frac{P_e}{2A_r}, t) = (u, v, A, B, C)(x, \frac{P_e}{2A_r}, t) \tag{5.23}$$

In the above equations $P_e = \frac{U_{ch} L_x}{D\phi}$ is the Péclet number and $A_r = \frac{L_x}{L_y}$ is the cell aspect-ratio.

5.2.3 Numerical technique

The problem can be solved by splitting the variables into a base-state part and a perturbation term, where the base-state is a numerical solution of the reactive-diffusive-convective equations (5.4)-(5.6). The perturbation is initiated as a random noise centred at the initial interface between the reactants, and that decays rapidly far from the interface. The magnitude of the initial perturbation may increase, decrease or stay constant depending on the density and viscosity mismatch between the different species. This approach where the problem is solved in term of a perturbation allows to use the highly accurate spectral methods.

Following previous studies; [129], [27], [120], the Hartley-Pseudo-spectral method is used to evaluate the perturbation part of the problem. This method allows to cast the original partial differential equation in time and space into an ordinary differential equation in time. The solution for the time stepping of the reactive-diffusive-convective equations was generated by using a semi-implicit predictor-corrector method along with an operator-splitting algorithm [120].

5.3 Results

5.3.1 Validation and convergence of the numerical code

The numerical code was validated by comparing the time evolution and the related finger structures for the case where the chemical reaction is complete ($\alpha = 0$) with those presented by Hezaji and Azaiez [125] for the non-reversible case. It has been noted that the dynamics of fingering were identical when the same parameters that characterize the flow were used along with the same spatial resolution and time step size. In this study, a spatial resolution of 256 x 256 with at time step $\triangle t = 0.005$ are used to present the non-linear simulation results for the effect of reversibility on the instability of the displacement process.

5.3.2 Concentration iso-surfaces contours

The flow evolution will depend on both viscosities and densities mismatch between the chemical species, in addition to Pe, A_r, D_a and D_r. In order to limit the analysis to the effects of the reversibility of the chemical reaction, the following parameters are fixed as $A_r = 2$, $P_e = 1000$ and $D_a = 1$. Furthermore, the analysis will first examine the cases where instability is only driven by densities mismatch ($R_b = R_c = 0$) for both scenarios involving stable ($G_A < G_B$) and unstable ($G_A > G_B$) initial fronts. The effects of mobility mismatch are examined afterwards. For each case, concentration iso-surfaces of the product (C) are presented for a complete chemical reaction ($\alpha = 0$) and for one or two different non-zero values of reversibility coefficient (α) in order to illustrate the effect of reversibility on the dynamics of fingering.

5.3.3 Effect of densities mismatch at equal mobility ratios

In this part, it is assumed that there is no viscosity mismatch between the chemical species ($R_b = R_c = 0$) and therefore, the frontal instability depends only on the variation of densities between the reactants and the product. Flows with an unstable initial reactive fronts ($G_A >$

G_B) are presented first followed by cases with stable initial fronts ($G_A < G_B$).

Unstable initial reactive front ($G_A > G_B$)

In a vertical displacement process, the initial interface between the displacing and displaced fluid is unstable if the top fluid (A) is heavier than the bottom one (B) ($G_A > G_B$). The density of the chemical product (C) can be either smaller than, larger than or in between the densities of (A) and (B). As a result, regardless of the density of product (C), instability will take place at least at the trailing or leading fronts if not at both. In what follows, various cases of instability are discussed.

The case where the density of the product (C) is higher than those of both reactants; i.e. $G_C > G_A > G_B$, resulted in a stable trailing front and an unstable leading front. As a result, fingers appeared and extended in the direction of the flow on the leading front as shown in figure 5.2. The figure shows results for the cases where the chemical reaction is complete ($\alpha = 0$), weakly reversible ($\alpha = 0.3$) and strongly reversible ($\alpha = 0.8$). It is clear that in this case, reversibility tends to attenuate the instability of the flow at the unstable leading front, while there was a noticeable increase in the instability at the trailing front. In this particular case ($G_A = 4, G_B = 1, G_C = 10$), It can be noticed that the number of developed fingers increases as the reaction reverse. However, fingers are less developed and more diffuse than in the non-reversible case. Furthermore, for reversible cases ($\alpha > 0$), there is a noticeable variation in the number of fingers as well as their structure as the magnitude of α varies.

It is worth mentioning that, the effects of reversibility on the instability of the reactive system may vary based on the particular choice of densities gaps between the chemical species. To illustrate this, another simulation was carried out for the previous case of frontal instability, where instability takes place at the leading front using a different magnitude of densities ($G_A = 2, G_B = 1, G_C = 4$). In this case, the densities mismatch at the initial interface be-

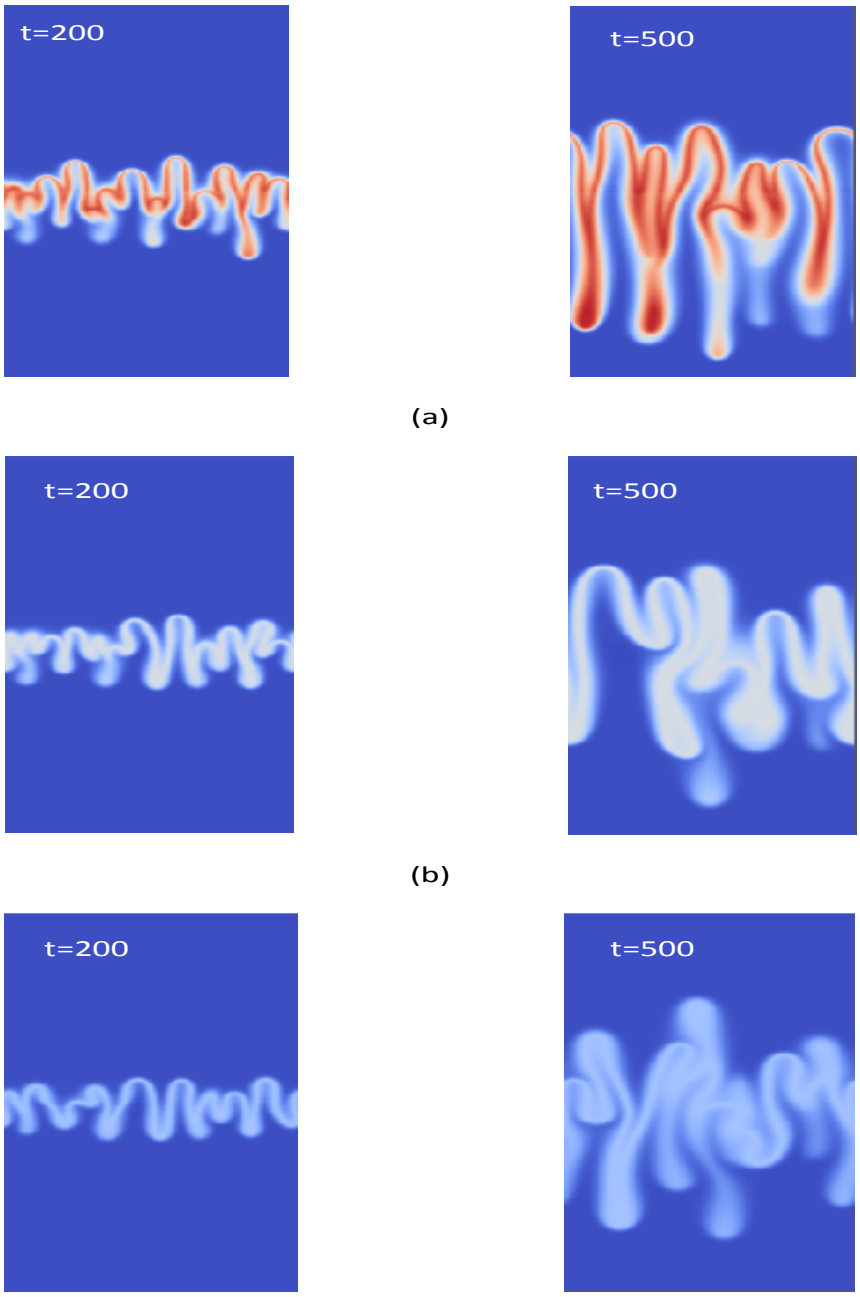

Figure 5.2: Concentration iso-surfaces for $G_A = 4$, $G_B = 1$, $G_C = 10$ (Stable trailing front, Unstable leading front): (a) $\alpha = 0.0$, (b) $\alpha = 0.3$, (c) $\alpha = 0.8$

tween the reactants as well as that at the unstable leading front are smaller compared to the previous case ($G_A = 4, G_B = 1, G_C = 10$) and the results for both complete and reversible reactions are presented in Figure 5.3. From the figure, it can be noticed that reversibility still attenuates the instability of the system. However, the variation in the magnitude of reversibility had no effect on both the development and structure of fingers.

When the density of the product (C) is smaller than those of both reactants, the variation of densities is favourable at the trailing front ($G_C > G_B$) and unfavourable at the leading one($G_A < G_C$). This combination of densities mismatches triggers instability at the trailing front, while the leading front will be stable. A simulation was carried out for ($G_A = 4, G_B = 2, G_C = 1$) and It was found that here too, reversibility acts towards reducing the growth of fingers and results in more diffuse less developed fingers as shown in figure 5.4. In addition, similar fingers structures were observed for reversible reactions with different α as the variation in densities decreases ($G_A = 3, G_B = 2, G_C = 1$).

In a reactive displacement process, instability will not grow at the unstable front till a certain amount of product (C) is produced. Furthermore, for cases with an unstable initial front, where instability appears at only one of the trailing or the leading fronts the densities mismatch at the unstable front is always higher than that of the initial interface. As the reaction reverses and part of product (C) is converted to (A) and (B), the variation of densities between the reactants will attenuate the instability by decreasing the densities divergence at the unstable trailing or leading front. Furthermore, The existence of a stable front limits the degree of mixing between the reactants and this, in addition to the reduction in the amount of chemical product, attenuate the instability of the flow. This also explains the unnoticeable effect of increasing the magnitude of reversibility in the development and fingering structure in the case where a small variation between the densities mismatch at

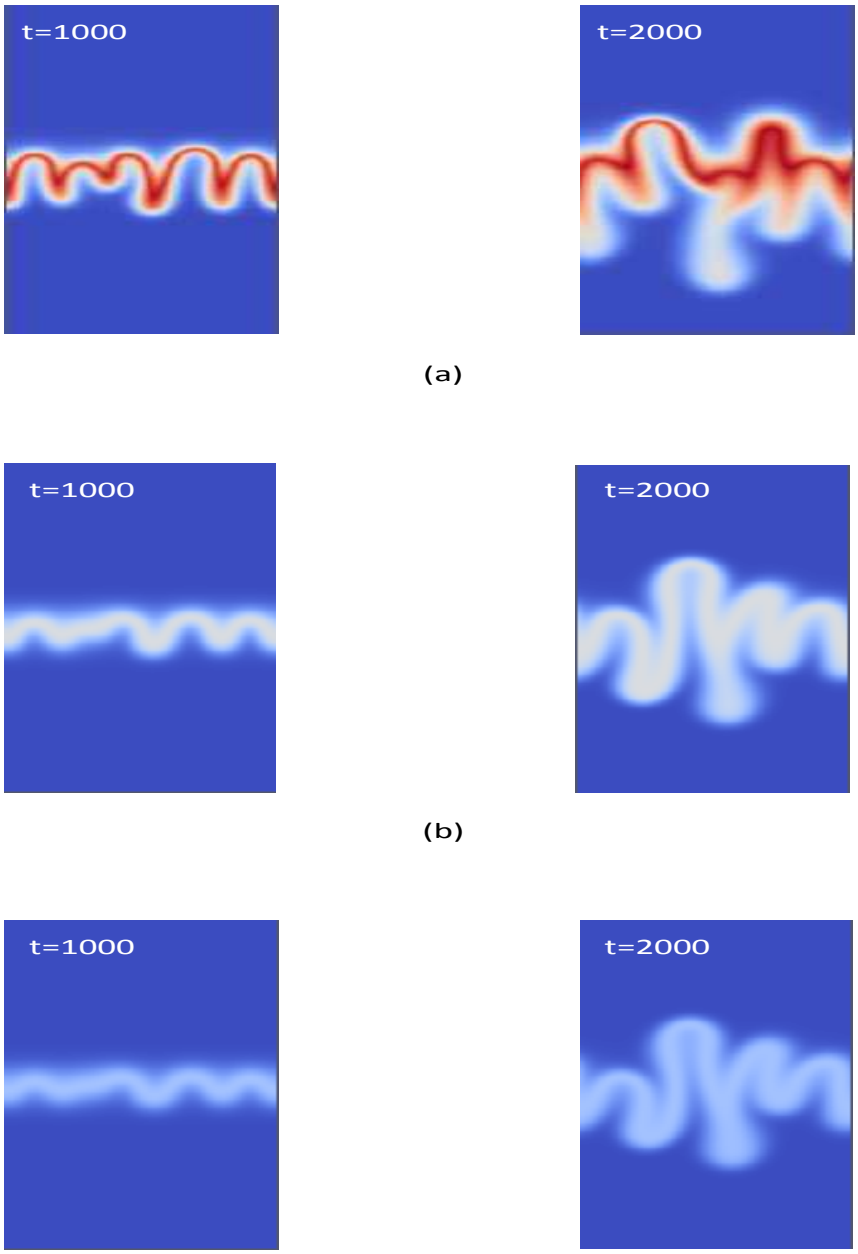

Figure 5.3: Concentration iso-surfaces for $G_A = 2$, $G_B = 1$, $G_C = 4$ (Stable trailing front, Unstable leading front): (a) $\alpha = 0.0$, (b) $\alpha = 0.3$, (c) $\alpha = 0.8$

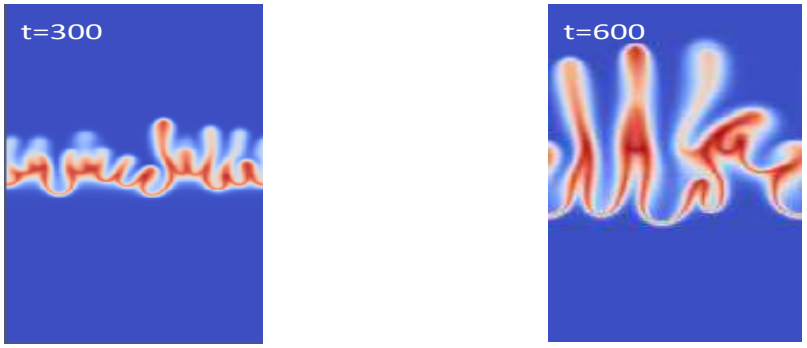

(a)

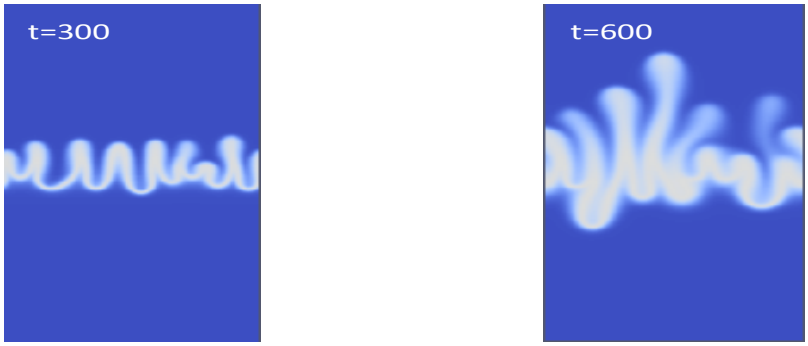

(b)

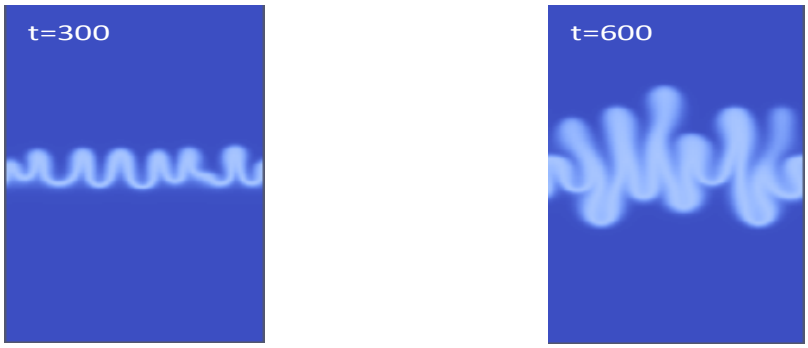

(c)

Figure 5.4: Concentration iso-surfaces for $G_A = 4$, $G_B = 2$, $G_C = 1$ (Unstable trailing front, Stable leading front): (a) $\alpha = 0.0$, (b) $\alpha = 0.3$, (c) $\alpha = 0.8$

the initial and the unstable leading fronts is considered ($G_A = 2, G_B = 1, G_C = 4$)

For displacements where the density of the product (C) lies between those of the two reactants, the trailing and leading fronts are both unstable ($G_C > G_B$, $G_C < G_A$) as shown in Figure 5.5 for $G_A = 3, , G_B = 1$ and $G_C = 2$. In this particular case, it can be noticed that reversibility has small tendency to attenuate the instability of the system. The limited effect of reversibility in the instability of such a system is due to the fast mixing between the reactants as instability takes place at both the trailing and the leading fronts. In addition, the variations between densities at both fronts are less than that of the initial interface and as the reaction reverses, the favourable densities mismatch between the reactants helps instability to keep growing regardless of how fast product (C) is converted back to (A) and (B). It should be noted that in this particular case, stronger reversibility has a hardly noticeable effect on the structure of fingers.

In all previous cases, reversibility tends to attenuate or slightly enhance the instability of the reactive system. However, the effect of reversibility on the instability where both the trailing and the leading fronts are unstable may vary as the densities gap between the reactants increases. This is well illustrated in figure 5.6 where $G_A = 4, G_B = 1$ and $G_C = 2$. For this choice of the density coefficients, there is actually a tendency for the fingers at both the trailing and leading fronts to extend more and have more interactions, when the reaction is reversible. Here, the fingers are more diffuse but more developed in the reversible cases, and the change in the degree of reversibility ($i.e.\alpha$) does actually have a strong noticeable effect on the fingers structures.

The strong effect of reversibility in increasing the instability at the leading front can be explained by looking at the variation of density coefficients at that interface. When the

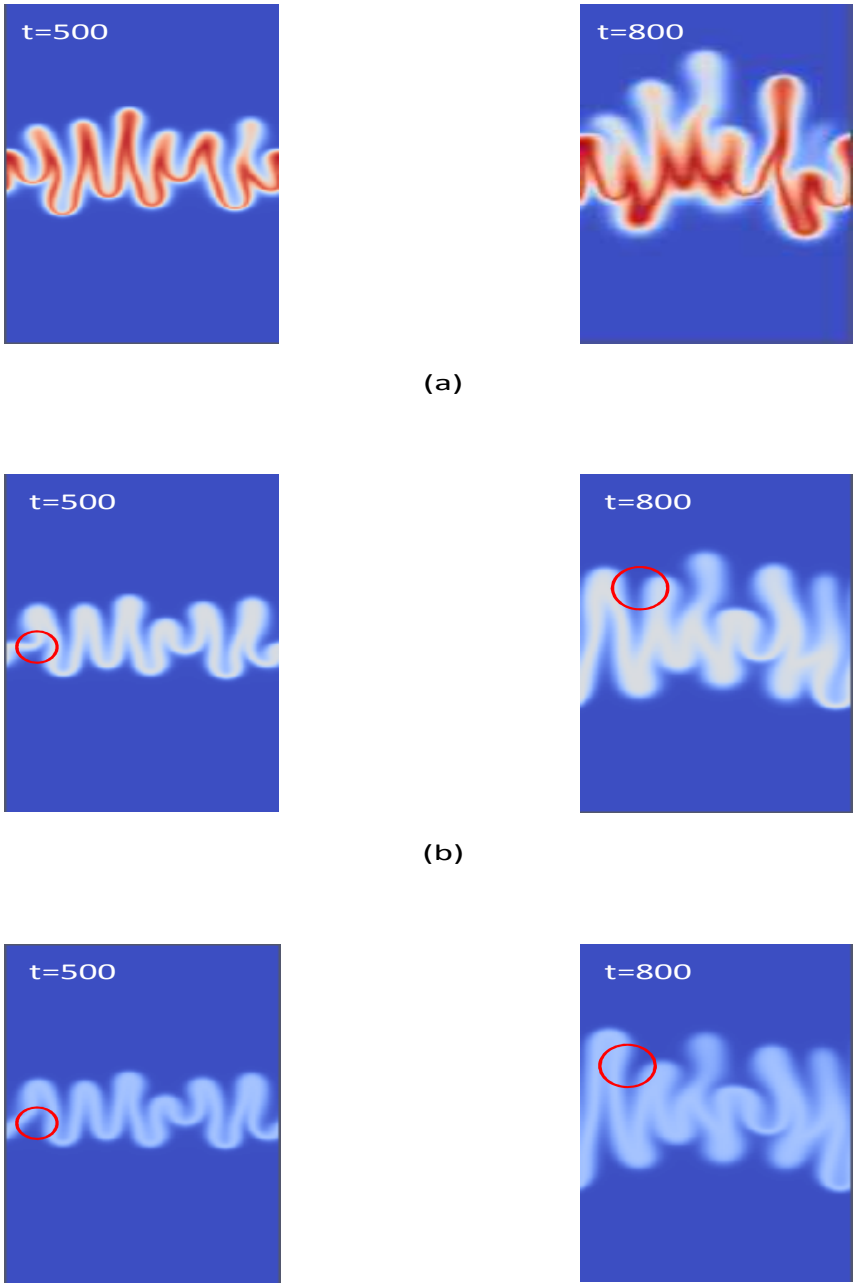

Figure 5.5: Concentration iso-surfaces for $G_A = 3$, $G_B = 1$, $G_C = 2$ (Unstable trailing front, Unstable leading front): (a) $\alpha = 0.0$, (b) $\alpha = 0.3$, (c) $\alpha = 0.8$

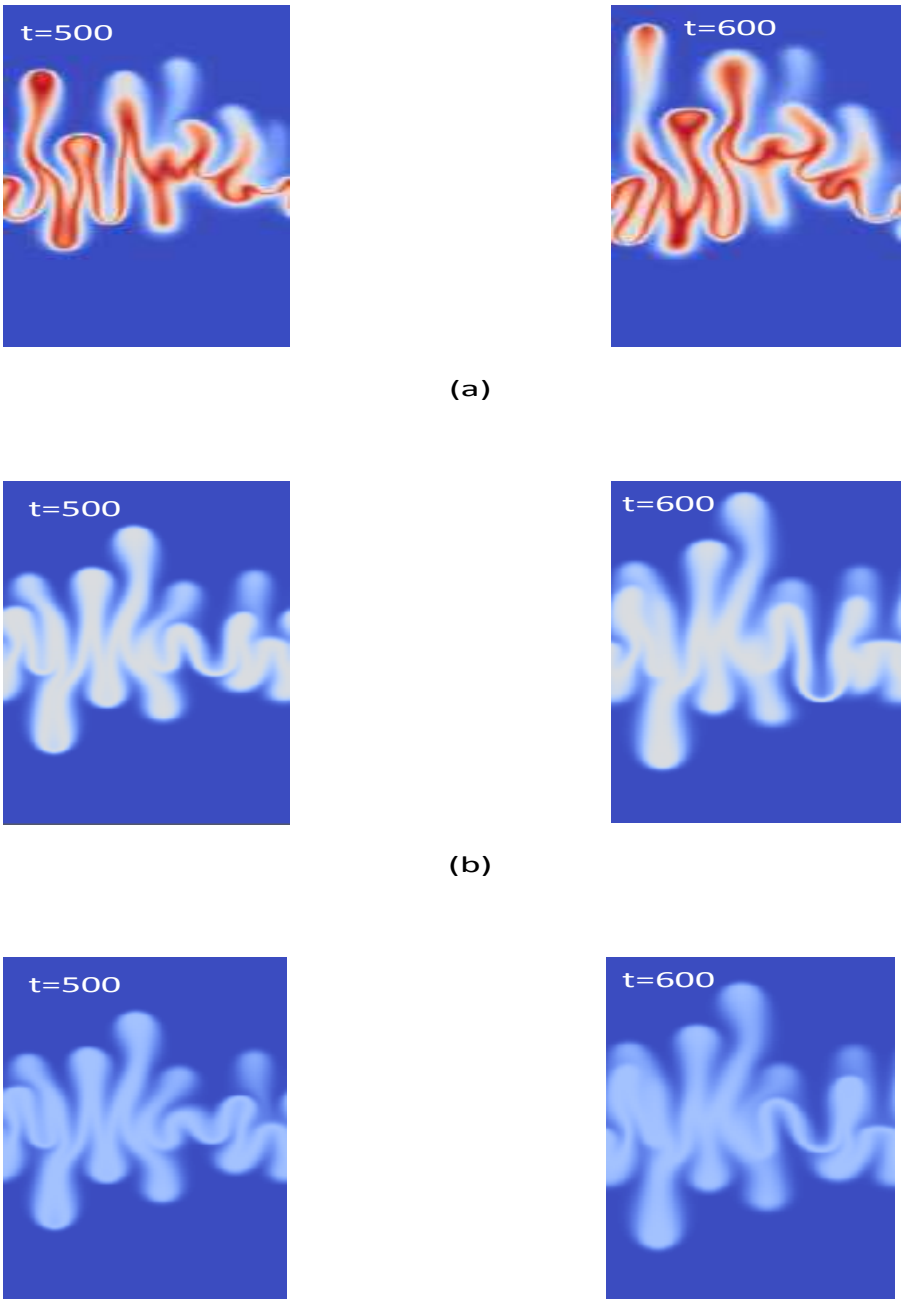

Figure 5.6: Concentration iso-surfaces for $G_A = 4$, $G_B = 1$, $G_C = 2$ (Unstable trailing front, Unstable leading front): (a) $\alpha = 0.0$, (b) $\alpha = 0.3$, (c) $\alpha = 0.8$

chemical reaction is complete, the growth of instability at the leading front depends on the densities gap between reactant (B) and product (C) ($G_B = 1, G_C = 2$). However, as the reaction reverses, the favourable densities mismatch of the initial interface ($G_A = 4, G_B = 1$) increases the variation in densities mismatch at the leading front, which explains the effect of reversibility in boosting instability at that front. On the other hand, the small variation in densities gaps at the initial and the trailing fronts explains the limited effect of reversibility on the instability at the trailing front.

Stable or neutrally stable initial reactive front ($G_A \leq G_B$)

The initial interface between the two reactants is stable or neutrally stable if the density of the displacing fluid is either smaller or equal to that of the displaced fluid ($G_B \leq G_A$). However, as the reaction takes place and product (C) appears at the initial interface, instability may develop at either the trailing or the leading front, but not both based on the density of the product. The case where the density of (C) lies between those of (B) and (A) or equal to both or any of them ($G_B \geq G_C \geq G_A$) will result in a stable displacement process and therefore, will not be discussed. In what follows, the two cases where instability appears at only one of the trailing or the leading fronts are discussed.

An unstable trailing front and a stable leading front is observed in the case where density of (C) is smaller than that of both reactants. On the other hand, an unstable leading front and a stable trailing front is observed when the density of product (C) is higher than those of both reactants ($G_A = 1, G_B = 2, G_C = 5$) as shown in figure 5.7. It is worth mentioning that unlike the previously discussed cases with an unstable initial front, the mixing between the two reactants when the initial front is stable is mainly controlled by diffusion. As a result, the growth of fingers is rather slow compared to cases with unstable initial fronts. In both cases, reversibility tends to reduce the instability at the unstable front and may actually result in a stable system for a period of time. This reduction in instability is due to the fact

that the unfavourable densities gap between the reactants reduces the variation of densities at the unstable front. However, depending on the magnitude of reversibility coefficient and the variation of densities at the unstable front, instability will eventually appear at the unstable front at later times. A small reversibility coefficient combined with a large densities gap will result in an earlier development of the instability at the unstable front as shown in figure 5.9. The complete stabilization of the system in these cases is due to the limited amount of the product (C) at the unstable front, which in addition to the very weak mixing between the reactants delay the development of instability.

The case where instability takes place at the trailing front ($G_A = 2, G_B = 4, G_C = 1$) was also examined. Here too, reversibility attenuated the instability and resulted in stable system for a period of time as shown in figure 5.8.

5.3.4 Effect of mobility ratios

In a displacement process, the variations in the densities of the fluids involved are not the only source of instability. In fact, frontal instability can also be encountered as the viscosities of these fluids vary. In a displacement process, The interface between the displacing and displaced fluid is unstable or stable, if the viscosity of the displacing fluid is lower or higher than that of the displaced one, respectively. In this part, the effect of viscosities mismatch on the instability of a reversible-reactive displacement process is examined by including the variations of viscosities in addition to densities of the species involved in the displacement.

In a vertical displacement process, a stable or neutrally stable viscous interface ($R_b \leq 0$) between the fluids will limit the degree of mixing between the chemical species and consequently attenuates the instability of the system. Moreover, a favourable mobility ratio ($R_b > 0$) at the initial interface will help the mixing between the species and enhance the instability of the system. However, in absence of injection, the mixing between the species

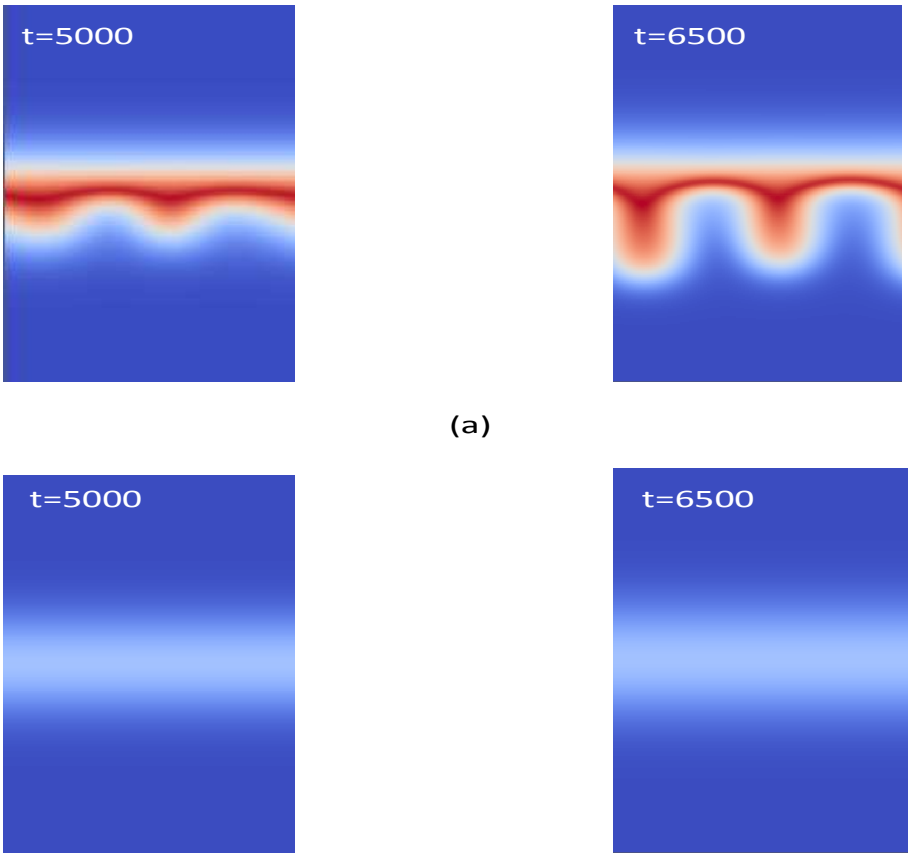

Figure 5.7: Concentration iso-surfaces for $G_A = 1$, $G_B = 2$, $G_C = 5$ (Stable trailing front, Unstable leading front): (a) $\alpha = 0.0$, (b) $\alpha = 0.8$

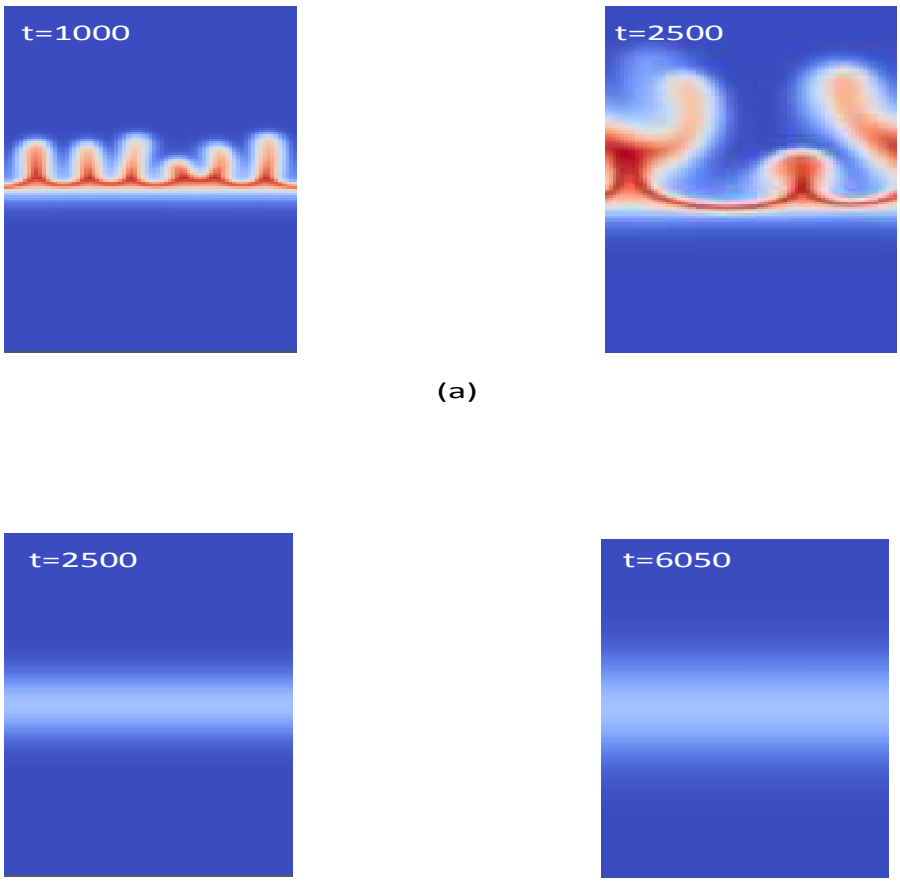

Figure 5.8: Concentration iso-surfaces for $G_A = 2$, $G_B = 4$, $G_C = 1$ (Unstable trailing front, Stable leading front): (a) $\alpha = 0.0$, (b) $\alpha = 0.8$

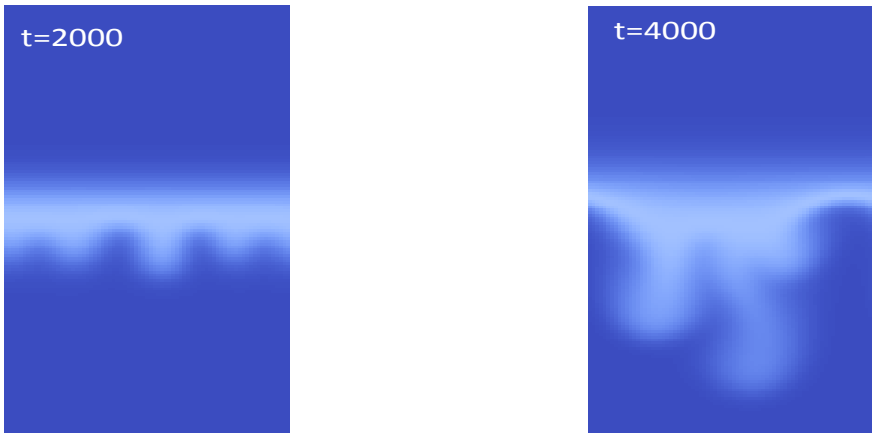

Figure 5.9: Concentration iso-surfaces for $G_A = 1$, $G_B = 2$, $G_C = 10$, $\alpha = 0.8$ (Stable trailing front, Unstable leading front)

is controlled by diffusion rather than convection.

Starting with the unstable initial viscous interface, mobility ratios of $R_b = 2$ and $R_c = 3$, which make both the trailing $(R_C/2)$ and the leading $(R_b - R_c/2)$ fronts viscously unstable. Figure 5.10 depicts the non-linear simulation results for the examined case for both complete $(\alpha = 0)$ and extremely reversible reactions $(\alpha = 0.8)$. From the figure, it can be noticed that the growth of the instability is much weaker compare to the same case in absence of mobility ratios (figure 5.6).

The case where the viscous initial interface between the reactants is stable $(R_b < 0)$ is examined using mobility ratios of $R_b = -2$ and $R_c = 3$. Here, the trailing front is viscously unstable $(R_c/2)$, while the leading front is viscously stable. The non-linear simulation results are presented for both cases of complete $(\alpha = 0)$ and extremely reversible $(\alpha = 0.8)$ reactions in figure 5.11. In this case, the unfavourable mobility ratio between the reactants (R_b) enhances the mixing between the chemical species, which enriched the instability of the system and resulted in an earlier development of the instability compare to the same case in absence of viscosities mismatch (figure 5.3).

It is worth mentioning that in the previous two cases, reversibility had an opposite influence on the instability where it enhanced/attenuated the instability instead of attenuating/enhancing the instability for the cases $(G_A = 2, G_B = 1, G_C = 4)$ and $(G_A = 4, G_B = 1, G_C = 2)$, respectively. Furthermore, the previous two cases were considered as one of the densities or viscosities mismatch was in favour of the growth of the instability while the other was not. Whereas, the instability will be enhanced/attenuated when both densities and viscosities mismatches are in favour of the growth/reduction of the instability. Finally, it should be stressed that these results are observed in absence of injection and the effect of

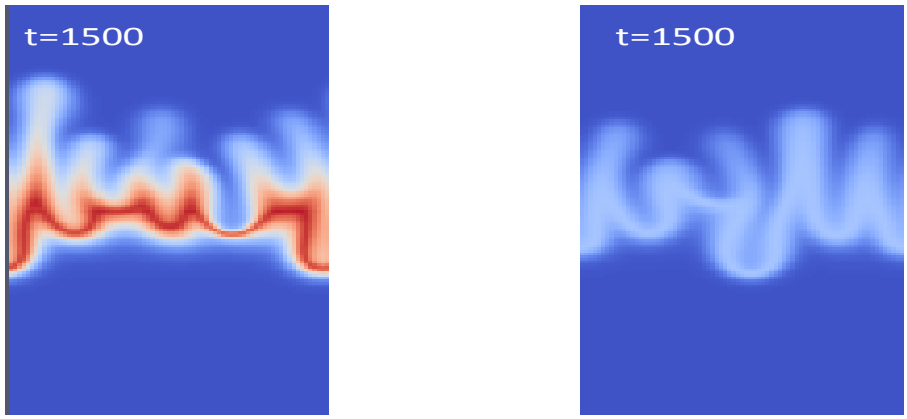

Figure 5.10: Concentration iso-surfaces for $G_A = 4$, $G_B = 1$, $G_C = 2$, $R_b = 2$, $R_c = 3$: (a) $\alpha = 0.0$, (b) $\alpha = 0.8$

viscosities on the instability may vary with the speed of injection.

The observed effects of the variation of viscosities can be explained by the countered relation between viscosity and diffusion [31], [130]. In absence of injection, the mixing is controlled by diffusion and the increased/decreased mobility ratio between the reactants limits/helps the mixing between the reactants and consequently attenuates/enhances the instability.

5.3.5 Quantitative analysis

In this part, the effect of reversibility on the instability of the reactive system is illustrated by presenting the relative contact areas (R.C.A.) of the system, which is defined as the area of contact between the species involved in the displacement process scaled by the cross-sectional area of the cell. This contact area is determined by measuring the length of a contour that corresponds to a specific concentration's value of one of the species, which is the product(C) in this case. There are two contact interfaces to be measured one correspond to the leading front and the other to the trailing front. The contour that correspond to concentration of 0.01 of the chemical product ($C = 0.01$), is used to determine the length of the contact areas

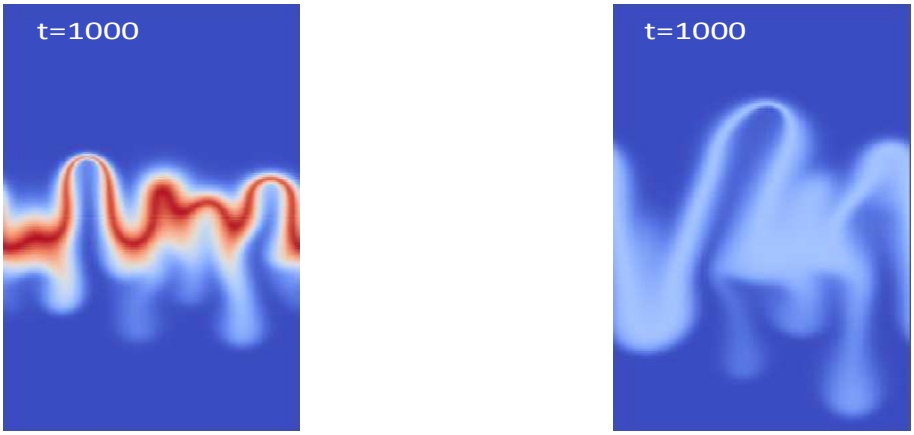

Figure 5.11: Concentration iso-surfaces for $G_A = 2$, $G_B = 1$, $G_C = 4$, $R_b = -2$, $R_c = 3$: (a) $\alpha = 0.0$, (b) $\alpha = 0.8$

at both fronts.

Measuring the contact area between the species is a good criteria to quantify the complexity of instability. Moreover, this contact area is expected to increase as the complexity of fingering structure increases. Here, the R.C.A for the case where an increase in the instability of the reactive front was observed ($G_A = 4, G_B = 1, G_C = 2$) is calculated. Figure 5.12 illustrates the variation in R.C.A with time for the case, where densities mismatch triggers instability at both fronts in absence of mobility ratios between the chemical species. The results confirm what have been reported in the qualitative part where an increase in the instability of the leading front has been observed as the reaction reverses. Furthermore, it can be noticed that the growth of instability or equivalently the contact area between the species at the trailing front is higher than that at the leading one, which is a result of the higher densities mismatch at the trailing front. Furthermore, the relative contact areas were also calculate for the cases were instability is triggered by both densities and viscosities mismatch and it was observed that the contact areas grow faster/slower than cases with densities mismatch only as the viscosities mismatches enhanced/attenuated the instability

as the reactions reverse.

It is worth mentioning that the growth of the instability when the reaction reverses is always slower than that of complete reactions at both the trailing and the leading fronts at early stages, which is a result of the reduction in the total amount of the chemical product (C). However, as time proceed and more products accumulate at the reactive interfaces, the effect of converting part of (C) back to (A) and (B) become more pronounced.

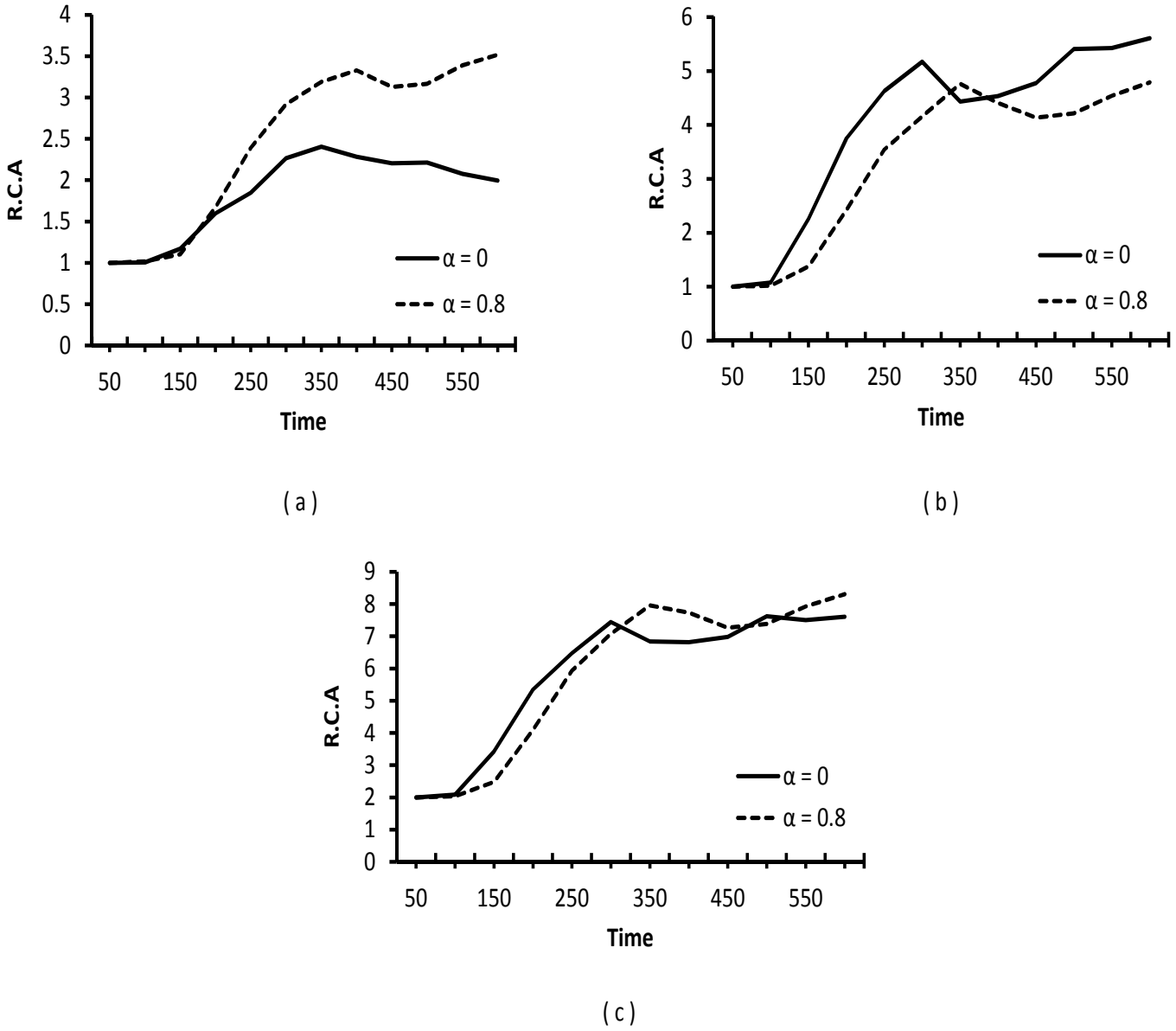

Figure 5.12: Concentration iso-surfaces for $G_A = 4$, $G_B = 1$, $G_C = 2$, $R_b = R_c = 0$: (a) R.C.A. at Leading Front, (b) R.C.A. at Trailing Front, (c) Total R.C.A.

5.4 Conclusion and discussion

The main objective of this study was to illustrate the effect of reversibility on the overall efficiency of a vertical reversible reactive displacement process, where frontal instability is triggered by the densities combined or not with viscosities mismatch between the reactants and the product. The non-linear interaction between the fluids was capture for different scenarios of frontal instability at a specific set of parameters. It was found that, the fate of the displacement process can be dramatically influenced when a reversible chemical reaction takes place between the displacing and the displaced fluids, which introduces a new fluid with a viscosity and density that might be different than those of both reactants. The dynamics of fingering were mainly controlled by the viscosities and densities mismatch at the initial as well as the trailing and the leading fronts in addition to the magnitude of reversibility.

The development of instability was much faster in cases where the initial front between the reactant was unstable ($G_A > G_B$) compare to cases with a stable initial front ($G_A < G_B$) and this is due to the higher production rate in former cases, which is a result of the quick mixing between the reactants. The frontal instability of the reactive leading and trailing fronts determine the direction of fingers development, where they develop in the upstream or downstream direction when instability appears only at the trailing or the leading front, respectively if not in both directions when both fronts are unstable.

In absence of mobility ratios, the effect of reversibility of the chemical reaction was found to be similar for cases where only one of the trailing or the leading front is unstable regardless of the stability of the initial front. For those cases, the reduction in fingering instability increases analogously with the increase in the magnitude of reversibility. Indeed, a complete stabilization of the system was reported for cases with stable initial fronts ($G_A < G_B$). Moreover, for unstable initial fronts similar fingering structures were observed for reversible reactions

with different magnitude of reversibility as the densities gap between the reactants decreases. Furthermore, it was found that reversibility has a weak tendency to attenuate the instability when both of the reactive fronts are unstable combined with a hardly noticeable change in fingering structure when there is a small variation in densities ($G_a = 3, G_B = 1, G_C = 2$). However, an enhancement of the instability was observed as the variation of densities increases ($G_a = 4, G_B = 1, G_C = 2$). The quick mixing between the reactants in addition to the favourable densities mismatch between the reactants helped the continuous growing of instability regardless of the magnitude of reversibility.

Finally, it was observed that increasing the viscosities mismatch between the chemical species in order to achieve a viscously unstable trailing and leading fronts ($R_b = 2, R_c = 3$), attenuated the instability of the system by limiting the degree of mixing between the species. On the other hand, the stable initial viscous interface ($R_b < 0$) enhanced the instability of the displacement process.

Chapter 6

Conclusions and Recommendations

The reversibility of the chemical reaction has been shown to dramatically influence the properties of the chemical species and consequently the dynamics of reactive displacement processes in porous media. In this thesis, a model where a simple reversible bimolecular chemical reaction ($BRCR$) $A + B \leftrightharpoons C$ develops, is adopted. The reaction produces a new chemical species with properties that can be different that those of the reactants. The study focuses on the case where the initial interface between the displacing (A) and the displaced (B) reactants may be stable or unstable based on the physical properties of the chemical species. However, once the reactants come in contact and the chemical reaction takes place to produce (C), two reaction zones are defined. The trailing zone between reactant (A) and the product (C) and the leading zone between reactants (B) and the product (C) where the variations in the species properties trigger hydrodynamical instability at one or both of these zones. Here, the effects of reversibility on the instability of the different scenarios were examined in both horizontal and vertical geometry.

In the horizontal geometry, a detailed linear stability analysis was performed in order to investigate analytically and numerically the capability of the reversibility of the chemical reaction in modifying the flow instability. Here, the variation in the concentrations of the chemical species as a result of the reversible reaction induces the instability by modifying the viscosity profile. For unstable initial fronts, the effect of the reversibility varied between enhancing and attenuating the instability based on the particular choice of the mobility ratios at the initial as well as the trailing and the leading fronts. On the other hand, it was observed that reversibility always attenuates the instability when the initial front between

the reactants is stable.

For the same geometry, the non-linear interactions between the chemical species were illustrated by performing non-linear simulations. In agreement with the linear stability analysis, it was observed that reversibility may stabilize the unstable system for a period of time that increases analogously with increasing and decreasing the reversibility coefficient (α) and the mobility ratio, respectively at the unstable front when the initial interface is stable. Furthermore, the capability of reversibility to enhance the instability was also illustrated. This particular case was observed when the effects of the direction of the flow, which is in favour of the growth of the instability at the leading but not the trailing fronts, were combined with the role of reversibility in increasing the mobility ratio at the leading front. In addition, the enrichment of the instability as the reaction reverses was presented by determining the relative contact areas between the chemical species at both the trailing and the leading fronts.

In parallel, the effects of reversibility on the instability of the reactive displacements have also been examined in a vertical geometry. Here, the growth of the instability can be influenced by either the densities or both the densities and the viscosities mismatches between the chemical species. In absence of viscosity mismatch, reversibility was found to attenuate the instability when the initial buoyancy interface is stable. Indeed, the unstable system can be stabilized for a period of time before stability takes place at the unstable trailing or leading front. The time at which instability takes place depends on both the strength of the reversibility as well as the densities gap at the unstable trailing or leading front. Furthermore, it was observed that based on the particular choice of densities gaps at the trailing and the leading fronts, reversibility may enhance the instability when the initial interface is unstable. Counter relation between the viscosity and the diffusion coefficient resulted in an earlier development of the instability when the initial front was viscously stable.

The scope of the present research can be expanded for future studies on the same topic. In the present study it was assumed that the porous media is homogeneous with a simple isothermal bimolecular reversible chemical reaction taking place between the reactants with no interactions with the medium. However, since many chemical reactions are actually endothermic or exothermic, it would be interesting to consider the influence of the temperature on the physical properties of the chemical species and the role of the variation of the temperature on the instability of the reversible reactive flows. Furthermore, it is recommended for future studies to consider the effects of the chemical interactions between the fluids and the medium such as precipitation in addition to the heterogeneity of the porous medium.

Appendix A

Derivation of The Stability Characteristic Equation

The continuity conditions are obtained by taking the integral of equations (3.30)–(3.32) across the initial interface ($x = 0$). Starting with integrating the velocity perturbation equation (3.32) from 0^- to 0^+:

$$\int_{0^-}^{0^+} \left[\mu_0 \frac{d^2\phi}{dx^2} + \frac{\partial \mu_0}{\partial x}\frac{d\phi}{dx}\right] \mathrm{d}x - \int_{0^-}^{0^+} \mu_0 k^2 \phi \, \mathrm{d}x = \int_{0^-}^{0^+} \mu_0 k^2 \left[R_b - \frac{R_c}{2}\right] \psi_B \, \mathrm{d}x - \int_{0^-}^{0^+} \mu_0 k^2 \frac{R_c}{2} \psi_A \, \mathrm{d}x \tag{A.1}$$

The continuity of the perturbation and the velocity impose that the last three integrals in (A.1) are zeros, which result in:

$$\int_{0^-}^{0^+} \frac{d}{dx}\left[\mu_0 \frac{d\phi}{dx}\right] \mathrm{d}x = 0 \tag{A.2}$$

and as a result:

$$\left[\mu_0 \frac{d\phi}{dx}\right]_{0^-}^{0^+} = 0 \tag{A.3}$$

The above equation (A.3) expresses the continuity of pressure across the initial interface. The second condition is obtained by taking the integral of equation (3.32) twice, which results in:

$$[\phi]_{0^-}^{0^+} = 0 \tag{A.4}$$

The other conditions are obtained by integrating once and twice equations (3.30) and (3.31) across $x = 0$:

$$\int_{0^-}^{0^+} -\frac{d^2}{dx^2}\psi_A \, \mathrm{d}x + \int_{0^-}^{0^+} \left[\sigma(t_0) + k^2 + D_a B_0 + \frac{D_r}{2}\right] \psi_A \, \mathrm{d}x = -\int_{0^-}^{0^+} \frac{\partial A_0}{\partial x}\phi \, \mathrm{d}x - \int_{0^-}^{0^+} (D_a A_0 + \frac{D_r}{2})\psi_B \, \mathrm{d}x, \tag{A.5}$$

Imposing the continuity of perturbation and velocity across the initial interface ($x = 0$) and the property of the delta function ($\partial A_0/\partial x = \partial H(-x)/\partial x = -\delta(x)$) yields

$$\int_{0^-}^{0^+} -\frac{d^2}{dx^2}\psi_A \, \mathrm{d}x = -\int_{0^-}^{0^+} -\delta(x)\phi \, \mathrm{d}x, \tag{A.6}$$

Which can me simplified to:

$$\left[\frac{d\psi_A}{dx}\right]_{0^-}^{0^+} = -\phi(0). \tag{A.7}$$

Integrating equation (3.30) twice across $x = 0$ yields

$$[\psi_A]_{0^-}^{0^+} = 0 \tag{A.8}$$

Similarly for equation (3.31), the integral once and twice across $x = 0$ yields

$$\left[\frac{d\psi_B}{dx}\right]_{0^-}^{0^+} = \phi(0) \tag{A.9}$$

and

$$[\psi_B]_{0^-}^{0^+} = 0. \tag{A.10}$$

The above conditions result in a system of six algebraic equations for the unknowns and the determinant of the coefficient matrix has to be zero for non-trivial solutions

$$\begin{pmatrix}
1 & -\frac{D_r}{2D_a+D_r} & 1 & -1 & 0 & 0 \\
1 & -1 & -\frac{D_r}{2D_a+D_r} & -1 & 0 & 0 \\
\gamma_0 + \frac{(R_b-R_c)k^2}{\gamma_0^2-k^2} & -\frac{\gamma_1 D_r}{2D_a+D_r} & \gamma_1 + \frac{(R_b(2D_a+D_r)-R_cD_a)k^2}{(\gamma_1^2-k^2)(2D_a+D_r)} & \gamma_0 & 1 & 0 \\
\gamma_0 - \frac{(R_b-R_c)k^2}{\gamma_0^2-k^2} & \gamma_1 & -(\frac{(R_b(2D_a+D_r)-R_cD_a)k^2}{(\gamma_1^2-k^2)(2D_a+D_r)} + \frac{\gamma_1 D_r}{2D_a+D_r}) & \gamma_0 & -1 & 0 \\
\frac{(R_b-R_c)k^2}{\gamma_0^2-k^2} & \frac{(R_b(2D_a+D_r)-R_cD_a)k^2}{(\gamma_1^2-k^2)(2D_a+D_r)} & \frac{(R_bD_r+R_cD_a)k^2}{(\gamma_1^2-k^2)(2D_a+D_r)} & \frac{(R_c-R_b)k^2}{\gamma_0^2-k^2} & 1 & -1 \\
e^{R_b}\frac{(R_b-R_c)k^2}{\gamma_0^2-k^2}\gamma_0 & -\frac{(R_bD_r+R_cD_a)k^2}{(\gamma_1^2-k^2)(2D_a+D_r)}\gamma_1 & e^{R_b}\frac{(R_b(2D_a+D_r)-R_cD_a)k^2}{(\gamma_1^2-k^2)(2D_a+D_r)}\gamma_1 & \frac{(R_b-R_c)k^2}{\gamma_0^2-k^2}\gamma_0 & ke^{R_b} & k
\end{pmatrix}$$

$$\times \begin{pmatrix} A^+ \\ A^- \\ B^+ \\ B^- \\ G^+ \\ G^- \end{pmatrix} = \begin{pmatrix} 0 \\ 0 \\ 0 \\ 0 \\ 0 \\ 0 \end{pmatrix} \tag{A.11}$$

Solving the above system results in the implicit relation (equation 3.48) between the growth rate σ and the wavenumber k.

Appendix B

Non-linear Simulation - Pseudo-Spectral Method

In this thesis, the non-linear simulation numerical code was performed based on the pseudo-spectral method. The Hartley transform based on pseudo-spectral method, which is a special case of Fourier transformation, was used to solve the dynamics equations for the reactive flow. Hartley transformation was first used by [27] to solve viscous fingering related problems. The general form of the Hartley transform is:

$$G(s) = \mathcal{H}\langle g(t)\rangle = \int_{-\infty}^{\infty} g(t) cas(2\pi st)\,\mathrm{d}t. \tag{B.1}$$

Where $\mathcal{H}$ represent the transform function and $cas(\alpha) = \cos(\alpha) + \sin(\alpha)$. Here, a two-dimensional discrete Hartley transform is used [131], which for an arbitrary function $g(x, y)$ gives

$$G(k_x, k_y) = \mathcal{H}\langle g(x, y)\rangle = \frac{1}{\sqrt{N_x N_y}} \sum_x \sum_y g(x, y) cas\left(\frac{2\pi k_x x}{N_x}\right) cas\left(\frac{2\pi k_y y}{N_y}\right). \tag{B.2}$$

Where k_x and k_y represent the discrete wave-numbers and N_x and N_y are the number of spectral modes in the x and y directions, respectively. The transform of a derivative of a function using the Hartley derivative theorem is obtained as

$$\mathcal{H}\left\langle \frac{\partial}{\partial x} g(x, y) \right\rangle = -2\pi k_x G(-k_x, k_y). \tag{B.3}$$

For brevity the numerical procedure is presented for only one of the chemical species (A). Here, A_0 and A' represent the base state and the perturbation concentrations, respectively and the total concentration is

$$A(x, y, t) = A_0(x, t) + A'(x, y, t), \tag{B.4}$$

Recall the RDC equation for transport of (A) and vorticity equation as:

$$\frac{\partial A}{\partial t} + \mathbf{u}.\nabla A = \nabla^2 A - D_a AB + D_r C, \tag{B.5}$$

$$\omega = R_b\left(\frac{\partial\psi}{\partial x}\frac{\partial B}{\partial x} + \frac{\partial\psi}{\partial y}\frac{\partial B}{\partial y} + \frac{\partial B}{\partial y}\right) + R_c\left(\frac{\partial\psi}{\partial x}\frac{\partial C}{\partial x} + \frac{\partial\psi}{\partial y}\frac{\partial C}{\partial y} + \frac{\partial C}{\partial y}\right), \tag{B.6}$$

Where ψ is the stream-function and is related to the vorticity as:

$$\nabla^2\psi = -\omega, \tag{B.7}$$

Using the expressions for total concentration in (B.5) yeilds:

$$\frac{\partial A'}{\partial t} = \left(\frac{\partial^2}{\partial x^2} + \frac{\partial^2}{\partial y^2}\right)A' - J_A, \tag{B.8}$$

Where J_A represents the non-linear terms in the above equation:

$$J_A(x,y,t) = \frac{\partial\psi}{\partial y}\left(\frac{\partial A_0}{\partial x} + \frac{\partial A'}{\partial x}\right) - \frac{\partial\psi}{\partial x}\frac{\partial A'}{\partial y} + D_a(A'B' + A'B_0 + A_0B') - D_rC', \tag{B.9}$$

While the Base-State solution $A_0(x,t)$:

$$\frac{\partial A_0}{\partial t} = \frac{\partial^2 A_0}{\partial x^2} - D_aA_0B_0 + D_rC_0, \tag{B.10}$$

The two dimensional domain of size $P_e \times P_e/Ar$ is divided into $N_x \times N_y$ domain of size dx and dy where $P_e = N_x.dx$ and $P_e/A = N_y.dy$. The collocation points are defined as

$$x_m = \frac{m}{N_x}.P_e, \quad m = 0, 1, 2, ..., N_x - 1. \tag{B.11}$$

$$y_n = \frac{n}{N_y}.\frac{P_e}{A_r}, \quad n = 0, 1, 2, ..., N_y - 1. \tag{B.12}$$

In Hartley modes, flow variables (A'), (ψ), (ω) and (J_A) are expanded as:

$$A'(x,y,t) = \frac{1}{\sqrt{N_xN_y}}\sum_{m=0}^{N_x-1}\sum_{n=0}^{N_y-1}\check{A}(t)cas(k_mx + k_ny), \tag{B.13}$$

$$\psi(x,y,t) = \frac{1}{\sqrt{N_xN_y}}\sum_{m=0}^{N_x-1}\sum_{n=0}^{N_y-1}\check{\psi}(t)cas(k_mx + k_ny), \tag{B.14}$$

$$\omega(x,y,t) = \frac{1}{\sqrt{N_xN_y}}\sum_{m=0}^{N_x-1}\sum_{n=0}^{N_y-1}\check{\omega}(t)cas(k_mx + k_ny), \tag{B.15}$$

$$J_A(x,y,t) = \frac{1}{\sqrt{N_xN_y}}\sum_{m=0}^{N_x-1}\sum_{n=0}^{N_y-1}\check{J}_A(t)cas(k_mx + k_ny), \tag{B.16}$$

where

$$k_m = \frac{2\pi m}{P_e}, \quad k_n = \frac{2\pi n}{P_e/A_r}, \quad m, n = 0, 1, 2, ... \tag{B.17}$$

First, the non-linear terms ω and J_A are evaluated in the real space before they are transformed to the Hartley space.

The equations (B.6) - (B.8) in Hartley space are

$$\frac{d\check{A}}{dt} = -\check{J}_A - (k_m^2 + k_n^2)\check{A}, \tag{B.18}$$

$$\check{\psi} = \frac{\check{\omega}}{(k_m^2 + k_n^2)}, \tag{B.19}$$

The Hartley transform allows recasting the partial differential equations in space and time into ordinary differential equations in time. known variables at a given time t can be used to predict the concentration at time $t + \Delta t$ according to (B.18) and then the stream-function can be updated with (B.19). A semi-implicit predictor-corrector scheme along with operator-splitting techniques are used for time stepping of the dynamic equations. Equation (B.18) can be rearranged as:

$$\left(\frac{d\check{A}}{dt} + (k_m^2 + k_n^2)\check{A}\right)e^{-(k_m^2+k_n^2)t} = -\check{J}_A e^{-(k_m^2+k_n^2)t}, \tag{B.20}$$

Using the fact that $\check{A} = \check{A}e^{(k_m^2+k_n^2)t}$, the left hand side is further simplified to

$$\frac{d\check{A}}{dt} = -\check{J}_A e^{-(k_m^2+k_n^2)}, \tag{B.21}$$

The nonlinear convective reactive terms $\check{J}_A$ is advanced with a second order Adams-Bashforth method to compute a conditional value $\tilde{\check{A}}$ at $t + \Delta t$

$$\frac{\tilde{\check{A}}(t + \Delta t) - \check{A}(t)}{\Delta t} = \left(\frac{3}{2}\check{J}_A(t) - \frac{1}{2}\check{J}_A(t - \Delta t)\right)e^{-(k_m^2+k_n^2)t}, \tag{B.22}$$

and the predicted concentration value of $\tilde{A}(t + \Delta t)$ is computed by:

$$\tilde{A}(t + \Delta t) = \left[\check{A}(t) - \Delta t\left(\frac{3}{2}\check{J}_A(t) - \frac{1}{2}\check{J}_A(t - \Delta t)\right)\right]e^{-(k_m^2+k_n^2)\Delta t}, \tag{B.23}$$

The vorticity is updated using the predicted concentration from (B.23) then the velocity fields is updated using (B.19) before the correction evaluation sequence is imposed over the predicted values using the trapezoid rule for the nonlinear terms.

$$\check{A}(t+\Delta t) = \frac{1}{1+\Delta t(k_m^2+k_n^2)}\left[\check{A}(t) - \frac{1}{2}\Delta t(\tilde{J}_A(t+\Delta t) + \check{J}_A(t))\right]. \tag{B.24}$$

Bibliography

[1] W.-Z. Li, B. Dong, and Y.-C. Song, "Lbm simulation of viscous fingering phenomenon in a horizontal channel," *Dalian Ligong Daxue Xuebao/Journal of Dalian University of Technology*, vol. 52, no. 3, pp. 343 – 349, 2012.

[2] L. Riolfo, Y. Nagatsu, S. Iwata, R. Maes, P. Trevelyan, and A. De Wit, "Experimental evidence of reaction-driven miscible viscous fingering," *Physical Review E - Statistical, Nonlinear, and Soft Matter Physics*, vol. 85, no. 1, 2012.

[3] R. L. Slobod and B. H. Caudle, "X-ray shadowgrath studies of areal sweepout efficiencies," *Transactions of the American Institute of Mining and Metallurgical Engineers*, vol. 195, pp. 265–270, 1952.

[4] P. G. Saffman and G. Taylor, "The penetration of a fluid into a porous medium or hele-shaw cell containing a more viscous liquid," *Proceedings of the Royal Society of London. Series A, Mathematical and Physical Sciences*, vol. 245, no. 1242, pp. 312–329, 1958.

[5] G. M. Homsy, "Viscous fingering in porous media," *Annual Review of Fluid Mechanics*, vol. 19, pp. 271–311, 1987.

[6] K. V. McCloud and J. V. Maher, "Experimental perturbations to saffman-taylor flow," *Physics Report*, vol. 260, no. 3, pp. 139–185, 1995.

[7] W. X. Zhang, "Nanoscale iron particles for environmental remediation: An overview," *Journal of Nanoparticle Research*, vol. 5, no. 3-4, pp. 323–332, 2003.

[8] J. Ennis-King and L. Paterson, "Coupling of geochemical reactions and convective mixing in the long-term geological storage of carbon dioxide," *International Journal of Greenhouse Gas Control*, vol. 1, no. 1, pp. 86–93, 2007.

[9] C. B. Castells and R. C. Castells, "Peak distortion in reversed-phase liquid chromatography as a consequence of viscosity differences between sample solvent and mobile phase," *Journal of Chromatography A*, vol. 805, no. 1-2, pp. 55–61, 1998.

[10] D. W. Elliott and W.-X. Zhang, "Field assessment of nanoscale bimetallic particles for groundwater treatment," *Environmental Science and Technology*, vol. 35, no. 24, pp. 4922–4926, 2001.

[11] R. D. Ludwig, C. Su, T. R. Lee, R. T. Wilkin, S. D. Acree, R. R. Ross, and A. Keeley, "In situ chemical reduction of cr(vi) in groundwater using a combination of ferrous sulfate and sodium dithionite: A field investigation," *Environmental Science and Technology*, vol. 41, no. 15, pp. 5299–5305, 2007.

[12] A. B. Cundy, L. Hopkinson, and R. L. D. Whitby, "Use of iron-based technologies in contaminated land and groundwater remediation: A review," *Science of the Total Environment*, vol. 400, no. 1-3, pp. 42–51, 2008.

[13] J. Kotz, P. Treichel, and J. Townsend, *Chemistry & Chemical Reactivity*. Brooks Cole/Cengage Learning, 2009.

[14] H. Darcy, *Les fontaines publiques de la ville de Dijon*. Paris: Dalmont, 1856.

[15] S. Hill, "Channeling in packed columns," *Chemical Engineering Science*, vol. 1, no. 6, pp. 247–253, 1952.

[16] G. Taylor, "The instability of liquid surfaces when accelerated in a direction perpendicular to their planes. i," *Proceedings of the Royal Society of London. Series A, Mathematical and Physical Sciences*, vol. 201, no. 1065, pp. 192–196, 1950.

[17] D. J. Lewis, "The instability of liquid surfaces when accelerated in a direction perpendicular to their planes. ii," *Proceedings of the Royal Society of London. Series A, Mathematical and Physical Sciences*, vol. 202, no. 1068, pp. 81–96, 1950.

[18] R. L. Chuoke, P. van Meurs, and C. van der Poel, "Instability of slow, immiscible, viscous liquid-liquid displacements in permeable media," *Journal of Petroleum Technology*, vol. 11, no. 7, p. 6473, 1959.

[19] D. W. Peaceman and J. H. H. Rachford, "Numerical calculation of multidimensional miscible displacement," *Society of Petroleum Engineers Journal*, vol. 2, no. 4, pp. 327–339, 1962.

[20] C. W. Park and G. M. Homsy, "The instability of long fingers in hele-shaw flows," *Physics of Fluids*, vol. 28, no. 6, pp. 1583–1585, 1985.

[21] J. Nittmann and H. E. Stanley, "Tip splitting without interfacial tension and dendritic growth patterns arising from molecular anisotropy," *Nature*, vol. 321, no. 6071, pp. 663–668, 1986.

[22] E. Ben-Jacob and P. Garik, "The formation of patterns in non-equilibrium growth," *Nature*, vol. 343, no. 6258, pp. 523–530, 1990.

[23] E. Brener, H. Levine, and Y. Tu, "Nonsymmetric saffman-taylor fingers," *Physics of Fluids A*, vol. 3, no. 4, pp. 529–534, 1991.

[24] C. T. Tan and G. M. Homsy, "Stability of miscible displacements in porous media: Rectilinear flow," *Physics of Fluids*, vol. 29, no. 11, pp. 3549–3556, 1986.

[25] C. T. Tan and G. M. Homsy, "Simulation of nonlinear viscous fingering in miscible displacement," *Physics of Fluids*, vol. 31, no. 6, pp. 1330–1338, 1988.

[26] Y. C. Yortsos and M. Zeybek, "Dispersion driven instability in miscible displacement in porous media," *Physics of Fluids*, vol. 31, no. 12, pp. 3511–3518, 1988.

[27] W. B. Zimmerman and G. M. Homsy, "Viscous fingering in miscible displacements: Unification of effects of viscosity contrast, anisotropic dispersion, and velocity depen-

dence of dispersion on nonlinear finger propagation," *Physics of Fluids A*, vol. 4, no. 11, pp. 2348–2359, 1992.

[28] C. T. Tan and G. M. Homsy, "Viscous fingering with permeability heterogeneity," *Physics of Fluids A*, vol. 4, no. 6, pp. 1099–1101, 1992.

[29] M. A. Christie, A. H. Muggeridge, and J. J. Barley, "3d simulation of viscous fingering and wag schemes," *SPE Reservoir Engineering*, vol. 8, no. 1, pp. 19–26, 1993.

[30] H. A. Tchelepi and J. F. M. Orr, "Interaction of viscous fingering, permeability heterogeneity, and gravity segregation in three dimensions," *SPE Reservoir Engineering*, vol. 9, no. 4, pp. 266–271, 1994.

[31] O. Manickam and G. M. Homsy, "Fingering instabilities in vertical miscible displacement flows in porous media," *Journal of Fluid Mechanics*, vol. 288, pp. 75–102, 1995.

[32] A. Rogerson and E. Meiburg, "Shear stabilization of miscible displacement processes in porous-media," *Physics of Fluids A*, vol. 5, no. 6, pp. 1344–1355, 1993.

[33] A. Rogerson and E. Meiburg, "Numerical simulation of miscible displacement processes in porous media flows under gravity," *Physics of Fluids A*, vol. 5, no. 11, pp. 2644–2660, 1993.

[34] M. Ruith and E. Meiburg, "Miscible rectilinear displacements with gravity override. part 1. homogeneous porous medium," *Journal of Fluid Mechanics*, vol. 420, pp. 225–257, 2000.

[35] A. Riaz and E. Meiburg, "Radial source flows in porous media: Linear stability analysis of axial and helical perturbations in miscible displacements," *Physics of Fluids*, vol. 15, no. 4, pp. 938–946, 2003.

[36] B. K. Singh and J. Azaiez, "Numerical simulation of viscous fingering of shear-thinning fluids," *Canadian Journal of Chemical Engineering*, vol. 79, no. 6, pp. 961–967, 2001.

[37] A. De Wit, Y. Bertho, and M. Martin, "Viscous fingering of miscible slices," *Physics of Fluids*, vol. 17, no. 5, pp. 1–9, 2005.

[38] M. N. Islam and J. Azaiez, "New viscous fingering mechanisms at high viscosity ratio and Péclet number miscible displacements," *Journal of Porous Media*, vol. 10, no. 4, pp. 357–376, 2007.

[39] G. Rousseaux, M. Martin, and A. De Wit, "Viscous fingering in packed chromatographic columns: Non-linear dynamics," *Journal of Chromatography A*, vol. 1218, no. 46, pp. 8353 – 8361, 2011.

[40] M. C. Kim, "Linear stability analysis on the onset of the viscous fingering of a miscible slice in a porous medium," *Advances in Water Resources*, vol. 35, pp. 1 – 9, 2012.

[41] M. C. Kim and C. K. Choi, "Linear analysis on the stability of miscible dispersion of shear-thinning fluids in porous media," *Journal of Non-Newtonian Fluid Mechanics*, vol. 166, no. 21-22, pp. 1211 – 1220, 2011.

[42] B. Jha, L. Cueto-Felgueroso, and R. Juanes, "Fluid mixing from viscous fingering," *Physical Review Letters*, vol. 106, no. 19, pp. 194502 (4 pp.) –, 2011.

[43] K. Nsir, G. Schafer, R. d. C. Roupert, O. Razakarisoa, and R. Toussaint, "Laboratory experiments on dnapl gravity fingering in water-saturated porous media," *International Journal of Multiphase Flow*, vol. 40, pp. 83 – 92, 2012.

[44] E. O. Dias, E. Alvarez-Lacalle, M. S. Carvalho, and J. A. Miranda, "Minimization of viscous fluid fingering: A variational scheme for optimal flow rates," *Phys. Rev. Lett.*, vol. 109, p. 144502, Oct 2012.

[45] M. Mishra, A. De Wit, and K. C. Sahu, "Double diffusive effects on pressure-driven miscible displacement flows in a channel," *Journal of Fluid Mechanics*, vol. 712, pp. 579 – 597, 2012.

[46] H. A. Nasr-El-Din, K. C. Khulbe, V. Hornof, and G. H. Neale, "Effects of interfacial reaction on the radial displacement of oil by alkaline solutions," *Revue - Institut Francais du Petrole*, vol. 45, no. 2, pp. 231–244, 1990.

[47] V. Hornof and F. U. Baig, "Influence of interfacial reaction and mobility ratio on the displacement of oil in a hele-shaw cell," *Experiments in Fluids*, vol. 18, no. 6, pp. 448–453, 1995.

[48] M. R. Carey, S. W. Morris, and P. Kolodner, "Convective fingering of an autocatalytic reaction front," *Physical Review E*, vol. 53, no. 6 SUPPL. A, pp. 6012–6015, 1996.

[49] M. Bockmann and S. C. Muller, "Growth rates of the buoyancy-driven instability of an autocatalytic reaction front in a narrow cell," *Physical Review Letters*, vol. 85, no. 12, pp. 2506–2509, 2000.

[50] Y. Nagatsu and T. Ueda, "Effects of reactant concentrations on reactive miscible viscous fingering," *AIChE Journal*, vol. 47, no. 8, pp. 1711–1720, 2001.

[51] Y. Nagatsu and T. Ueda, "Effects of finger-growth velocity on reactive miscible viscous fingering," *AIChE Journal*, vol. 49, no. 3, pp. 789–792, 2003.

[52] J. Fernandez and G. M. Homsy, "Viscous fingering with chemical reaction: Effect of in-situ production of surfactants," *Journal of Fluid Mechanics*, no. 480, pp. 267–281, 2003.

[53] Y. Nagatsu, K. Matsuda, Y. Kato, and Y. Tada, "Experimental study on miscible viscous fingering involving viscosity changes induced by variations in chemical species concentrations due to chemical reactions," *Journal of Fluid Mechanics*, vol. 571, pp. 475–493, 2007.

[54] Y. Nagatsu, Y. Kondo, Y. Kato, and Y. Tada, "Effects of moderate damkohler number on miscible viscous fingering involving viscosity decrease due to a chemical reaction,"

Journal of Fluid Mechanics, vol. 625, pp. 97–124, 2009.

[55] T. Podgorski, M. C. Sostarecz, S. Zorman, and A. Belmonte, "Fingering instabilities of a reactive micellar interface," *Physical Review E*, vol. 76, no. 1, pp. 16202:1–6, 2007.

[56] Y. Nagatsu, S. K. Bae, Y. Kato, and Y. Tada, "Miscible viscous fingering with a chemical reaction involving precipitation," *Physical Review E*, vol. 77, no. 6, pp. 67302:1–4, 2008.

[57] S. Li, J. S. Lowengrub, J. Fontana, and P. Palffy-Muhoray, "Control of viscous fingering patterns in a radial hele-shaw cell," *Phys. Rev. Lett.*, vol. 102, p. 174501, Apr 2009.

[58] S. Berg, S. Oedai, A. Landman, N. Brussee, M. Boele, R. Valdez, and K. van Gelder, "Miscible displacement of oils by carbon disulfide in porous media: Experiments and analysis," *Physics of Fluids*, vol. 22, no. 11, p. 113102 (14 pp.), 2010.

[59] Y. Nagatsu, C. Iguchi, K. Matsuda, Y. Kato, and Y. Tada, "Miscible viscous fingering involving viscosity changes of the displacinginvolving viscosity changes of the displacing fluid by chemical reactions," *Physics of Fluids*, vol. 22, no. 2, p. 024101 (13 pp.), 2010.

[60] M. Buchgraber, T. Clemens, L. Castanier, and A. Kovscek, "A microvisual study of the displacement of viscous oil by polymer solutions," *SPE Reservoir Evaluation and Engineering*, vol. 14, no. 3, pp. 269 – 280, 2011.

[61] J. Chadam, D. Hoff, E. Merino, P. Ortoleva, and A. Sen, "Reactive infiltration instabilities," *IMA J Appl Math*, vol. 36, no. 3, pp. 207–221, 1986.

[62] P. Lichtner, E. Oelkers, and H. Helgeson, "Exact and numerical solutions to the moving boundary problem resulting from reversible heterogeneous reactions and aqueous diffusion in a porous medium," *Journal of Geophysical Research*, vol. 91, no. B7, pp. 7531 – 44, 1986.

[63] C. Wei and P. Ortoleva, "Reaction front fingering in carbonate-cemented sandstones," *Earth Science Reviews*, vol. 29, no. 1-4, pp. 183–198, 1990.

[64] E. J. Hinch and B. S. Bhatt, "Stability of an acid front moving through porous rock," *Journal of Fluid Mechanics*, vol. 212, pp. 279–288, 1990.

[65] E. Aharonov, J. A. Whitehead, P. B. Kelemen, and M. Spiegelman, "Channeling instability of upwelling melt in the mantle," *Journal of Geophysical Research*, vol. 100, no. B10, pp. 20433–20450, 1995.

[66] A. De Wit and G. M. Homsy, "Nonlinear interactions of chemical reactions and viscous fingering in porous media," *Physics of Fluids*, vol. 11, no. 5, pp. 949–951, 1999.

[67] M. Jahoda and V. Hornof, "Concentration profiles of reactant in a viscous finger formed during the interfacially reactive immiscible displacements in porous media," *Powder Technology*, vol. 110, no. 3, pp. 253–257, 2000.

[68] J. Chadam, P. Ortoleva, Y. Qin, and R. Stamicar, "The effect of hydrodynamic dispersion on reactive flows in porous media," *European Journal of Applied Mathematics*, vol. 12, pp. 557–569, 2001.

[69] A. De Wit, "Fingering of chemical fronts in porous media," *Physical Review Letters*, vol. 87, no. 5, pp. 54502:1–4, 2001.

[70] J. Yang, A. D'Onofrio, S. Kalliadasis, and A. De Wit, "Rayleigh-taylor instability of reaction-diffusion acidity fronts," *Journal of Chemical Physics*, vol. 117, no. 20, pp. 9395–9408, 2002.

[71] Q. J. Kang, D. X. Zhang, S. Y. Chen, and X. Y. He, "Lattice boltzmann simulation of chemical dissolution in porous media," *Physical Review E*, vol. 65, no. 3, pp. 036318:1–8, 2002.

[72] R. Demuth and E. Meiburg, "Chemical fronts in hele-shaw cells: Linear stability analysis based on the three-dimensional stokes equations," *Physics of Fluids*, vol. 15, no. 3, pp. 597–602, 2003.

[73] P. Grosfils and J. P. Boon, "Viscous fingering in miscible, immiscible and reactive fluids," *International Journal of Modern Physics B*, vol. 17, no. 1-2, pp. 15–20, 2003.

[74] P. Grosfils, J. P. Boon, J. Chin, and E. S. Boek, "Structural and dynamical characterization of hele-shaw viscous fingering," *Philosophical Transactions Royal Society London A*, vol. 356, no. 1821, pp. 1723–1734, 2004.

[75] D. A. Vasquez and A. De Wit, "Dispersion relations for the convective instability of an acidity front in hele-shaw cells," *Journal of Chemical Physics*, vol. 121, no. 2, pp. 935–941, 2004.

[76] T. Kai-Xuan, W. Qing-Liang, L. Ze-Hua, and W. M. Hu, "Nonlinear dynamics of flow-reaction coupling in porous media and application to in situ leaching uranium mining," *International Journal of Modern Physics B*, vol. 18, pp. 2663–8, 2004.

[77] S. Kalliadasis, J. Yang, and A. De Wit, "Fingering instabilities of exothermic reaction-diffusion fronts in porous media," *Physics of Fluids*, vol. 16, no. 5, pp. 1395–1409, 2004.

[78] A. De Wit, "Miscible density fingering of chemical fronts in porous media: Nonlinear simulations," *Physics of Fluids*, vol. 16, no. 1, pp. 163–175, 2004.

[79] J. D'Hernoncourt, S. Kalliadasis, and A. De Wit, "Fingering of exothermic reaction-diffusion fronts in hele-shaw cells with conducting walls," *Journal of Chemical Physics*, vol. 123, no. 23, pp. 234503:1–9, 2005.

[80] E. G. Bruneau, P. C. Macpherson, D. Goldman, R. I. Hume, and M. Akaaboune, "The effect of agrin and laminin on acetylcholine receptor dynamics in vitro," *Developmental Biology*, vol. 288, no. 1, pp. 248–258, 2005.

[81] A. Zadrazil, I. Z. Kiss, J. D'Hernoncourt, H. Sevcikova, J. H. Merkin, and A. De Wit, "Effects of constant electric fields on the buoyant stability of reaction fronts," *Physical Review E*, vol. 71, no. 2, pp. 26224:1–11, 2005.

[82] D. Lima, A. D'Onofrio, and A. De Wit, "Nonlinear fingering dynamics of reaction-diffusion acidity fronts: self-similar scaling and influence of differential diffusion," *Journal of Chemical Physics*, vol. 124, no. 1, pp. 14509–1, 2006.

[83] J. D'Hernoncourt, A. Zebib, and A. De Wit, "On the classification of buoyancy-driven chemo-hydrodynamic instabilities of chemical fronts," *Chaos*, vol. 17, no. 1, pp. 13109:1–9, 2007.

[84] S. Swernath and S. Pushpavanam, "Viscous fingering in a horizontal flow through a porous medium induced by chemical reactions under isothermal and adiabatic conditions," *The Journal of Chemical Physics*, vol. 127, no. 20, pp. 204701:1–14, 2007.

[85] S. Swernath and S. Pushpavanam, "Instability of a vertical chemical front: Effect of viscosity and density varying with concentration," *Physics of Fluids*, vol. 20, no. 1, pp. 012101:1–10, 2008.

[86] K. Ghesmat and J. Azaiez, "Viscous fingering instability in porous media: Effect of anisotropic velocity-dependent dispersion tensor," *Transport in Porous Media*, vol. 73, no. 3, pp. 297–318, 2008.

[87] L. Rongy, P. M. J. Trevelyan, and A. De Wit, "Dynamics of A + B $\rightarrow$ C reaction fronts in the presence of buoyancy-driven convection," *Physical Review Letters*, vol. 101, no. 8, pp. 84503:1–4, 2008.

[88] T. Gérard and A. De Wit, "Miscible viscous fingering induced by a simple A + B $\rightarrow$ C chemical reaction," *Physical Review E*, vol. 79, no. 1, pp. 016308:1–10, 2009.

[89] S. H. Hejazi, P. M. J. Trevelyan, J. Azaiez, and A. De Wit, "Viscous fingering of a miscible reactive A + B → C interface: a linear stability analysis," *Journal of Fluid Mechanics*, vol. 652, pp. 501–528, 2010.

[90] S. H. Hejazi and J. Azaiez, "Nonlinear interactions of dynamic reactive interfaces in porous media," *Chemical Engineering Science*, vol. 65, no. 2, pp. 938–949, 2010.

[91] S. H. Hejazi and J. Azaiez, "Hydrodynamic instability in the transport of miscible reactive slices through porous media," *Physical Review E*, vol. 81, no. 5, pp. 056321:1–12, 2010.

[92] C. Almarcha, P. M. J. Trevelyan, P. Grosfils, and A. De Wit, "Chemically driven hydrodynamic instabilities," *Physical Review Letters*, vol. 104, no. 4, pp. 044501:1–44, 2010.

[93] Y. Nagatsu and A. De Wit, "Viscous fingering of a miscible reactive $a+b \rightleftharpoons c$ interface for an infinitely fast chemical reaction: Nonlinear simulations," *Physics of Fluids*, vol. 23, no. 4, 2011.

[94] S. Hejazi and J. Azaiez, "Stability of reactive interfaces in saturated porous media under gravity in the presence of transverse flows," *Journal of Fluid Mechanics*, vol. 695, pp. 439 – 466, 2012.

[95] S. Davison, H. Yoon, and M. Martinez, "Pore scale analysis of the impact of mixing-induced reaction dependent viscosity variations," *Advances in Water Resources*, vol. 38, pp. 70 – 80, 2012.

[96] B. Chopard, M. Droz, T. Karapiperis, and Z. Racz, "Properties of the reaction front in a reversible $a + b \rightleftharpoons c$ reaction-diffusion process," *Physical Review E. Statistical Physics, Plasmas, Fluids, and Related Interdisciplinary Topics*, vol. 47, no. 1, pp. R40 – R40, 1993.

[97] M. Sinder, H. Taitelbaum, and J. Pelleg, "Reversible and irreversible reaction fronts in two competing reactions system," *Nuclear Instruments and Methods in Physics Research, Section B: Beam Interactions with Materials and Atoms*, vol. 186, no. 1-4, pp. 161 – 165, 2002.

[98] N. E. Benes, R. Verzijl, and H. Verweij, "Numerical scheme for simulating multicomponent mass transport accompanied by reversible chemical reactions in porous media," *Computers and Chemical Engineering*, vol. 23, no. 8, pp. 975 – 985, 1999.

[99] I. Gopich and A. Szabo, "Asymptotic relaxation of reversible bimolecular chemical reactions," *Chemical Physics*, vol. 284, no. 1-2, pp. 91 – 102, 2002.

[100] K. U. Mayer, E. O. Frind, and D. W. Blowes, "Multicomponent reactive transport modeling in variably saturated porous media using a generalized formulation for kinetically controlled reactions," *Water Resources Research*, vol. 38, no. 9, pp. 131 – 1321, 2002.

[101] Z. Koza, "Reaction fronts in reversible $a + b \rightleftharpoons c$ reaction-diffusion systems," *Physica A: Statistical Mechanics and its Applications*, vol. 330, no. 1-2, pp. 160 – 166, 2003.

[102] M. Sinder, V. Sokolovsky, and J. Pelleg, "Reversible $a \rightleftharpoons b$ reaction diffusion process with initially mixed reactants: Boundary layer function approach," *Physica B: Condensed Matter*, vol. 406, no. 15-16, pp. 3042 – 3049, 2011.

[103] H. Alhumade and J. Azaiez, "Stability analysis of reversible reactive flow displacements in porous media," *Submitted*, 2013.

[104] S. Havlin and D. Ben-Avraham, "Diffusion in disordered media," *Advances in Physics*, vol. 51, no. 1, pp. 187 – 292, 2002.

[105] V. Alvarado, H. Davis, and L. Scriven, "Effects of pore-level reaction on dispersion in porous media," *Chemical Engineering Science*, vol. 52, no. 17, pp. 2865 – 2881, 1997.

[106] L. Galfi and Z. Racz, "Properties of the reaction front in an a + b → c type reaction-diffusion process," *Physical Review A*, vol. 38, no. 6, pp. 3151–3154, 1988.

[107] Z. Jiang and C. Ebner, "Simulation study of reaction fronts," *Physical Review A*, vol. 42, no. 12, pp. 7483–7486, 1990.

[108] M. Cross and P. Hohenberg, "Pattern-formation outside of equilibrium," *Review Modern Physics*, vol. 65, pp. 851–1112, 1993.

[109] J. Bansagi, T., D. Horvath, A. Toth, J. Yang, S. Kalliadasis, and A. De Wit, "Density fingering of an exothermic autocatalytic reaction," *Physical Review E*, vol. 68, no. 5, pp. 55301:1–4, 2003.

[110] M. Mishra, M. Martin, and A. de Wit, "Miscible viscous fingering with linear adsorption on the porous matrix," *Physics of Fluids*, vol. 19, no. 7, pp. 073101:1–9, 2007.

[111] J. G. Weissman, "Review of processes for downhole catalytic upgrading of heavy crude oil," *Fuel Processing Technology*, vol. 50, no. 2-3, pp. 199–213, 1997.

[112] D. Horvath, J. T. Bansagi, and A. Toth, "Orientation-dependent density fingering in an acidity front," *The Journal of Chemical Physics*, vol. 117, no. 9, pp. 4399–4402, 2002.

[113] T. Bansagi, D. Horvath, and A. Toth, "Nonlinear interactions in the density fingering of an acidity front," *Journal of Chemical Physics*, vol. 121, no. 23, pp. 11912–15, 2004.

[114] A. Zadrazil and H. Sevcikova, "Influence of an electric field on the buoyancy-driven instabilities," *Journal of Chemical Physics*, vol. 123, no. 17, pp. 174509:1–9, 2005.

[115] T. Rica, D. Horvth, and g. Tth, "Density fingering in acidity fronts: Effect of viscosity," *Chemical Physics Letters*, vol. 408, no. 4-6, pp. 422–425, 2005.

[116] B. F. Edwards, J. W. Wilder, and K. Showalter, "Onset of convection for autocatalytic reaction fronts: laterally unbounded system," *Physical Review A*, vol. 43, no. 2, pp. 749–760, 1991.

[117] A. De Wit and G. M. Homsy, "Viscous fingering in reaction-diffusion systems," *Journal of Chemical Physics*, vol. 110, no. 17, pp. 8663–8675, 1999.

[118] J. Huang and B. F. Edwards, "Pattern formation and evolution near autocatalytic reaction fronts in a narrow vertical slab," *Physical Review E*, vol. 54, no. 3, pp. 2620–2627, 1996.

[119] K. Ghesmat and J. Azaiez, "Miscible displacements of reactive and anisotropic dispersive flows in porous media," *Transport in Porous Media*, vol. 77, pp. 489–506, 2009.

[120] M. N. Islam and J. Azaiez, "Fully implicit finite difference pseudo-spectral method for simulating high mobility-ratio miscible displacements," *International Journal for Numerical Methods in Fluids*, vol. 47, no. 2, pp. 161–183, 2005.

[121] M. Mishra, M. Martin, and A. De Wit, "Differences in miscible viscous fingering of finite width slices with positive or negative log-mobility ratio," *Physical Review E*, vol. 78, no. 6, pp. 206–221, 2008.

[122] C. Bacri, D. Salin, and Y. Yortsos, "Analyse linéaire de la stabilite de l'écoulement de fluides miscibles en milieux poreux," *C. R. Acad. Sci. Paris*, vol. 314, pp. 139–144, 1992.

[123] Y. Nagatsu, Y. Kondo, Y. Kato, and Y. Tada, "Miscible viscous fingering involving viscosity increase by a chemical reaction with moderate damkohler number," *Physics of Fluids*, vol. 23, no. 1, pp. 014109:1–8, 2011.

[124] H. Alhumade and J. Azaiez, "Numerical simulations of reversible reactive flows in homogenous porous media," *Submitted*, 2013.

[125] S. H. Hejazi and J. Azaiez, "Chemically buoyancy driven convective mixing in porous media under transverse flows," *Submitted*, 2011.

[126] T. C. Flowers and J. R. Hunt, "Viscous and gravitational contributions to mixing during vertical brine transport in water-saturated porous media," *Water Resources Research*, vol. 43, no. 1, pp. W01407:1–18, 2007.

[127] K. Ghesmat, H. Hassanzadeh, and J. Abedi, "The impact of geochemistry on convective mixing in a gravitationally unstable diffusive boundary layer in porous media: Co2 storage in saline aquifers," *Journal of Fluid Mechanics*, vol. 673, pp. 480 – 512, 2011.

[128] S. Gruner and A. Kienle, "Equilibrium theory and nonlinear waves for reactive distillation columns and chromatographic reactors," *Chemical Engineering Science*, vol. 59, no. 4, pp. 901 – 918, 2004.

[129] C. Canuto, M. Hussaini, A. Quarteroni, and T. Zang, *Spectral Methods in Fluid Dynamic*. New York: Springer-Verlag, 1987.

[130] I. Avramov, "Relationship between diffusion, self-diffusion and viscosity," *Journal of Non-Crystalline Solids*, vol. 355, no. 10-12, pp. 745 – 747, 2009.

[131] R. N. Bracewell, O. Buneman, H. Hao, and J. Villasenor, "Fast two-dimensional hartley transform," *Proceedings of the IEEE*, vol. 74, no. 9, pp. 1282–1283, 1986.